PHARMACOPHORIC MODELS OF SODIUM CHANNEL ANTAGONISTS

Poon Thong Yuen
(B.Sc. (Pharm. Hons.), NUS)

A THESIS SUBMITTED
FOR THE DEGREE OF DOCTOR OF PHILOSOPHY
DEPARTMENT OF PHARMACY
NATIONAL UNIVERSITY OF SINGAPORE
2004

ACKNOWLEDGEMENTS

I wish to express my sincere gratitude to Dr. Chui Wai Keung for his patience, guidance and mentorship. His advice and pertinent questions helped to direct the course of this project. He taught me the virtues of caution and prudence, and I hold him in high esteem for his expertise and knowledge.

I would like to express my heartfelt appreciation to Dr. J. C. Thenmozhiyal for her selfless tutelage and assistance.

I wish to thank Assoc. Prof Wong Tsun Hon and Mrs. Ting Wee Lee from the Pharmacology department for their assistance in radioligand and animal studies.

I also wish to thank the Pharmacy department for providing the necessary facilities for this project, and the National University of Singapore for providing the research scholarship.

Throughout these years, my wife has given me never-ending encouragement and support, which helped me overcome all obstacles and barriers to complete my Ph. D studies. Words cannot express my gratitude to her. Last but not least, I would like to thank my parents and siblings for their understanding and emotional support.

CONTENTS

	PAGE
ACKNOWLEDGEMENTS	**i**
CONTENTS	**ii**
SUMMARY	**vi**
LIST OF TABLES	**viii**
LIST OF FIGURES	**ix**
ABBREVIATIONS	**x**

INTRODUCTION

1 COMPUTER-AIDED DRUG DESIGN IN THE DRUG DISCOVERY PROCESS

1.1	Definition and Role of Computer-aided Drug Design in the Drug Discovery Process	1
1.2.	CADD Strategies and their Usage	2
1.2.1	CADD Strategies based on Known 3D Structures of Target Receptor	2
1.2.2	CADD Strategies based on Ligands	4
1.2.3	Genetic Algorithms in CADD Strategies	6
1.3	Methodology in Computer-aided Drug Design	6
1.3.1	Quantum Mechanics and Molecular Mechanics Calculation Methods	7
1.3.2	Conformational Search Techniques	9

2. PHARMACOLOGY AND MEDICINAL CHEMISTRY OF NEURONAL VOLTAGE–GATED SODIUM CHANNEL BLOCKERS

2.1	Structure and Function of Voltage-gated Sodium Channels	11
2.1.1	Structure	11
2.1.2	Function	12
2.1.3	Neurotoxin Binding Sites	12
2.2	Medicinal Chemistry of Sodium Channel Blockers	14
2.2.1	*In Vitro* Test Systems	15
2.2.2	*In Vivo* Test Systems	17
2.2.3	Sodium Channel Blockers as Anticonvulsants	19
2.2.4	Sodium Channel Blockers as Neuroprotective Agents	27
2.2.5	Sodium Channel Blockers as Antinociceptive Agents	30

3. RATIONALE AND OBJECTIVES

3.1 The Need for New Sodium Channel Blockers 35
3.2 Previous Studies on Sodium Channel Blockers 36
3.3 Hypotheses and Objectives 39
3.3.1 Hypotheses 39
3.3.2 Objectives 39

RESULTS AND DISCUSSION

4. A NEW PHARMACOPHORIC MODEL FOR NEURONAL (TYPE II) SODIUM CHANNEL BLOCKERS.

4.1 Choice of a CADD Strategy 41
4.2 Selection of a Training Set of Compounds 43
4.2.1 Characteristics of the Compounds in the Training Set 43
4.2.2 *In Vitro* Method for Assessment of Biological Activity of Compounds used for Modelling and Validating the Pharmacophoric Model 46
4.2.3 Compounds Selected as the Training Set 48
4.3 A Search for Pharmacophoric Models
4.3.1 Methodology of Conformational Analysis 49
4.3.2 DISCO 50
4.4 Validation of Pharmacophoric Models 51
4.5 Results and Discussion of Pharmacophoric Modelling 55
4.6 Proposed Pharmacophoric Model for Neuronal (Type II) Sodium Channels 63

5. ADAPTATION OF THE PHARMACOPHORIC MODEL FOR IDENTIFYING POTENTIAL SODIUM CHANNEL BLOCKERS

5.1 Criteria for a Screening Process for Potential Sodium Channel Blockers 67
5.2 Limitations of the Screening Process 69

6. VERIFICATION OF PREDICTIONS THROUGH CHEMICAL SYNTHESIS AND *IN VITRO* TESTING

6.1 Identification of Potential Sodium Channel Blockers 71
6.2 Chemical Synthesis and *In Vitro* Testing of Compounds 72
6.2.1 Chemistry 72
6.2.2 BTX Radio-ligand Binding Assay 73
6.3 Results of CADD and *In Vitro* Testing of 4,6-Diamino-1,2-dihydro-2,2-substituted-1-phenyl-1,3,5-triazines (Phenyldihydro-1,3,5-triazines) 75
6.3.1 *In Vitro* Testing of 4,6-Diamino-1,2-dihydro-2,2-dimethyl-1-phenyl-1,3,5-triazines (Series (I)) 75
6.3.2 *In Vitro* Testing of 4,6-Diamino-1,2-dihydro-2,2-cyclohexyl-1-phenyl-1,3,5-triazines (Series (II)) 77
6.3.3 Structural Activity Relationships of Phenyldihydro-1,3,5-triazines and PLS Analysis 82
6.4 Results of CADD and *In Vitro* Testing of Benzyloximes 87

7. POTENTIAL PHARMACOLOGICAL ACTIONS RELATED TO SODIUM CHANNEL BLOCKADE

7.1 Choice of Pharmacological Assays 90
7.2 Anticonvulsant and Sedative Effects of the Phenyldihydro-1,3,5-triazines and Benzyloximes in the MES and Rotarod Assays 92
7.3 Analgesic Effects of the Phenyldihydro-1,3,5-triazines and Benzyloximes in the Hot-plate Assay 97
7.4 Inhibitory Activity of the Phenyldihydro-1,3,5-triazines against DHFR 99
7.5 Pharmacological Profile of Phenyldihydro-1,3,5-triazines and Benzyloximes 103

CONCLUSIONS AND FUTURE WORK

8. CONCLUSIONS AND FUTURE WORK

8.1 CADD and its Application in the Development of a Pharmacophoric model for Sodium Channel Blockers 105
8.2 Adaptation of the Pharmacophoric Model into a Screening Process for Potential Neuronal Sodium Channel Blockers 106
8.3 Screening of Pharmacological Activities 108
8.4 Future Work 109

MATERIALS AND METHODS

9 MATERIALS AND METHODS

9.1 Computer-aided Drug Design 112
9.1.1 Systematic Conformational Search 112
9.1.2 Distance Comparison (DISCO) 112
9.1.3 Quantitative Structural Activity Relationship (QSAR) 113

9.2 Chemical Synthesis 113
9.2.1 Materials and Equipments 113
9.2.2 General Three-component Synthesis of 4,6-Diamino-1-(substituted)phenyl-1,2-dihydro-2,2-substituted-1,3,5-triazine HCl. 114
9.2.3 General Synthesis of Benzyloximes. 123

9.3 Pharmacological Assays 127
9.3.1 Sodium Channel Binding Assay 127
9.3.2 MES and Rotarod Test 128
9.3.3 Hot-plate assay 129
9.3.4 DHFR Inhibition Assay 129

BIBLIOGRAPHY 133

SUMMARY

The functions of neuronal sodium channels can be antagonised by blocking the ion flux. It is hypothesized that all compounds that exhibit blockade activity against the neuronal sodium channels, as characterized by the BTX assay, share a common pharmacophore, and that such a pharmacophore is able to discern good blockers from weaker blockers. As such, the main objective of the study was to derive and validate a pharmacophoric model for sodium channel blockers, by computer-aided molecular modelling. The pharmacophoric model was derived from five good neuronal sodium channel blockers, and was subsequently validated with 20 compounds. The model consists of one H-bond donor (D), one H-bond acceptor (A) and one hydrophobic group (H), and the A-H, A-D and D-H distances are 4.02 ± 1.26Å, 5.65 ± 1.26Å, and 3.27 ± 1.26Å respectively. Results from correlation studies between Relative Binding Potential (RBP) and Total Difference (TD) values were used to separate the good blockers from the weaker blockers.

The study was able to demonstrate that the pharmacophoric model could identify potential sodium channel blockers. According to the model, active sodium channel blockers should have the three stipulated pharmacophoric elements, a TD value less than 3.50, and a charged nitrogen at physiological pH. The model identified the 4,6-diamino-1,2-dihydro-2,2-substituted-1-phenyl-1,3,5-triazines (phenyldihydro-1,3,5-triazines) as good blockers. In addition, the pharmacophoric model was also used to help in optimising the blockade activity of the phenyldihydro-1,3,5-triazines. 4,6-diamino-1,2-dihydro-2,2-dimethyl-1-phenyl-1,3,5-triazine was synthesized and its sodium channel blockade activity was observed at an IC_{50} value of 195.1 ± 10.8μM. The pharmacophoric model suggested the substitution of the dimethyl group at the 2-position, with a more hydrophobic group, would give better binding affinity to the

sodium channels. Among the new phenyldihydro-1,3,5-triazines synthesized, the most potent compound was 1-(*m*-chlorophenyl)-2,2-cyclohexyl-4,6-diamino-1,2-dihydro-1,3,5-triazine (compound **34**) and its IC_{50} value was 4.0 ± 0.5μM. In contrast, the benzyloximes were predicted to be weak blockers. All the 11 benzyloximes synthesized exhibited poor sodium channel blockade activity and the most active compound (compound **51**) had an IC_{50} value of 0.44 ± 0.02mM.

Finally, the study also investigated the pharmacological activities of the new compounds. The phenyldihydro-1,3,5-triazines did not show epileptic protection in the Maximal Electroshock (MES) assay but were found to have antinociceptive properties in the hot-plate assay. Phenyldihydro-1,3,5-triazines **38** and **41** have mean hot-plate latency values of 13.6s and 13.1s at the dose of 50mg/Kg, in comparison to morphine sulphate (positive control), which has a mean hot-plate latency value of 13.9s at 5mg/Kg. The benzyloximes displayed epileptic protection in the MES assay, with compound **51** providing full epileptic protection (MES score of 4) at the dose of 150mg/Kg. However, compound **51** only have a mean hot-plate latency value of 9.3s at the dose 100mg/Kg.

Keywords: neuronal sodium channels, pharmacophore, model, triazines, benzyloximes, BTX, MES, hot-plate, screening.

LIST OF TABLES

TABLE		PAGE
1	Pharmacophoric models and inter-pharmacophoric distances (Å)	55
2	TD and RBP values of the compounds	56
3	Correlation of TD with RBP values	57
4	Physical parameters of Phenyldihydro-1,3,5-triazines as calculated *in silico*	84
5	Mean hot-plate latency values of selected phenydihydro-1,3,5-triazines and benzyloximes	98
6	Volume of reagents, enzyme and inhibitors used in the DHFR enzyme assay	131

LIST OF FIGURES

FIGURE		PAGE
1	Training set of compounds	49
2	Validation set of compounds	54
3	Correlation plot of RBP vs TD (from model A) using compounds in the training set	59
4	Correlation plot of RBP vs TD (from model A) using compounds **1** to **7**	60
5	Correlation plot of RBP vs TD (from model A) using compounds **8** to **14**	60
6	Compound **(17)** is shown with an arrow indicating the H-bond donor atom.	62
7	Proposed pharmacophoric model	64
8	Flowchart for the screening process	68
9	Chemistry of phenyldihydro-1,3,5-triazines	73
10	Chemistry of benzyloximes	73
11	Binding affinity of compounds in series (**I)** in the BTX assay	76
12	Compound **21** overlapped onto the pharmacophoric triangle	78
13	Binding affinity of compounds in series (**II)** in the BTX assay	80
14	PCA scores scatter plot	85
15	PLS scores scatter plot	85
16	PLS loadings plot	86
17	PLS Variable Importance Plot (VIP)	86
18	Binding affinity of compounds in the benzyloximes series	88
19	MES scores and Rotarod values of phenyldihydro-1,3,5-triazines	94
20	MES scores and Rotatrod values of benzyloximes	96
21	DHFR inhibitory activity of phenyldihydro-1,3,5-triazines	102

ABBREVIATIONS

3-BEP	3-Benzyl-3-ethyl-2-piperidinone
3D	Three-Dimensional
5-HT	5-Hydroxytryptamine
A	Hydrogen-bond acceptor
AMPA	α-Amino-3-hydroxy-5-methyl-4-isoxazolepropionic acid
BAPTA	Bis-(*o*-aminophenoxy)-N, N, N', N'-tetraacetic acid
BTX	Batrachotoxin
CADD	Computer-Aided Drug Design
CADR	Computer-Aided Drug Refinement
CoMFA	Comparative Molecular Field Analysis
CoMSIA	Comparative Molecular Similarity Index Analysis
COSMO	Conductor-like Screening Model
CPK	Corey-Pauling-Koltun
D	Hydrogen-bond donor
DDT	1,1-Trichloro-2,2-bis(4-chlorophenyl)ethane
DHF	Dihydrofolate
DISCO	Distance Comparison
DUCKs	N-substituted 4-ureido-5, 7-dichloro-quinolines
GA	Genetic Algorithms
GABA	γ-Aminobutyric Acid
$GEFS^+$	Generalized Epilepsy with Febrile Seizures Plus
GMEC	Global Minimum Energy Conformer
H	Hydrophobic group
HAD	Hydrogen bond acceptor/donor unit

H-bond	Hydrogen bond
HIV	Human Immuno-deficiency Virus
HOMO	Highest Occupied Molecular Orbital
IC_{50}	Concentration of inhibitor that causes 50% of inhibition
K_i	Inhibitory constant
LMEC	Local Minimum Energy Conformer
LUMO	Lowest Unoccupied Molecular Orbital
MCAO	Middle Cerebral Artery Occlusion
MDR	Multidrug Resistance
MES	Maximal Electroshock
MM	Molecular Mechanics
MR	Molecular Refractivity
NMDA	N-methyl-*D*-aspartate
NMR	Nuclear Magnetic Resonance
PCA	Principal Component Analysis
PKUDDS	Peking University Drug Design System
PLS	Partial Least Squares
QM	Quantum Mechanics
QSAR	Quantitative Structural Activity Relationship
RBP	Relative Blocking Potential
SAS	Solvent Accessibility Surface
SBFI	Selective dye Benzofuran Isophthalate
s. c. Met/PTZ	Subcutaneous Metrazol/pentylenetetrazol
TD	Total Difference
THF	Tetrahydrofolate

TTE	Threshold Tonic Extension
TTX	Tetrodotoxin
UV	Ultra Violet
VIP	Variable Importance Plot

1. COMPUTER-AIDED DRUG DESIGN IN THE DRUG DISCOVERY PROCESS

1.1 Definition and Role of Computer-aided Drug Design in the Drug Discovery Process

Drug discovery is a long and costly process, requiring about US$802 million to bring a new drug to the end of a phase III clinical testing.[1] The traditional approach to drug design starts with the screening of a large number of compounds, for one or more biological targets, until a suitable lead compound is identified. Lead identification is usually the most time-consuming and expensive stage of the drug discovery process. Rational drug design, also known as structure-based design, is a more time and cost efficient alternative. For rational drug design, structural information on a target receptor is first elucidated, which is then used to design specific ligands to interact with it. When compared to the traditional trial and error method of drug discovery, rational drug design drastically reduced the number of compounds synthesized and screened in biological assays.

One approach to rational drug design is Computer-aided Drug Design (CADD), which is the development or improvement of drug candidates with the assistance of computers. CADD approaches can be divided into two general categories, those that are based on the three-dimensional (3D) structure of the target receptor, and those that gained information by studying ligands that bind to the receptors. In the former category, the 3D structure of the receptor is first elucidated by techniques such as X-ray crystallography, before being used for *in silico* experiments of receptor-ligand binding. In the later category, the approaches used were based on the concept of molecular recognition, which specifies that in order for ligands to bind well to their receptors, they must possess significant structural and chemical characteristics

complementarily to their targets. These approaches usually combine the biological data (such as radioligand-binding studies) and *in silico* data, so as to deduce the geometrical and physiochemical requirements for favorable binding to the target receptor. A recent example of CADD includes the development of a receptor-based pharmacophore model for *Bascillus stearothermophilus* alanine racemase. [2] The group was able to utilize the conformations of the alanine racemase dimer (with a D-alanine and a non-covalent inhibitor attached to the receptor sites) obtained during molecular dynamics simulations to generate a dynamic pharmacophore model.

1.2. CADD Strategies and their Usage

The interest in CADD by researchers in academia and industry lead to the development of a plethora of CADD strategies. The choice of which strategy to use is largely dependent on whether the 3D structure of the target receptor is available, as it is often ideal to work with a known receptor structure to avoid questions about the reliability of the receptor structure prediction. In practice, however, the structure of the receptor is usually unknown, and alternative methods have to be employed.

1.2.1 CADD Strategies based on Known 3D Structures of Target Receptor

Knowledge of the 3D structure of a receptor can accelerate the drug discovery process tremendously, as can be seen by the development of purine nucleoside phosphorylase inhibitors and Human Immuno-deficiency Virus (HIV) reverse transcriptase inhibitors. [3-4] The most common method of obtaining information on the 3D structure is to employ X-ray crystallography. Protein nuclear magnetic resonance (NMR) also contributes valuable data on protein-ligand interactions, such as the NMR solved structure of glutamate mutase (B12-binding subunit) complexed with the

vitamin B12 nucleotide.[5] A homology model of the receptor can be constructed if structural information about homologous receptors is available. One example is the homology model of thymidine kinase from *Varicella zoster* virus, using homology modelling based on thymidine kinase from *Herpes simplex* virus type 1 structure as template.[6] Another example is the homology model of human cytochrome P450 2E1 (CYP2E1), based on the CYP2C5 crystallographic template.[7]

The most common CADD strategy for use with a known 3D structure of a target receptor is docking. Docking is a computational method that is used to determine the geometry of the receptor-ligand complex. The docking procedure can be done manually, using interactive computer graphics. However, this manner of docking requires a lot of input from the user, and can be successful only if the user has a good idea of the expected binding mode. Automatic docking algorithms are less biased than human modellers and usually consider more possibilities. There are many docking strategies available, such as those that consider the receptor-ligand complex as being a rigid entity. Sometimes only the ligand or the region around the receptor is considered as flexible.[8-10]

Gehlhaar *et. al*. has described a *de novo* ligand designer, which made use of the 3D structure of the target receptor.[11] The group utilized a program, which starts by filling the receptor site with a closely packed array of carbon atoms, and subsequently makes adjustments to the atoms (adding, removing or changing the types of atoms). Their effects on the receptor-ligand interactions assessed the resulting changes, and a metropolis algorithm was used to determine whether or not to accept the changes. The program was tested successfully with the HIV protease receptor.

1.2.2 CADD Strategies based on Ligands

The problem most familiar to researchers is the one in which the structure of the target receptor is unknown, and only little information can be inferred through biological screening of compounds. In such situations, CADD can be utilized to combine the data from biological screening with *in silico* data, such as geometrical and physicochemical data, to form receptor models or quantitative structure-activity relationship (QSAR) models.

Pharmacophore and pharmacophoric elements are central concepts in medicinal chemistry, and have been used for a long time in two dimensional pharmacophoric models. CADD has enormously facilitated the 3D use of the concept, and the most commonly used strategy is the active analog approach. [12] This approach starts by selecting a set of biologically active compounds and then obtaining their energetically accessible conformations. These conformations were then superimposed according to their pharmacophoric elements and the possible 3D-pharmacophoric models were subsequently examined. Pharmacophoric elements used in the development of the models are most often atoms or functional groups which may interact with receptor binding sites via hydrogen bonds, electrostatic forces or *van der waals* interactions. Examples of pharmacophoric elements include heteroatoms such as oxygen and nitrogen and polar functional groups such as carboxylic acids, amides and hydroxyl groups. Other approaches to pharmacophoric models have been proposed, and they include the ensemble distance geometry method by Sheriden *et. al*. and the constrained minimization of active compounds by Naruto *et. al*. [13-14] Poulsen *et. al.* recently developed a neurokinin 2 antagonist pharmacophoric model using five non-peptide antagonists from several structurally diverse classes. [15]

The steric and electrostatic properties of ligands influence their ability to form stable receptor-ligand complexes. These properties, together with biological data, can be developed into a 3D QSAR model using the comparative molecular field analysis (CoMFA) approach. CoMFA begins by aligning a set of compounds of known biological data to optimize the overlapping of their steric and electrostatic fields, which is then followed by partial least squares analysis. The program will then map out 3D areas where particular steric and electrostatic features are either advantageous or detrimental to biological activity. The most significant drawback of CoMFA is the process of selecting the conformations of the ligands to be used for alignment. The selection is either done manually or a weighted average of many conformations will be used to determine the molecular fields. Another development of the 3D QSAR approach is comparative molecular similarity index analysis (CoMSIA), which differs from CoMFA by using some arbitrary 'descriptors' that consider the spatial similarity or dissimilarity of molecules. CoMFA and CoMSIA are often used together, such as in the work of Tsakovska. [16] The author made use of the two 3D-QSAR methods to derive models for phenothiazine type multidrug resistance (MDR) modulators in P388/ADR cells, confirming the role of hydrophobicity as a 3D property and also found that hydrogen bond acceptor interactions contribute to anti-MDR activity. Paier *et. al.* used both CoMFA and CoMSIA to generate models for predicting the catalytic abilities of four different bacteria that contain epoxide hydrolase. [17] The models were used to predict the enantiomeric ratio of the products of the hydrolysis, and thus can identify the most suitable epoxide hydrolase for a given substrate.

1.2.3 Genetic Algorithms in CADD Strategies

Genetic algorithms (GA) are techniques relatively new to CADD. [18] The basic concept of genetic algorithms is the 'survival of the fittest'. These techniques start by randomly generating a population of solutions, and these solutions were evaluated for their 'fitness'. The program would then select 'fit' solutions and 'breed' (that is, to further explore) them, resulting in a new population of solutions. The whole process would be repeated till satisfied solutions were obtained.

GA can be applied to many CADD strategies, such as pharmacophore elucidation, docking and QSAR. Genetic algorithms can differ in their approach to the evaluation of 'fit' solutions. One approach is to 'screen' the solutions *in silico*, such as by docking to a known receptor. Another method is to evaluate the solutions based on biological screening. The latter method can be carried out by robotic synthesis, and the guiding computer system would direct the contents of the next library based.

Hou *et. al.* developed a molecular simulation software package, Peking University Drug Design System (PKUDDS), for rationale drug design.[19] The software package applied genetic algorithms to various CADD strategies such as molecular docking, conformational analysis, 2D-QSAR and CoMFA. The software package was verified using molecular docking studies of unbound complexes, a 2D-QSAR study of some cinnamamides and a CoMFA study of β–carboline ligands.

1.3 Methodology in Computer-aided Drug Design

In order to utilize CADD strategies, it is a prerequisite to model the molecules used in the study. The process starts by constructing a trial molecular geometry (conformation) *in silico*. For molecular mechanics calculations, the atoms of the molecule are then iteratively moved using an energy minimization technique until the

net forces on all atoms vanish and the total energy of the molecule reaches a minimum. For quantum mechanics, both the positive nuclei and negative electrons are considered. The conformer corresponding to this energy minimum is called the Local Minimum Energy Conformer (LMEC). The energy minimization methods cannot move the molecule across energy barriers, thus to find other LMECs, the process has to be repeated with another starting geometry or more efficiently by using a conformational search technique. The LMEC with the lowest energy is known as the Global Minimum Energy Conformer (GMEC).

1.3.1 Quantum Mechanics and Molecular Mechanics Calculation Methods

Calculations of conformational properties of molecules can be done using either the quantum mechanics (QM) methods or the molecular mechanics (MM, also known as force field) methods. The basis of QM methods is the Schrödinger equation, which is solved by treating the molecules as a collection of positive nuclei and negative electrons moving under the influence of coulombic potentials. This allowed both the calculation of the energy of the molecule and the associated wave function, from which electronic properties, such as electron density, can be derived. In the *ab initio* methods, all the electrons were included in the calculations; thus these QM methods can be extremely expensive in terms of the computer resources needed. Semi-empirical methods, which consider only the valence electrons of the system, were developed to reduce computation effort. In addition, many terms in the equation were omitted, and scaling factors that were derived from experiments were used instead.

MM methods consider a molecule as a collection of atoms held together by classical forces. These methods completely ignore the electrical motions and calculate

the energy of a system as a function of nuclear positions only. The energy of the molecule (E_{total}) is calculated as a sum of terms as in the equation below.

$$E_{total} = E_{stretching} + E_{bending} + E_{torsion} + E_{van\ der\ Waals} + E_{electrostatic} + \text{cross terms}$$

The first four terms in the sum are the energies due to deviations of bond length, bond angles, torsional angles and non-bonded distances, respectively, from their reference values. $E_{electrostatic}$ gives the electrostatic attraction or repulsion between bond dipoles or partial atomic charges while cross-terms are hybrid terms such as stretch-bend and torsion-bend. Atom types define reference values used in the above equation, which give information about the atomic number, hybridization state, and sometimes the local environment of the atom. For example, a carbon atom can be typed as sp, sp^2, sp^3, carbonyl, or cyclopropane. A carbon atom typed as sp^3-hybridized will have a reference angle of 109.5°.

QM methods, like MM methods, can be used for energy minimization or in conformational searches. However, QM methods require a far greater amount of computer resource than MM calculations. This difference between the two methods become more pronounced in cases where a fast and accurate computation of structures of appreciably large molecules, an extensive conformational search, dynamic processes or docking are the objectives of a study.

QM calculations are based on the electrons in the system, thus it is possible to derive properties that depend upon the electronic distribution, and can be used in situations when covalent bonds are broken or formed. In contrast, MM methods consider only the position of the nuclei, and therefore provide no information on the

electronic structure. Furthermore, MM methods cannot be used when the molecule is not in the ground state, or when covalent bonds are broken or formed.

In view of the strengths and limitations of the two groups of methods, researchers combined the two into a QM/MM hybrid, which is used mainly for investigating the structure and properties of large systems. [20] The system is divided into two regions: a small QM region and a significantly larger MM region. This method is well suited for studying biomolecular systems. For example, to simulate the mechanisms of enzyme reactions, the active site can be modeled in the QM region, while the rest of the macromolecule is modeled in the MM region. The most challenging aspect of the QM/MM method is the treatment of the bonds that connect atoms positioned on different sides of the QM/MM boundary. Many approaches had been suggested, and ongoing research is being performed to solve this problem.

1.3.2 Conformational Search Techniques

During an energy minimization of a molecule, the molecule changes from the initial trial conformation to the closest LMEC. For molecules with three or more rotatable bonds, the number of LMECs increases, thus a computer implemented search method is necessary. The three main conformational search methods are grid search, molecular dynamics and Monte Carlo simulations.

Grid search generates new conformers by using all combinations of torsional angle values at a preset angle increment. The major advantage of this method is that all the LMECs are located within the space examined. Being a combinatorial approach, the number of conformers handled is equal to $(360/m)^n$, where n is the number of rotatable bonds and m is the angle of increment. This method of conformational search is very time consuming and is only suitable for small and/or relatively rigid molecules.

Most grid search approaches reduce the number of conformers being minimized to save computational resources. This can be accomplished by eliminating strained conformers, such as when two atoms in the molecule become too close to each other.

Molecular dynamics make use of Newton's laws of motion to model a trajectory that specifies how the positions and velocities of the particles in the system vary with time. Sampling at a series of time points yield conformers which can be minimized to their closest LMECs. The time steps used for advancing the atom motions, usually in femtoseconds, must be shorter than the highest-frequency molecular motion, otherwise two bonded atoms may move too far from each other to the extent that they cannot form a bond. Therefore this method can be very time-consuming if applied to large molecular systems.

The Monte Carlo method generates conformers by making random changes to the 3D positions of the atoms in a structure. The resulting conformers are usually highly strained systems, which are then minimized to obtain LMECs. Through multiple sampling, an overview of the energy surface is obtained and sufficient sampling may place confidence limits on the conformer that is found to be the GMEC.

Both the molecular dynamics and Monte Carlo methods are suitable for flexible molecules and macromolecules, but there are cases where one is more suitable than the other. For example, molecular dynamics is required for calculation of time-dependent quantities such as transport coefficients, while Monte Carlo methods are more suitable for performing simulations at exact temperatures and pressures. In general, molecular dynamics is more useful for exploration of the local phase space as it advances the positions and velocities of all the particles simultaneously, while Monte Carlo simulations are more effective for conformational changes, as it jumps to completely different area of phase space.

3. PHARMACOLOGY AND MEDICINAL CHEMISTRY OF NEURONAL VOLTAGE–GATED SODIUM CHANNEL BLOCKERS

2.1 Structure and Function of Voltage-gated Sodium Channels

3.1.1 Structure

The sodium channel consists of a 260-kDa α-subunit, a 36-kDa β1-subunit, a 33-kDa β2-subunit and a β3-subunit.[21] The α-subunit forms the ion pore and demonstrates the basic pharmacology and physiology of the native channel, while β-subunits appear to be modulators of α-subunit's function. No drug has been reported to interact directly with the β-subunits. The three-dimensional structure of sodium channels has not been solved, as attempts to obtain crystallographic information have so far been unsuccessful.

The ion channel (aqueous pore and gating processes) resides in the α-subunit, which consists of four repeated sequences of amino acids (homologous domains DI-DIV). [22] Each of these repeats spans the membrane six times (transmembrane segments S1-S6), and it was postulated that DI-DIV form the 'four walls' of the aqueous pore. Several investigations have enabled the assigning of functions to particular regions or even specific amino acids. Mutation studies indicated that the lysine and alanine residues in DIII and DIV are critical determinants of the ion selectivity of the sodium channel while an intracellular loop that connects DIII and DIV is critical for the sodium channel inactivation process. Since the signal for activation of the sodium channel is depolarization, the ion channel needs a voltage sensor to detect such changes. The S4 regions are highly conserved between sodium channels from different species and are also homologous to the equivalent regions of

voltage-gated potassium and calcium channels. Furthermore, it has positively charged arginine or lysine at every third position. Therefore the S4 regions are widely accepted as the voltage sensor of the sodium channel.

3.1.2 Function

Information can be transferred throughout the nervous system via neurons, and other excitable cells, in the form of action potentials. Such action potentials are in the form of all or none signals that are generated by ion channels, such as the voltage-gated sodium channel. The voltage–gated sodium channels can be visualized as water-filled tunnels that provide an aqueous route for sodium ions through the hydrophobic cell membrane. During depolarization of the membrane, the voltage sensor detects electric field changes in the membrane and alters the conformation of the channel protein, thus opening the channel. The increase in permeability resulting from activation of the sodium channel is biphasic. Upon depolarization, permeability to sodium increases dramatically and then decreases to the baseline level. The voltage-gated sodium channel can exist in three functionally distinct states; resting, active and inactivated. Both resting and inactivated states are non-conducting, and channels that have been inactivated by prolonged depolarization are refractory unless the cell is repolarized to allow them to return to the resting stage.

3.1.3 Neurotoxin Binding Sites

Neurotoxins that bind with high affinity and specificity to the channel complex were used as molecular probes to determine the subunit structure of the rat brain sodium channel. Five groups of neurotoxins that act at different receptor sites on the sodium channel were described.[23] Tetrodotoxin (TTX), saxitoxin, and μ-conotoxin,

which inhibit transportation of sodium ions across the channels and thus block ion conductance, bind to site 1. Batrachotoxin (BTX), veratridine, grayanotoxin, and aconitine bind to site 2, resulting in persistent activation of the sodium channel. Polypeptide α-scorpion toxins and sea anemone toxins, which enhance persistent activation, slow inactivation and/or block inactivation of the sodium channels, bind to site 3. A second class of scorpion toxins (β-scorpion toxins) that shift the voltage dependence of activation of the sodium channels to more negative membrane potentials without modifying sodium channel inactivation binds to site 4. The brevetoxins and ciguatoxins, agents that cause repetitive neuronal firing, shift the voltage dependence of sodium channel activation, and block sodium channel inactivation bind to site 5.

More recently, four additional sites were reported, which consist of neurotoxin and insecticide binding sites.[24] The δ-conotoxins, which cause inhibition of activation, binds to site 6 binds. 1,1,1-trichloro-2,2-bis(4-chlorophenyl)ethane (DDT), DDT analogues and pyrethroids bind to site 7, which inhibit inactivation of sodium channels and shift their voltage dependence. The goniopora coral toxin and conus stratius toxin bind to site 8 and inhibit the activation of the sodium channels. The local anaesthetics, anticonvulsants and dihydropyrazoles bind to site 9 and inhibit the transportation of the sodium ions across the channels.

McPhee *et al* showed that mutations at positions 1764 and1771 in the DIV S6 of SCN2A segment significantly reduced the binding affinity of the channels for a range of sodium channel blocking drugs. [25] Linford *et al* further showed that these mutated sodium channels have reduced binding affinity for tritiated BTX.[26] Thus it was concluded that the BTX binding site shares overlapping but not identical molecular determinants with the binding site of sodium channel blockers.

2.2 Medicinal Chemistry of Sodium Channel Blockers

Neuronal voltage-gated sodium channels have been targeted for various ailments, including epilepsy, stroke and other brain injuries, and neuralgia. The discovery of the structure and function of sodium channels allowed better understanding of how the functions of the sodium channels can be antagonised. Antagonists of sodium channels block the ion flux and therefore are also commonly known as sodium channel blockers. As such, the term sodium channel blockers will be used throughout the text to represent sodium channel antagonists. Various chemical classes of compounds had been developed as sodium channel blockers and multiple *in vivo* and *in vitro* tests allowed the assessments of potential sodium channel blockers.

A much better understanding of sodium channels and drugs interacting with them had made it clear that local anaesthetics such as procaine, class I antiarrhythmics such as lidocaine and mexiletine, and anticonvulsants such as phenytoin and carbamazepine actually work by modulating sodium channel conductance. Phenytoin and carbamazepine were important in the characterization of the role of sodium channels first in epilepsy, then in neuroprotection, and analgesia.

Various *in vitro* and *in vivo* assay methods have been developed to explore the medicinal chemistry of sodium channel blockers. There is a need to differentiate test systems for studying the mechanisms of action of sodium channel blockers from test systems intended to identify therapeutic sodium channel blockers. Clinical activity of sodium channel blockers can be studied definitively only *in vivo*, whereas analysis of the mechanism of action requires *in vitro* test systems. *In vitro* test systems have the advantage that drug concentrations can be precisely controlled and complications introduced by absorption, distribution, metabolism and elimination can be largely avoided.

2.2.1 *In Vitro* Test Systems

In vitro test systems for sodium channel blockers include radioligand binding assays, radioactive flux assays, fluorescence-based assays, voltage-sensitive dyes assays and the patch-clamp technique.

Radioligand binding assays revealed the presence of multiple neurotoxin binding sites on sodium channels and were extensively used to measure ability of drugs to bind selectively to the channels that were at a particular stage of the activated/ inactivated/resting cycle of channel activity. Among the radioligand binding assays designed for sodium channel blockers, the most commonly used was the BTX assay.[27] It was shown that sodium channel blockers like phenytoin and carbamazepine were able to displace BTX, thus the pharmacological activity of sodium channel blockers can be predicted by measuring the ability of these drugs to displace [^{3}H]-BTX. It is reasonable to assume that the use of such a high-throughput binding assays should lead to the identification of novel sodium channel blockers.

Exposure to neurotoxins such as veratridine was used to stabilize the sodium channels in the open state, thus allowing a flux of radioactive tracers into cells or synaptosomal preparations that have sodium channels. The most commonly used radioactive tracers are the [^{22}Na] and [^{14}C]-guanidinium. When a sodium channel blocker was added to such a preparation, the flux of radioactive tracers was reduced. Thus the inhibition of radioactive tracer influx is a valid model for the identification of sodium channel blockers, which allows high-throughput analysis of compounds. For example, Maillard *et. al.* expressed the cloned type IIA sodium channels, derived from the rat brain, in a Chinese hamster cell line. [28] The authors then examined the ability of a series of aralkylguanidines to inhibit the flux of [^{14}C]-guanidinium ions.

Fluorescence-based assays are high-throughput screening techniques, which provide information content unavailable in other screening techniques due to its high sensitivity, use of homogeneous medium and ability to measure true equilibrium conditions. The application of this technology to sodium channel studies was mainly for measurement of membrane potentials with voltage-sensitive dyes and for the measurement of the concentration of particular ions with ion-selective fluorescent dyes. For example, Leong *et. al.* made use of rhodamine 6G fluorescence to calculate synaptoneurosomal membrane potential. [29] Knowing that veratridine will increase intracellular sodium concentration, Deffois *et. al.* measured this characteristic using fluorescence imaging, with the help of the sodium ion selective dye benzofuran isophthalate (SBFI). [30] The authors subsequently showed that the veratridine-induced increase in intracellular sodium concentration was inhibited by the addition of sodium channel blockers, thereby accessing their ability to block the sodium channel.

Electrophysiology is a low-throughput/high-information technique, which is able to determine the precise binding mode of active species. For example, Haeseler *et. al.* not only measured the extent of sodium channel blockade of ketamine, but also concentrated on the difference in affinity between resting and inactivated channel states. [31] Another example of high-information output by this technique was demonstrated by Grolleau *et. al.* [32] The group was able to demonstrate that oxaliplatin and its metabolite oxalate were able to reduce the inward sodium current amplitude, and more importantly, it was shown that their effects were mimicked by intracellularly applied bis-(*o*-aminophenoxy)-N, N, N', N'-tetraacetic acid (BAPTA). Since BAPTA is a chelator of calcium ions, the group was able to conclude that oxaliplatin was capable of altering the voltage-gated sodium channels through a pathway involving calcium ions.

Cell viability can be used as an assay for sodium channel blockers. For example, cell death can be caused by addition of high concentrations of veratridine. Such cell death possessed characteristics of apoptosis, which can be assessed by morphology, or by techniques such as DNA laddering on agarose gel. Ability of compounds to block sodium channels can be induced from the extent these blockers inhibit the veratridine-induced apoptosis.

2.2.2 *In Vivo* Test Systems

White *et al* summarized the various *in vivo* test systems for anticonvulsant screening.[33] The assays described were the Maximal electroshock (MES) test, subcutaneous pentylenetetrazol (s. c. Met/PTZ) test and the threshold tonic extension (TTE) test. In the MES test, an alternating current was delivered to the mouse (or rat) via electrodes, either through connections to the cornea or ear. The shock was usually given at a fixed time after drug administration. Following stimulation, the animal was observed for the entire duration of the seizure. The anticonvulsant activity of the test substance was graded upon the limb tonic extensor component.

In the s. c. Met/PTZ (subcutaneous metrazol/pentylenetetrazol) test, a convulsive dose of pentylenetetrazol was injected subcutaneously. The animals were placed in isolation cages and observed for presence or absence of an episode of clonic spasms. Absence of a clonic seizure suggested that the test substance have the ability to raise the seizure threshold. The two above-mentioned tests are able to predict the type of seizures that can be controlled. It is generally agreed that substances that obtund only the tonic extension of maximal seizures (in MES test) may be clinically useful in generalized tonic-clonic seizures, while substances which only elevate

minimal seizure threshold (in s. c. Met test) may be useful in generalized absence seizures.

The TTE test is a non-selective, electroconvulsive seizure model that identifies substances that block seizures induced in the MES and/or s. c. Met tests. However, this test will also identify a small number of compounds that are inactive in the MES and s. c. Met tests. The TTE test is similar to the MES test except that the TTE test uses sufficient current to elicit threshold limb tonic extension, while the MES test uses a supra maximal current (four to five times threshold). The results from these identification tests can provide important preliminary information pertaining to oral bioavailability, species variation, duration of action, toxicity, efficacy, and overall potential of novel anticonvulsant substances.

Antinociceptive effects of compounds can be investigated using a plethora of methods, with the hot plate and tail-flick tests being the most common. In the hot plate test, mice were put on a hot plate that was heated, usually to 55° C. Response measured includes front and hind paw licking or jumping. For the tail-flick test, only the tail of a rat was immersed in either hot or cold water, and the time taken for the rat to flick its tail was the end-point. A commonly used visceral pain model test is the writhing syndrome test, where compounds to be tested can be injected into various sites for comparison. [34] The number of writhes was then noted over 10 minutes periods for about 1 hour.

Neuroprotection is usually measured by the reduction in cell damage due to cerebral ischemia as compared to a negative control. The most common method used was the middle cerebral artery occlusion (MCAO) technique that can be performed in rats or gerbils. Surgery was subsequently performed and the cerebral artery was

occluded for a short period of about 5 minutes. The animal was sacrificed several days later, and the area of infarct was examined through histological preparations.

2.2.3 Sodium Channel Blockers as Anticonvulsants

Epilepsy is a leading neurological disorder in man, characterized by recurrent seizures that have a sudden onset. Idiopathic epilepsies, which accounted for up to 40% of all epilepsies, were mainly caused by genetic factors. [35] Recently, researchers found a link between mutation of the sodium channel and abnormal neuronal excitability that resulted in epilepsy. It was found that a clinical subset termed generalized epilepsy with febrile seizures plus ($GEFS^+$) was associated with a mutation of the sodium channel β1 subunit SCN1B gene. [36] Similarly, $GEFS^+$ type 2 was associated with a mutation of the α subunit SCN1A gene. [37]

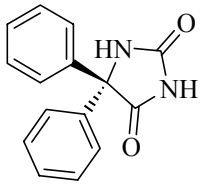

Phenytoin

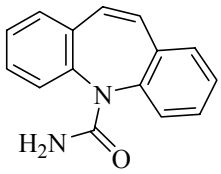

Carbamazepine

Phenytoin and carbamazepine were established as anticonvulsants long before their mechanism of action was established. Phenytoin is most certainly the reference standard of anticonvulsants that act via sodium channel blockade. Many analogues of phenytoin were synthesized in order to achieve better activity and selectivity. The focuses of these syntheses were usually the hydantoin moiety or its bioisostere. For example, Brouilette *et al* designed a series of hydantoins containing conformationally constrained 5-phenyl substitutions, phenyl-substituted bicyclic 2,4-oxazolidinediones

and bicyclic hydantoins with a bridgehead nitrogen. [38-40] Scholl *et al* explored the lipophilicity of a representative number of hydantoins derivatives and used the results, combined with structure similarities, to propose a pharmacological model for binding the hydantoins derivatives along the sodium channel. [41] Solubility of phenytoin was improved by formulating the salt form, fosphenytoin (Cerebyx). [42] Brown *et al* synthesized a series of compounds with the hydantoin moiety and then used comparative molecular field analysis (CoMFA) to build a model of the binding site of this structure. [43] Further development of carbamazepine resulted in several derivatives, such as oxcarbazepine and SGB-017 (ADCI). Benes *et al* found the enantiomeric acetates of carbamazepine at the 10-position were more potent than both carbamazepine and oxcarbazepine. [44] SGB-017 produced its anticonvulsant activity by blocking both sodium- and NMDA-receptor. [45]

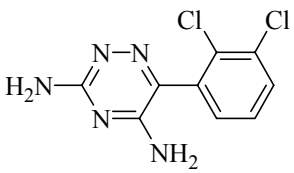

Lamotrigine

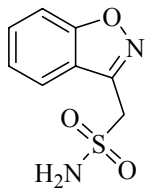

Zonisamide

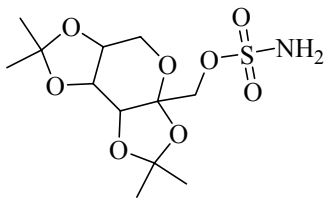

Topiramate

More recently, lamotrigine, zonisamide and topiramate were marketed as Lamictal, Excegran and Topamax respectively. Lang *et al* showed that lamotrigine inhibited sodium channels in a manner that was similar to that produced by phenytoin and carbamazepine. [46] Another study reported that lamotrigine caused concentration dependent inhibition of 5-hydroxytryptamine (5-HT) uptake in both human platelets and rat brain synaptosomes, probably reflecting an affinity for biogenic amine transporters. [47] Zonisamide was demonstrated to block voltage-sensitive sodium channels and also consistently prevented the tonic extensor component of maximal

electroshock seizure (MES) in animal models. [48] However, zonisamide was also shown to be a weak carbonic anhydrase inhibitor, and also a T-type calcium channel blocker. Taverna *et al* assessed the action of topiramate on sodium channels using whole-cell patch-clamp recordings. [49] The study reported that there was a slight but significant inhibition of the persistent fraction of the sodium current, obtained with the relatively low topiramate concentration. It was concluded that topiramate may contribute to its anticonvulsant effectiveness by modulating the near-threshold depolarizing events that were sustained by this small current fraction. McLean *et al* determined the ability of topiramate to limit depolarization-induced spontaneous repetitive firing in cultured mouse spinal neurons and compared the results with those of phenytoin and lamotrigine. [50] The study did not support the concept that sodium channel blockade is the primary mechanism responsible for the anticonvulsant activity of topiramate. Topiramate had been shown to modulate sodium channels, potentiate γ-aminobutyric acid (GABA) inhibition, block excitatory neurotransmission, and possibly modulate voltage- and receptor –gated calcium ion channels. [51]

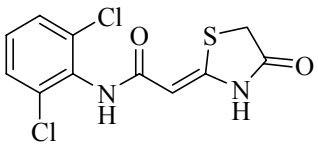

Ralitoline

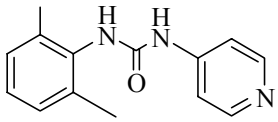

CI-953

Ralitoline (CI-446) and CI-953 were structurally similar and their profile of anticonvulsant activity was similar to those of phenytoin and carbamazepine. [52] These two compounds inhibited sustained repetitive action potentials from neuronal membrane depolarization and also inhibited the binding of BTX to rat synaptosomal membranes. U-54494A had potent and long-acting anticonvulsant activity without

antinociceptive or sedative effects on intact animals. [53] Two major metabolites of U-554494A, U-83892E and U-83894A, were synthesized and tested for anticonvulsant activity. The two compounds displayed anticonvulsant activity against electrical shock in experimental animals and blocked voltage-gated sodium channel in the resting stage.

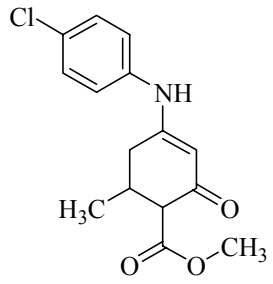

Methyl 4-[(p-chlorophenyl)amino]-
6-methyl-2-oxo-cyclohex-3-en-1-oate

Edafiogho *et al* synthesized a series of enaminones, with the most potent compound being methyl 4-[(p-chlorophenyl)amino]-6-methyl-2-oxo-cyclohex-3-ene-1-oate. [54] Free-Wilson analysis was applied for structure-activity correlation. Scott *et al* further developed the aniline-substituted enaminones that has 4'-, 3'- and 2'-substitution and polysubstitution. [55] *In vivo* assays discovered that *para*-substituted compounds generally had good anticonvulsant activity, while the meta-substituted compounds were largely inactive, and the *ortho*-substituted compounds had no clear relationship with biological activity.

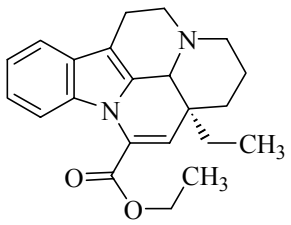

Vinpocetine

Vincanol and vinpocetine are derivatives of vincamine, the major alkaloid of *Vinca minor*. These compounds possess vasodilator/nootropic activity. [56] Vincamine

and vincanol also exhibit neuroprotective properties, like that of vinpocetine. Since vinpocetine was known to inhibit voltage-gated sodium channels, the compounds were tested for their effects on sodium channel. Vincamine, vincanol and vinpocetine reduced [^{3}H]-batrachotoxin binding with IC_{50} values of 1.9, 10.7 and 0.34 μM, and have MES ED_{50} values of 15.4, 14.6 and 27mg/kg respectively. It was observed that vinpocetine, according to results from BTX assays, was the most potent sodium channel blocker reported in the literature.

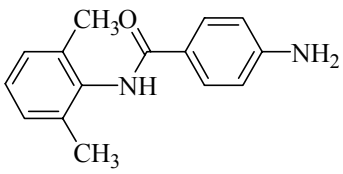

Ameltolide

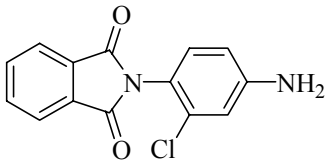

N-(2-Chloro-4-amino-phenyl)phthalimide

Clark *et al* developed amides having a primary amine in the 4-position of the benzamide moiety and an aromatic N-substitution of the 4-aminobenzamide pharmacophore, which resulted in the emersion of ameltolide; a potent anticonvulsant with structural similarities to lidocaine. [57] Vamecq *et al* synthesized 15 compounds related to ameltolide and tested them in both BTX and MES assays. [58] The correlation between the two assays suggested that the anticonvulsant properties of most compounds tested could be a direct result of their interaction with the neuronal voltage-dependent sodium channel. The 4-aminobenzamide unit seem to be essential and was compared with thalidomide to develop 4-amino-N-(2,6-dimethylphenyl)-phthalimide and eventually the substituted N-phenyl derivatives of the phthalimide pharmacophore. [59] Vamecq *et al* synthesized a series of compounds based on the phthalimide pharmacophore and found the 2-chloro-4-amino derivative to be the most potent compound of this series. It showed blockade of the neuronal voltage-dependent

sodium channels, potentiation of GABA-evoked current responses, and inhibition of kainite-evoked response. Therefore the 2-chloro-4-amino derivative may be of interest in a wide range of seizure models and neurological disorders due to its interaction with multiple ion channels.

Unverferth *et al* observed that there were numerous derivatives stemming from 5-, 6-, and 7-membered heterocycles, and that only few representatives with remarkable activity come from the pyrrole group. [60] Based on these observations, the group developed a series of 3-aminopyrroles and tested them for anticonvulsant activity using a variety of test models, including the MES test. The essential structural features, which could be responsible for an interaction with an active site of the voltage-dependent sodium channel, were established within a suggested pharmacophoric model.

Structure-activity relationships of a series of N, N'-diarylguanidines were used to develop several simpler diphenylguanidines with improved *in vitro* and *in vivo* activity. [61] Results indicated that N, N'-diphenylguanidines substituted with flexible and moderate size lipophilic groups were preferred over aryl and/or hydrophilic groups for biological activity. Compounds of this series showed only weak N-methyl-*D*-aspartate (NMDA) ion-channel blocking activity indicating that the anticonvulsant activity of these compounds are more likely to be via sodium channel blockade.

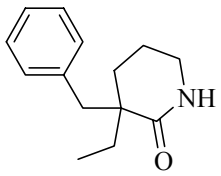

3-BEP

3-Benzyl-3-ethyl-2-piperidinone (3-BEP) belongs to a family of compounds that potentiate GABA mediated chloride currents. [62] This family of compounds,

including 3-BEP, had been shown to exhibit potent *in vivo* anticonvulsant activity in mice. The study reported that 3-BEP also modulates sodium channels, and thus may prevent seizures by both enhancing inhibition and diminishing neuronal excitability.

Antagonists of α-amino-3-hydroxy-5-methyl-4-isoxazolepropionic acid (AMPA) receptors and voltage-dependent sodium channels blockers both exhibited anticonvulsive and neuroprotective activity. BIIR 561 CL was identified in a screening campaign targeted to the identification of new structures active at AMPA receptors and voltage-gated sodium channels. [63] Weiser *et al* provided evidence that BIIR 561 CL was able to inhibit glutamate receptors of the AMPA subtype, as well as voltage-gated sodium channels.

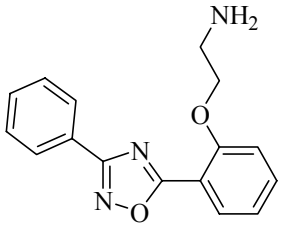

BIIR561CL

Diphenhydramine and many other H_1 histamine receptor antagonists, such as chlorpheniramine, have long been known for their local anaesthetic effect. However, the underlying mechanism of such an effect was unknown. Kuo *et al* explored the inhibition of the neuronal sodium current by diphenhydramine and other diphenyl compounds and found that diphenhydramine bound to the inactivated sodium channel with a dissociation constant of 10μM. [64] The study suggested that the two phenyl groups were the key ligands interacting with the channel.

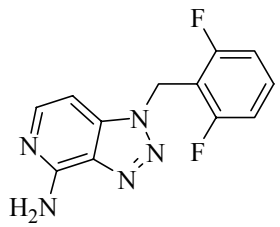

BW534U87

The pyridinotriazole BW534U87 had good activity in a variety of assays against seizures. [65] Preclinical evidence suggested that it would be free from side effects such as emesis and nausea, which had earlier cause the failure of the clinical development of its precessor, BW A78U. In a serendipitous approach to develop structurally novel central nervous system drugs, a series of two hundred 3-aminopyrrols were synthesized and tested. [66] AWD 140-190 was selected from this series based on its strong anticonvulsant activity and absence of side effects in experimental models. It was concluded, via the patch-clamp technique, that AWD 140-190 is a sodium channel blocker. PNU-151774E is a novel antiepileptic compound with potency comparable or superior to that of most classic anticonvulsant drugs, such as phenytoin and carbamazepine, in electrically and chemically induced seizure models. [67] PNU-151774E exerts its anticonvulsant activity, at least in part, through inhibition of sodium and calcium channels, stabilization neuronal membrane excitability and inhibition of transmitter release. Snell *et al* developed a novel series of N-substituted 4-ureido-5, 7-dichloro-quinolines (DUCKs) by combining parts of the structures of phenytoin, carbamazepine and dichlorokynurenate. [67] These compounds had combined actions: blockade of voltage-sensitive sodium channels and selective competitive antagonism at strychnine-insensitive glycine recognition site of NMDA receptor.

2.2.4 Sodium Channel Blockers as Neuroprotective Agents

Stroke had been reported to be the third leading cause of death in industrialized countries and the major cause of serious long-term disability. [69] A transient or permanent obstruction of blood flow in a major cerebral artery, usually the middle cerebral artery, will cause ischemic stroke. A reduction in blood flow will cause failure of ionic, metabolic and electronic homeostasis and irreversible death of neurons. It was reported that the effects occurred within minutes in the immediate area of the occlusion of blood flow, or over hours or days in adjacent areas that were supported by anastomoses with surrounding collateral arteries. [70, 71]

The development of a model of the ischemic cascade had provided much insight into the complex sequence of the pathophysiological changes. [72] The neurochemical sequelae following cerebral ischemia was reported to involve excess release of excitatory amino acids, particularly glutamate, disruption of ionic homeostasis due to sodium and calcium influx and generation of toxic free radicals, ultimately leading to cell death by necrosis and apoptosis. The progression of such events had been shown to depend on the extent and duration of the arterial occlusion and differed in the immediate and adjacent regions of the occlusion. [70, 73]

TTX, and various sodium channel blockers had been shown to have neuroprotective effects in various *in vitro* and *in vivo* studies. [74] The possible mechanisms of sodium channel blockers as neuroprotective agents were summarized in a review paper. [75] It was postulated that since the excitability of hippocampal and cortical neurons was inherently reduced during hypoxia by the inhibition of transient sodium ion current, it was possible that there was an endogenous neuronal mechanism, which decreased excitability and sodium ion influx via the sodium channel. Thus treatment with sodium channel blockers may further reduce the excitability of neurons

and protect neurons from hypoxia-induced injury. Another mechanism of action revolved around the idea that the non-inactivating sodium ion current (persistent sodium ion current that resists inactivation during depolarization) was involved in the entry of sodium ion during acute hypoxia. It was discovered that the non-inactivating sodium ion current was sensitive to TTX and other sodium channel blockers. During hypoxia, high intracellular concentration of sodium ions will increase calcium ion influx through the Na^+-Ca^+ exchangers. Since an increase in intracellular concentration of calcium ions constitutes a major cause of hypoxia-induced neuronal damage, sodium channel blockers may contribute to neuroprotection by reducing the intracellular concentration of calcium ions.

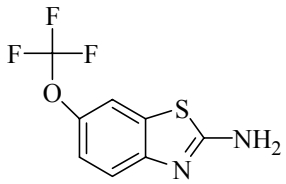

Riluzole

In vivo tests of rodent models showed that riluzole significantly reduced the extent of infarct in both global and focal cerebral ischemia. [76] These effects were attributed to the inhibition of sodium channel activity, which in turn inhibited glutamate release. Studies on cloned rat brain neuronal sodium channels verified that riluzole was able to bind selectively to inactivated sodium channels and not the open channel, which suggested that the stabilization of the inactivation state contributed to riluzole's neuroprotective properties. [77] Results had shown that riluzole, in addition to its ability to block sodium channels, was able to block glutamate release, reduce nonvesicular (calcium-independent) transmitter release, block potassium channels, inhibit certain NMDA-dependent responses and reduce neurotransmitter release in a

pertussis toxin-sensitive manner. [24] Cell-viability assays that utilized veratridine as the noxious substance showed that riluzole had better neuroprotective ability than phenytoin or lamotrigine. [78] Riluzole had been used clinically as a neuroprotective agent in cases of amyotrophic lateral sclerosis.

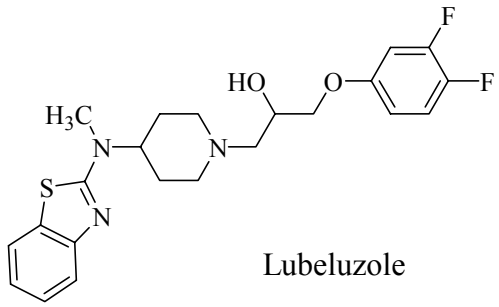

Lubeluzole

Lubeluzole had been shown to be effective in animal models of stroke in rats. [79,80] *In vitro* studies conducted on lubeluzole revealed that it inhibited nitric oxide synthesis, blocked sodium channels, and inhibited glutamate release, and these pharmacological actions were hypothesized to contributed to its neuroprotective effects. [81-83] Unfortunately, lubeluzole also blocked low-voltage and high-voltage calcium channel currents from both the extracellular and intracellular side, which is the cause of its side effects. In a review of all the randomized unconfounded trials comparing intravenous lubeluzole with placebo or open control in patients with clinical acute stroke, it was concluded that lubeluzole was not associated with a significant reduction of death or dependency at the end of scheduled follow-up period but seem to be associated with a significant increase of heart-conduction disorders (Q-T prolonged > 450msec). [84]

A few compounds were already in clinical trials for neuroprotection. Sipatrigine, or BW619C89, is a substituted pyrimidine derived from lamotrigine. Rodent models of global and focal ischemia showed that sipatrigine was effective as a neuroprotective agent by reducing cortical infarct. [85] In electrophysiological studies, sipatrigine inhibited neuronal sodium channels and calcium channels (L, N and P/Q

types), with similar potencies (IC_{50} of 5-16mM). Ramacemide is a non-competitive, low-affinity NMDA receptor antagonist. Ramacemide and its active metabolite also interact with sodium channels. These two pharmacological actions contribute to their neuroprotective effects. [86] Lifarizine, a piperizine, had been shown to be a sodium channel blocker, an inhibitor of intracellular calcium ion concentration rises and a neuroprotective agent in animal models. [87-90] Its analogues, lomerizine and flunarizine also shown promise as neuroprotective agents. [91,92] BIII 890 Cl, a benzomorphan derivative, had an IC_{50} value of 49 nM in the BTX assay and were shown to protect brain tissue from ischemia. [93]

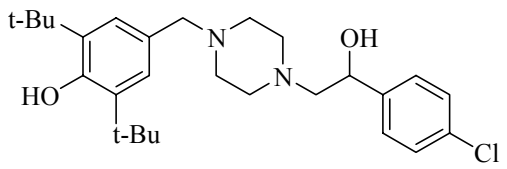

AM-36

In recent years, researchers have recognized the need to provide neuroprotection in a multi-prong approach. It was found that compounds that have multiple mechanism of actions, such as zonisamide, topiramate, T-477 and AM-36, more effectively prevented ischemic injury. [64, 94-96] For example, AM-36 has been shown to inhibit binding to the polyamine site of glutamate receptors, blocked neuronal sodium channels and had potent anti-oxidant activity.

2.2.5 Sodium Channel Blockers as Antinociceptive Agents

Neuropathic pain was reported to be due to hyperexcitability in primary sensory neurons following injury. Waxman *et al* detailed the molecular pathophysiology of pain with regards to sodium channels in a review article. [97] It had

been shown that in acute injury, activation of pre-existing sodium channels played an important role in the generation of the transient burst of impulses in primary sensory neurons. Subsequently, changes in gene expression resulted in down-regulation of some sodium channel subtypes, while some previously unexpressed sodium channel subtypes were up-regulated. There was also activity–related regulation of sodium channel expression in uninjured central neurons. In particular, there was a high proportion of TTX-insensitive (TTXi) sodium channels in hyperexcitable neurons.

Phenytoin and carbamazepine were tested for differential inhibition of sodium currents in small cells from adult rat dorsal root ganglia using the patch-clamp technique. [98] The results showed that both fast TTX-sensitive and slow TTX-resistant currents were inhibited by 10-100 mM of the drugs. Another study investigated the responses of inflamed and non-inflamed neurons to noxious substances. [99] It was showed that carbamazepine was able to significantly reduce the responses of neurons which were under inflammatory conditions, but not in non-inflamed conditions. This observation led to the conclusion that there were changes to the type, or proportion of sodium channels underlying the transmission of noxious messages. Carbamazepine and phenytoin were the first anticonvulsants to be used in controlled clinical trials of neuropathic pain and showed abilities to relieve painful diabetic neuropathy and paroxysmal attacks in trigeminal neuralgia. [100] The amide functional group was often found in sodium channel blockers, such as in phenytoin and carbamazepine. Therefore it was not surprising to find substituted 2-benzylamino-2-phenylacetamides, substituted 2-aminoacetamides and aminocycloalkyl cinnamide compounds being patented as analgesic that act via sodium channel blockade. [101-103]

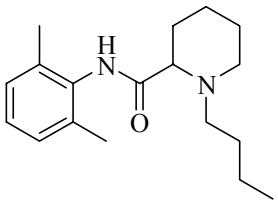

Bupivacaine

Based on the hypothesis that a selective blockade of the relay of messages by C-fibers into the spinal cord will reduce nociceptive transmission, the effects of bupivacaine and lamotrigine on these fibers were investigated. [104] The results showed that although both compounds were sodium channel blockers, only bupivacaine reduced the C-fibers-evoked responses while lamotrigine had a tendency to facilitate the responses. Thus it was concluded that lamotrigine may not be an antinociceptive. However, in a study of short- and long-term neuropathic models of hyperalgesia in rats done by Klamt *et. al*., intrathecally administered lamotrigine produced a spinal, dose-dependent, and long-lasting (24-48h) anti-hyperalgesic effect. [105] Lamotrigine was demonstrated to be effective in trigeminal neuralgia, painful peripheral neuropathy, and post-stroke pain in a controlled clinical trial. [100] Lamotrigine was subsequently used as a lead compound to develop GW4030W92. [106-108]

Plant extracts from the *Aconitum* species were used in traditional Chinese medication as anti-inflammatory and antinociceptive agents, and it was known that the active ingredients were aconitine and its derivatives. [109] In order to elucidate the mode of action of aconitine and its derivatives, a series of 10 aconitine-like derivatives were investigated. The first group of compounds, which consisted of aconitine, 3-acetylaconitine and hypaconitine had high affinity for the neuronal sodium channels (K_i of about 1.2mM) and good antinociceptive effects (ED_{50} of approximately 0.06 mg/kg). The second group of compounds, only consisting of lappaconitine, had lower affinity for the sodium channel (K_i of 11.5mM), and lesser antinociceptive effect (ED_{50} of approximately 2.8 mg/kg). The third group of compounds did not have any

significant pharmacological effects. A subsequent review paper characterized the aconitum alkaloids into three groups. [110] The first group of alkaloids activated voltage-gated sodium channels at resting potential and inhibited noradrenaline uptake, and had antinociceptive properties due to the eventual inexcitability of the sodium channel. The second group consisted of sodium channel blockers which are monoesters. These compounds were less toxic than the first group, and had strong antinociceptive, antiarrhythmic and antiepileptiform properties. The last group of compounds lacked an ester side chain and were only reported to have antiarrhythmic activity.

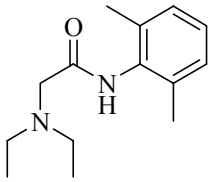

Lidocaine

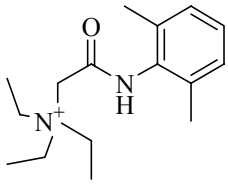

QX-314

Lidocaine, a well-known local anaesthetic, can be positively-charged in physiological conditions. Therefore QX-314, one of its positively-charged derivatives, was investigated in tandem with lidocaine in animal models of neuropathic pain.[111] Intravenously administered lidocaine inhibited ectopic nerve activity at the dorsal root ganglia, dorsal horn neurons and neromas (fine bundles of microfilaments) teased from the sciatic nerves in anesthetized and paralyzed rats. QX-314 induced dose-dependent inhibition of ectopic nerve activity at the dorsal root ganglia and neromas, but only a small inhibition of ectopic nerve activity at the dorsal horn neurons. The data suggested that intravenously administered QX-314 was able to acutely block sodium channels that contributed to the generation of ectopic nerve activity. Mexiletine, an oral dosage form of lidocaine, was further developed into N-[2-(2,6-dimethylphenoxy-

1-methylethyl)]ethylamine, which exhibited antinociceptive effect against mechanical allodynia. [112] Ketamine, a general anaesthetic, was tested for its ability to block TTX-sensitive and TTX-resistant sodium channels that were expressed in dorsal root ganglion neurons, using the patch-clamp technique. The results showed that ketamine was able to block both types of sodium channels, which suggested that high concentrations of ketamine might produce local anaesthetic action via this mechanism.

The extensive literature review showed that sodium channel blockers are chemically diverse, with the hydantoin moiety being the most prominent. Other chemical classes include amides, benzamide, and enaminones. Natural products, such as alkaloids from *Vinca minor* and the *Aconitum* species, were also used to develop sodium channel blockers. With so many different chemical classes that were tested for sodium channel blockade activity, the experimental data could be exploited to rationally design *de novo* compounds. One plausible approach to achieving this aim would be to use computer modelling methods, such as the search of a common pharmacophore, or modelling of the proposed receptor site.

3. RATIONALE AND OBJECTIVES

3.1 The Need for New Sodium Channel Blockers

The sodium channels play an important role in coordinating higher bodily functions, such as locomotive and cognitive processes, by transmitting electrical impulses rapidly throughout cells and cell networks. Excessive sodium channel activity may lead to disorders such as epilepsy, neurodegeneration, and extreme pain. Neuronal voltage-gated sodium channels blockers are therefore potential anticonvulsants, neuroprotectants and analgesics. Despite the large number of therapeutically useful sodium channel blockers, there are several reasons that justified the need for new therapeutic agents. It has been reported that most seizures can be treated to some extent, but with the existing anticonvulsants, either in monotherapy or in combination, complete or satisfactory seizure control can only be achieved in roughly 30% of all patients. [113] Furthermore, it is common to see manifestation of side effects despite the incomplete control of seizures. Thus there is a need to develop new anticonvulsants with higher therapeutic indexes and lesser side effects. In the field of pain management, there is a need for long-acting analgesic drugs because of the aging populations in the world, which will amplify the use of analgesics for treatment of neuropathic pain, rheumatoid arthritis, and cancer pain. [114] Such long-acting analgesic can also be used for post-operative pain, in place of morphine-like analgesics, or as pre-emptive analgesics. Treatment of stroke has been reported to be inefficient, as it is found that the neurochemical sequelae following cerebral ischemia are complex, and a single drug treatment is unlikely to be beneficial in its treatment. [69] Thus it is proposed to incorporate multiple neuroprotective mechanisms within one structure, such as inhibition of glutamate and sodium channel receptor, anti-oxidant activity and

inhibition of NMDA receptors. Therefore, the demand is high for effective and therapeutically distinct sodium channel blockers.

3.2 Previous Studies on Sodium Channel Blockers

A lot of information pertaining to the structure, function, and mechanism of action of the neuronal sodium channel receptors are available. However, the most prescribed sodium channel blockers are still phenytoin, carbamazepine and lamotrigine. Based on the vast amount of information that has been gathered over the years, new sodium channel blockers can be designed. Such information should be properly organized into forms which can facilitate novel drug design. The information gathered from the literature, clearly showed that there were several common structural moieties which were present in most sodium channel blockers, such as the amine and amide functional groups and aromatic rings. CADD is an effective tool for lowering the cost of drug discovery, both in terms of time and monetary expenses. It can be utilized to collate and process the data, into information that can be exploited for designing new compounds with potential sodium channel blocking activity. Ideally, these compounds will evolve into clinically useful therapeutic agents.

There have been several attempts to study the SARs of sodium channel blockers, such as the studies done on phenytoin, enaminones, ameltolides and their analogues. A CoMFA study on hydantoins carried out by Brown *et. al.,* suggested that features that enhanced the binding of hydantoins to the sodium channel include the orientation of the phenyl ring at the position C5 and a C5-alkyl chain of suitable length.[43] The CoMFA model was then used to design a structurally novel α-hydroxy-α-phenylamide, and the results showed that the actual and predicted biological activity of the compound was identical. From the results, it was concluded that the intact

hydantoin ring was not necessary for efficient binding to the sodium channels. However, since the compounds used to develop the CoMFA model were all hydantoins, the model had limited ability to predict the biological activity of compounds from other chemical classes. Although the α-hydroxy-α-phenylamides were structurally novel, they were actually analogues of the hydantoin moiety.

Unverferth *et. al*. summarized the previous attempts to explore the pharmacophoric model of different anticonvulsant classes , e.g., benzodiazepines, barbiturates, triazolines, enaminones and hydantoins, and also for structurally different compounds.[60] The group concluded that the various postulated pharmacophoric models showed no uniform picture. The previous studies were only concerned with pharmacophoric models for a single class of sodium channel blockers such as hydantoins. Since the compounds used had low structural diversity, the derived model can only be related to compounds in that particular class, and cannot be extended to other chemical classes acting at the sodium channel receptor. In view of the deficiencies in the pharmacophoric models available at that time, Unverferth *et. al*. used five well-known and structurally diverse sodium channel blockers with anticonvulsant activity, namely carbamazepine, phenytoin, lamotrigine, zonisamide and rufinamide to build a pharmacophoric model. The pharmacophoric model derived consisted of an electron donor, an aryl ring and a hydrogen bond acceptor/donor unit (HAD). However, the study did not choose the compounds based on their ability to block the neuronal sodium channel, but instead chose the compounds based on *in vivo* studies. *In vivo* studies were unable to estimate the binding affinity of the compounds to the sodium channel as it was confounded by pharmacokinetic parameters. Data on binding affinity of the compounds to the sodium channel receptor was necessary to estimate the ability of each compound to fit the receptor. When a set of compounds

with low binding affinities was used to create a pharmacophore model, the model developed would differ from the actual requirements needed to bind to the receptor-binding site. Carbamazepine and lamotrigine are known to have low binding affinities for the sodium channel according to BTX radio-ligand binding assays. A possible limitation of this study is that without binding affinity data, it was difficult to validate the consistency of the model. Binding data reflect how well a compound binds to the receptor, and should be correlated to their abilities to fit the proposed model. A good model should have a good correlation between these two properties. Unverferth *et. al.* validated their model using vinpocetine, remacemide hydrochloride, dezinamide and compounds that they synthesized. The authors concluded that only the hydrogen bond donor part of the HAD unit, together with the two other essential structure elements R and D may be sufficient for activity as blocker of the voltage-dependent sodium channel. He also concluded that compounds having R and D, and only a hydrogen bond acceptor were inactive.

Tasso *et. al.* made use of similarity analysis to generate a pharmacophoric model for antiepileptic drugs that act via sodium channel blockade. [115] The compounds used included 15 antiepileptic drugs that were active against the MES test and able to block the neuronal sodium channels. An inactive compound was also utilized to help define the structural factors that were important for the activity. However, the choice of the training set of compounds and the validation of the pharmacophoric model was not based on *in vitro* biological activity. The proposed pharmacophoric model consists of a polar group comprising two negative atoms and one positive atom, and a hydrophobic group that should be no smaller than three atoms. It must be emphasized that the polar group stated in the model represented local density charges restricted to the atoms, and does not refer to formal charges on atoms.

3.3 Hypotheses and Objectives

3.3.1 Hypotheses

Literature review shows that many compounds from diverse chemical classes bind to the neuronal sodium channels. In order for these compounds to bind to the sodium channel, they must have certain requisite pharmacophoric elements. Thus the current study hypothesizes is that all compounds that exhibit blockade activity against the neuronal (type II) sodium channel, as characterized by the BTX assay, share a common pharmacophore. In addition, it is hypothesized that the pharmacophore is able to discern good blockers from weaker blockers. As such, compounds that have the requisite pharmacophoric elements and fit well to the pharmacophore should have good binding affinity to the sodium channels in the BTX assay, and *vice versa* for compounds which do not possess the requisite pharmacophoric elements or do not fit well to the pharmacophore.

3.3.2 Objectives

It is proposed that the hypotheses are to be tested by setting up experiments that will:

- exploit existing information from the literature and use the active analogue approach to derive a pharmacophoric model for sodium channel blockers.
- validate the pharmacophoric model using a larger population of blockers of the sodium channels that have a variety of pharmacological activities.
- demonstrate that the pharmacophoric model can be used to discern good blockers from weaker blockers and therefore be recommended for use in a screening process for the identification of potential sodium channel blockers.

- use the model to identify potential sodium channel blockers and to optimise the blockade activity of the new compounds.
- investigate the pharmacological actions of the new compounds through *in vivo* experiments.

4. A NEW PHARMACOPHORIC MODEL FOR NEURONAL (TYPE II) SODIUM CHANNEL BLOCKERS.

4.1 Choice of a CADD Strategy

CADD is an effective tool for lowering the cost of drug discovery, both in terms of time and monetary expenses. In order to utilize this tool effectively, there is a need to fully understand the field to which it is to be applied. Literature search has shown that a 3D X-ray crystallographic structure of the sodium channel receptor is not available, due to the difficulties in the isolation of membrane-bound receptors. In view of such a circumstance, CADD strategies based on docking cannot be utilized.

Genetic algorithms (GA) is a high throughput method due to its combinatorial approach. GA has a major advantage over other combinatorial approaches due to the ability of the computer program to direct the library of compounds to be synthesized, thus it is possible to screen a lot of compounds for sodium channel blocking activity in a rational manner. Other than being used to screen for sodium channel blocking activity, GA can also be utilized in computer modelling, such as for elucidation of a pharmacophoric model, conformational analysis and QSAR studies. The major drawback of GA is the resources needed for its application. At the basic level where GA is used for computer modelling, it requires special computer modules, such as the PKUDDS. [19] When GA is utilized for screening of compounds, the cost of operations is innately high due to its combinatorial approach. Other than the basic combinatorial apparatus, the computer program needed to direct the synthesis is also expensive. Such high costs associated with this strategy have limited its use to mainly drug companies or well-funded institutions.

Extensive research had been done in the field of sodium channel blockers ever since it was discovered that phenytoin and carbamazepine work via blockade of

sodium channel receptors, thus many sodium channel blockers from different chemical classes had been reported in the literature. Such a situation is favourable for the development of a pharmacophoric model using the active analogue approach. [12] In the active analogue approach, a set of compounds with good biological activity, usually called the training set, is first chosen to define the pharmacophoric model. In order to get a good pharmacophoric model, it is important to have structural diversity in the training set. Structural diversity allows the model to map out a bigger volume in the receptor. It also helps in refining the location in the receptor that is essential for good activity and differentiating the location, if occupied, that is detrimental to activity. The second reason for structural diversity is to reduce redundancy. The inclusion of structurally similar analogues does not add new information to the solution, but instead adds time to the search for possible pharmacophoric models.

CoMFA is a 3D QSAR technique that is favoured by many researchers in computer modelling. Many articles have been published using the CoMFA approach but they are usually based on a single chemical class of compounds. This is a critical concern, as the results obtained from a single class of compounds cannot be extrapolated to compounds from other chemical classes, even if they act via the same mechanism. The only exception would be to extrapolate the results to analogues of the same class of chemicals. Some examples of CoMFA models, which were based on a single chemical class of compounds, include the CoMFA model of hydantoins by Brown *et. al*., or more recently the CoMFA and CoMSIA models of phenothiazines by Tsakovska. [43, 16] This trend can be partly attributed to the basic concept of CoMFA, where a group of compounds is aligned to optimize the overlapping of their steric and electrostatic fields. It is easier to overlap compounds of the same chemical class as there are already a ‘backbone’ and common functional groups. Comparatively, it is

difficult, if not impossible, to optimize the overlapping of sodium channel blockers from various chemical classes. It is unlikely that a good CoMFA model can be derived using the sodium channel blockers reported in the literature, as they are from different chemical classes.

Upon consideration of the various pros and cons of the CADD strategies, pharmacophoric modelling using the active analogue approach was chosen for the project. GA is a powerful strategy, but the lack of resources prevented its use. Pharmacophoric modelling was chosen over CoMFA, as diverse sodium channel blockers from numerous chemical classes would be better utilized for computer modelling.

4.2 Selection of a Training Set of Compounds

4.2.1 Characteristics of the Compounds in the Training Set

In the active analogue approach, the training set of compounds is first superimposed based on their pharmacophoric elements to derive a pharmacophoric model. As such, the choice of a training set of compounds is very important as the theoretical soundness of the pharmacophoric model depends on it. Furthermore, it determines whether the pharmacophoric model can be extrapolated to estimate biological activity of other compounds that are not studied during pharmacophoric modelling. The hypothesis of the current study is that sodium channel blockers utilize the same pharmacophoric elements to bind to the sodium channel receptor, and their binding affinities were based on the spatial relationships of these pharmacophoric elements. In order to determine whether the pharmacophoric model was theoretically sound, it was necessary to evaluate the training set of compounds from the pharmacological viewpoint.

The researcher must first be very clear about the parameters that are to be utilized for modelling. In pharmacophoric modelling, the *in silico* parameter being modelled is the binding affinity of the compound to the proposed receptor site. The binding affinity is usually represented by parameters that can be easily calculated, such as goodness of fit of the compound to the receptor or change in entropy during binding. The choice of a training set of compounds should thus be based on biological data that reflects binding affinity, and usually the compounds with the highest binding affinities should be chosen. Such a requirement is imposed because high affinity compounds tend to satisfy well all receptor-binding requirements in terms of conformation, pharmacophoric groups and inter-pharmacophoric group distances.

In vivo biological data gives information about the potency of the compound in a given clinical application, such as analgesia, but is unable to provide binding affinity data. The clinical effect measured in *in vivo* studies cannot be used to estimate binding affinity as its measurement can be confounded by pharmacokinetics of the compound. It should be noted that a pharmacophoric model does not model pharmacokinetic parameters of the compounds. For example, the researcher usually does not know the concentration of the compound at the site of action (e.g. brain) where the pharmacological effect is manifested. There are other confounding factors, such as whether the compound can cross the blood-brain-barrier to exert its pharmacological effect (e.g. anticonvulsants), active metabolites that may be present, or that the pharmacological effect may be missed because of rapid elimination. Another drawback of using *in vivo* biological data for choosing the training set of compounds is that they may have multiple mechanisms of action. For example, topiramate is an anticonvulsant that has been shown to modulate sodium channels, potentiate GABA inhibition, block excitatory neurotransmission, and possibly modulate voltage- and receptor-gated

calcium ion channels. [61] In such cases, the compound may be treated as having high binding affinity to the receptor due to its *in vivo* biological data, but the actual binding affinity to the receptor being evaluated (e.g. sodium channel receptor) is lower because the biological action is also mediated by another mechanism of action. In general, it is not suitable to choose a training set of compounds based on *in vivo* biological data, as the computer modelling data is not likely to correlate well with *in vivo* observations.

In vitro biological data, on the other hand, is preferred when selecting the training set of compounds for pharmacophoric modelling. Due to the nature of the assays, it is possible to accurately control the concentration of the compound being tested at the site of action. This is in sharp contrast with the *in vivo* assay methods which can be confounded by pharmacokinetics. Another advantage of *in vitro* biological data is that the parameter measured is usually based on the surrogate measure of one mechanism of action. For example, radio-ligand binding assays can be done using radio-ligands that are specifically displaced by sodium channel blockers. In this example, the biological data only represents the ability of the compound to bind to one receptor, namely the sodium channel receptor. The advantage of the specificity of the assay can be seen when the test compound has several mechanisms of action. For example, in the case of topiramate, the many mechanisms of action did not interfere with the measurement of the sodium channel blocking activity in the BTX assay. In summary, *in vitro* biological data is more suitable than *in vivo* biological data for selection of the training set of compounds. A good pharmacophoric model is likely to correlate well with, and may even predict, *in vitro* biological data.

The compounds in the training set should be from different chemical classes. Such a requirement allows the resultant pharmacophoric model to be extrapolated to other compounds acting at the same receptor site. As iterated above in the discussion

of the choice of CADD strategies, structural diversity in the training set of compounds will produce a pharmacophoric model which is more informative and representative. In contrast, if the training set of compounds is from a single chemical class, the conclusions gathered from the pharmacophoric model is limited to that particular chemical class and its analogues only, thus severely limiting the usefulness of the pharmacophoric model and lay to waste the immense amount of data available on sodium channel blockers.

4.2.2 *In Vitro* Method for Assessment of Biological Activity of Compounds used for Modelling and Validating the Pharmacophoric Model

When choosing an *in vitro* assay method for evaluating the training set of compounds and to eventually validate the pharmacophoric model, it is necessary to focus on the application of the pharmacophoric model. The pharmacophoric model is designed to discover more information about the receptor site, and thus aid in drug discovery of sodium channel blockers. Therefore the *in vitro* assay method chosen must be able to screen potential sodium channel blockers in a high-throughput manner. Among the *in vitro* assay methods available for sodium channel blockers, radioligand binding, radioligand flux and fluorescence based assays are considered to be high-throughput assays. The BTX assay is a radio-ligand binding assay that is frequently used by researchers to ascertain the binding affinity of sodium channel blockers to the neuronal type II sodium channel receptors. A lot of information can be obtained from the literature with regard to the binding affinity of sodium channel blockers as measured by this assay method, thus it was preferential to choose the training set of compounds using data derived from BTX assays. Therefore the BTX assay was used in the current project to assess the biological activity of sodium channel blockers used for

computational work, and also for compounds discovered by the current study to be potential sodium channel blockers. As such, only neuronal sodium channel blockers that were tested using the BTX assay were used for pharmacophoric modelling. As iterated in chapter 2, the work done by McPhee *et al* and Linford *et al* suggested that the BTX binding site shares overlapping but not identical molecular determinants with the binding site of sodium channel blockers. [25, 26] Therefore the BTX assay is suitable for comparing binding affinity of sodium channel blockers.

In order to standardize the potencies of the various sodium channel blockers for purpose of comparison, the relative blocking potential (RBP) was determined in the current study. The IC_{50} value of each selected sodium channel blocker was converted to the K_i value. The RBP was calculated as a ratio of the K_i value of phenytoin to the K_i value of the sodium channel blocker. Phenytoin was used as the reference in the calculation of RBP because it was a reference in most literatures. However in some studies, carbamazepine or veratridine were used as reference. In these situations, the relative RBP values ($RBP_{carbamazepine}$ and $RBP_{veretridine}$) of the compounds with respect to carbamazepine or veratridine were calculated. These values were then converted to RBP by correcting with a factor of 0.31 for carbamazepine, and 15.3 for veratridine. The factors used for correction are the RBP values of carbamazepine and veratridine respectively. A higher RBP value means that the test compound has higher binding affinity for the sodium channel receptor. Compounds of high RBP values were used to develop the pharmacophoric model because such compounds would tend to satisfy well all receptor-binding requirements in terms of conformation, pharmacophoric groups and inter-pharmacophoric group distances. Since BTX assay was used as a selection criterion, it would not matter if the compounds have multiple mechanisms of

action. This is because BTX assay is an objective measurement of the compounds' abilities to block sodium channels.

4.2.3 Compounds Selected as the Training Set

As stated in the preceding sections, a training set should consist of potent sodium channel blockers, and be chosen based on their binding affinity to the sodium channels in the BTX assay. It must be emphasized that the compounds were chosen from literature articles that presented data derived from a BTX assay that used synaptoneurosomes obtained from the rat brain. These preparations are known to contain high levels of neuronal (type II) sodium channels. The training set of compounds (**Figure 1**) was used to develop plausible pharmacophoric models, and they consisted of the most potent and representative members of the class of sodium channel blockers to which they belong. The five compounds in the training set were vinpocetine, **(1)** [56]; a 2-aminopropanamide analogue, **(2)** [116]; dextromethorphan, **(3)** [116]; BIIR561C1, **(4)** [63]; and lubeluzole, **(5)** [117]. It should be noted that the free acid of vinpocetine was used for computer modelling so as to reflect esterase activity in the physiological environment of the human body.

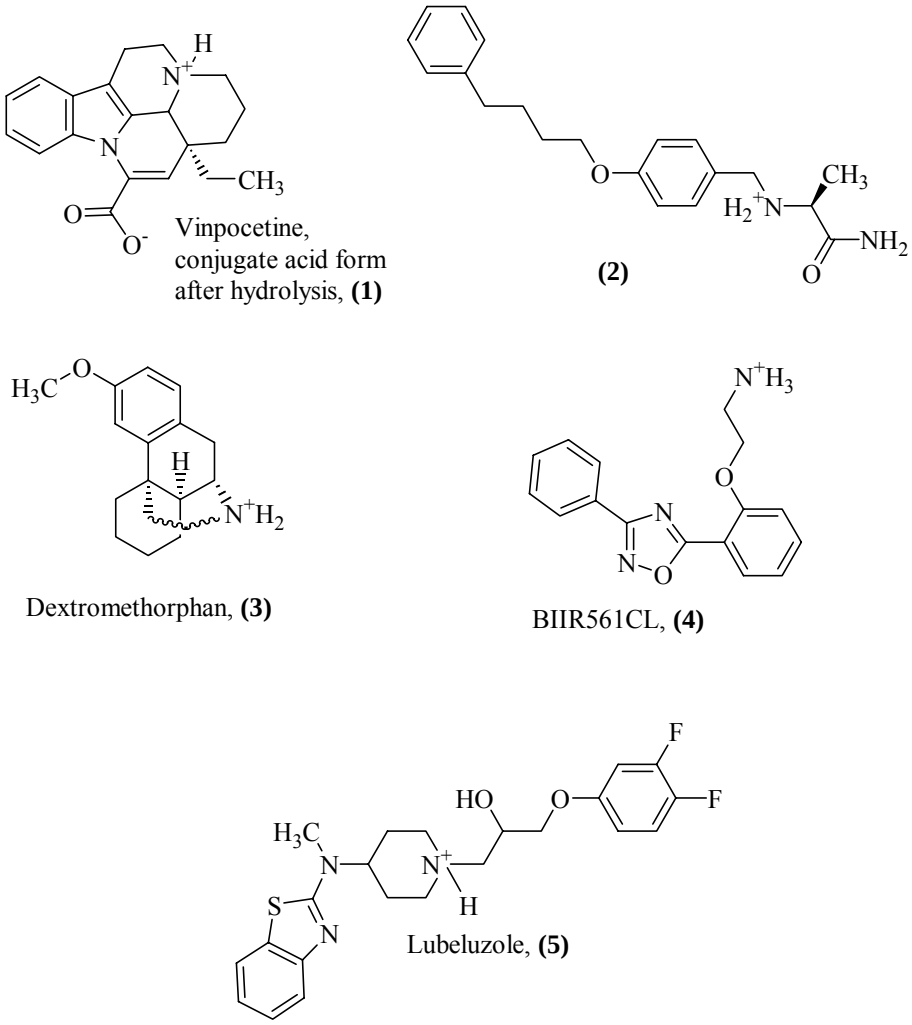

Figure 1. Training set of compounds.

4.3 A Search for Pharmacophoric Models

4.3.1 Methodology of Conformational Analysis

The great majority of drug molecules are able to assume a large number of conformations, through the rotations about bonds and/or inversions about atomic centres. Since the conformation of the drug molecule will dictate the spatial relationships between its pharmacophoric elements, it is necessary to find the particular conformation of each drug which has optimal complementarities to the receptor binding site during the search for a pharmacophoric model. It is well accepted

that any molecule will be in its GMEC most of the time as this conformation is more energetically favourable. Due to limitations in computation resources, GMECs instead of multiple conformations were used for the derivation of pharmacophoric models.

The choice of a conformational search methodology depends heavily on the drug molecules being investigated. As discussed in the first chapter, small molecules are best analysed using grid searches which can probably give the most complete number of conformations, even though it is more time consuming. On the other hand, molecular dynamics and Monte Carlo techniques are more suited for large molecules such as proteins. Most of the neuronal sodium channel blockers in the literature were small molecules, therefore the grid search approach was used.

Molecular mechanics or quantum mechanic can be used in the conformational analyses of small molecules. It was a matter of software availability that molecular mechanics was chosen for the current project. Since most of the compounds had either an amide or amine functional group, MMFF94s by Tripos was used for all the conformational analysis, because MMFF94s had its torsional and out-of-plane parameters modified to provide nearly planar structure for amide and unsaturated amine trigonal nitrogen.

4.3.2 DISCO

A systematic conformational search was performed for each compound in the training set in order to identify their low-energy conformations. The low energy conformers were then used in Distance Comparison (DISCO), a molecular superimposition program, to derive 3D-pharmacophores models. When a group of compounds with diverse chemical structures is used in DISCO, there is a tendency to

get multiple pharmacophoric models. Each of these models should then be tested and validated to identify the most credible one.

During superimposition of the compounds in DISCO, a 'template' compound was needed, so that the rest of the compounds in the training set could be superimposed onto it. The compound that could bind to the sodium channel receptors most effectively was used as the 'template' as it should be most capable in satisfying all receptor-binding requirements in terms of conformation, pharmacophoric groups and inter-pharmacophoric distances. Judging from BTX studies, vinpocetine was chosen as the 'template'. Pharmacophoric models could differ in tolerance. When compounds in the training set were fitted to vinpocetine, they were superimposed so that the distances between their respective pharmacophoric elements to the corresponding pharmacophoric elements of vinpocetine were minimal. Therefore tolerance would measure how large these distances were. In other words, a model with low tolerance would mean that the compounds in the training set had their pharmacophoric elements overlapped well with those of vinpocetine.

4.4 Validation of Pharmacophoric Models

The ultimate use of a pharmacophoric model is to design new compounds which have high binding affinity for the investigated receptor. The model should be validated with a set of compounds, from the literature, having a range of high to low binding affinities in biological assays, before being used to design new compounds. Conversely, if a pharmacophoric model, which was inaccurate or even invalid, was used indiscriminately for drug design, a lot of resources would be wasted. Validation can be done using molecular superimposition techniques. If a compound with low binding affinity in the BTX assay was found to have a poor fit to the model in any

conformation, or if it fitted the model well but in a high energy conformation, it would strengthen the credibility of the pharmacophoric model. However, if such a compound would fit the model well in its low energy conformation, then there would be three possibilities to rationalise this phenomenon. Firstly, the compound may be too voluminous in some parts of the molecule which may cause steric interactions with the receptor, thus causing low binding affinity. Secondly, the compound may have a very unfavourable free energy of solvation, and lastly, the electronic properties of the compound may not be complementary to the receptor site. If none of the three cases stated above are possible, then the pharmacophoric model would be deemed inaccurate or even invalid. On the other hand, a compound with high binding affinity in the BTX assay should be able to fit the model well. However, if such an active compound could not be fitted to the model, the pharmacophoric model would be considered invalid, unless it could be proven biologically to have a different binding mode.

Validation could be brought a step further by correlating *in silico* data with biological data. Ability of the compounds to fit the model could be quantified by the distances between each of the pharmacophoric elements of the compound to each of the corresponding pharmacophoric elements at the receptor site. This quantified parameter can then be correlated to binding affinity data using linear correlation. A good correlation between the two parameters would help to strengthen the pharmacophoric model's validity and predictive ability.

Validation of the models in the current study was carried out through the correlation of Total Difference (TD) with RBP. Each member of the training set was superimposed on the derived models and the TD was calculated. TD value is an arbitrary unit used to quantify the goodness of fit between the derived pharmacophoric model and each analyte. When the analyte was superimposed onto the pharmacophoric

model, the distance between each designated corresponding pharmacophoric element in the analyte and model was noted. TD is the sum of the three distances derived in the pharmacophoric triangle, and a low value would imply a better fit. Since higher RBP values equate to better binding affinity, RBP and TD values should therefore be inversely correlated. The compounds in the training set were correlated to ascertain the validity of the various pharmacophoric models.

The models were subsequently challenged to see if they could discern between good blockers from the poor blockers. This was carried out by first determining the TD values of a larger group of chemically diverse compounds (**Figure 2**, validation set) that exhibited different extent of sodium channel blockade activity. This larger group of compounds was later subjected to the same correlation study between the TD and RBP values. Similar to the compounds in the training set, compounds in the validation set were chosen from literature articles that performed the BTX assay using synaptoneurosomes obtained from the rat brain, which contained high levels of neuronal (type II) sodium channels.

The compounds in the validation set were lidocaine, **(6)** [118]; lamotrigine, **(7)** [116]; phenytoin, **(8)** [27]; carbamazepine, **(9)** [27]; a phenyl hydantoin, **(10)** [40]; ameltolide, **(11)** [58]; an ameltolide analogue, **(12)** [58]; a N-phenyl derivative of phthalimide, **(13)** [59]; ralitoline, **(14)** [52]; a 'smissmanone', **(15)** [39]; a carboxamide, **(16)** [44]; DCUKA-Ome, **(17)** [55]; an enaminone, **(18)** [68]; riluzole, **(19)** [67]; and Kavain, **(20)** [119].

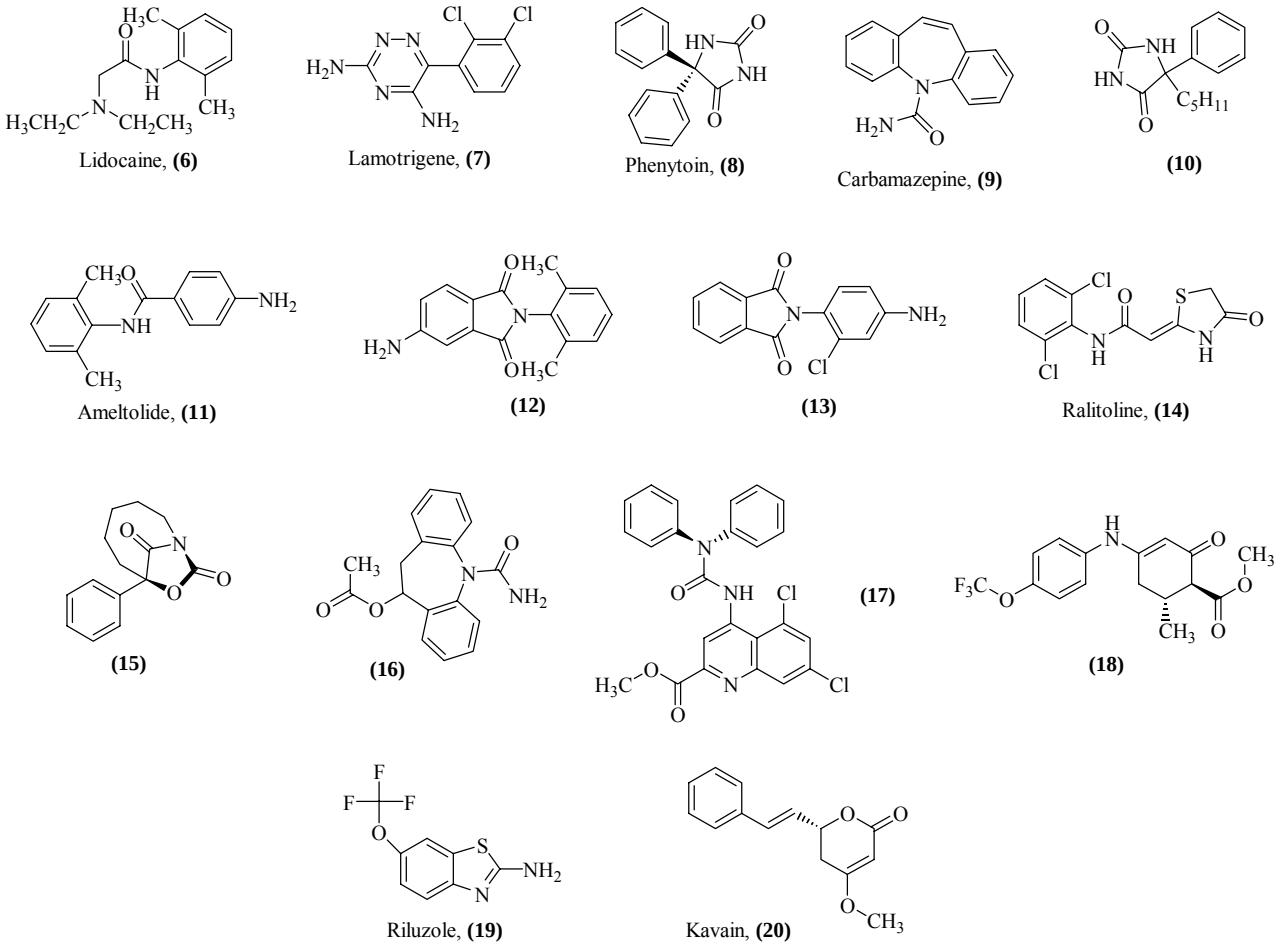

Figure 2. Validation set of compounds

4.5 Results and Discussion of Pharmacophoric Modelling

The use of vinpocetine as the 'template' in the DISCO study resulted in five pharmacophoric models, A to E. Each model was made up of one hydrogen-bond (H-bond) acceptor (A), one H-bond donor (D) and one hydrophobic group (H). The distances between each pharmacophoric element described the dimensions of each model. AH, AD and HD are distances between the H-bond acceptor and hydrophobic group; between H-bond acceptor and H-bond donor; and between hydrophobic group and H-bond donor respectively. Inter-pharmacophoric distances and tolerance of the five models are listed in **Table 1**. Model A had the lowest tolerance, followed by model C and then model B. Model D and E had large tolerance values and were less likely to be the correct models.

Table 1. Pharmacophoric models and inter-pharmacophoric distances (Å)

	Model A	Model B	Model C	Model D	Model E
AH[a]	4.02	3.60	4.31	5.39	5.42
AD[a]	5.65	6.12	5.65	5.65	5.65
HD[a]	3.27	2.61	5.33	1.41	1.46
Tolerance	1.26	1.88	1.65	2.88	2.88

[a]AH, AD and HD are distances between the H-bond acceptor and hydrophobic group; between H-bond acceptor and H-bond donor; and between hydrophobic group and H-bond donor respectively.

The proposed pharmacophoric models of drug-receptor interaction were validated by co-relationship study between RBP and the molecular modelling data (TD) using linear regression. This was done using both the compounds in the training set and validation set and goodness of correlations were represented with r^2 values. TD values for every

compound was calculated for each model and listed together with RBP values in **Table 2**. If the pharmacophoric models were plausible, then RBP and TD values

Table 2. TD and RBP values of the compounds

Compounds	TD values					RBP
	Model A	Model B	Model C	Model D	Model E	
1	0.00	0.00	0.00	0.00	0.00	122.0
2	2.63	3.64	4.36	6.25	4.87	36.4
3	3.34	4.09	4.02	5.15	4.27	30.8
4	2.23	6.43	1.11	5.80	7.70	29.2
5	1.67	2.10	2.07	3.59	3.72	98.6
6	4.20	5.50	6.39	5.54	5.04	0.6
7	3.11	4.01	2.65	5.22	4.95	0.2
8	4.16	3.35	2.78	6.79	5.60	1.0
9	7.19	8.54	6.14	6.82	8.27	0.3
10	4.05	3.36	5.77	5.55	5.77	1.0
11	2.54	2.23	5.34	4.21	4.26	0.9
12	0.74	1.06	2.07	3.91	3.30	7.8
13	2.04	1.42	3.24	3.94	3.45	6.2
14	2.85	2.94	4.57	6.18	6.07	1.6
15	NA[a]	NA[a]	NA[a]	NA[a]	NA[a]	0.3
16	0.72	1.31	1.05	5.13	3.82	0.6
17	1.69	1.13	2.43	3.75	3.14	0.5
18	1.88	2.99	6.89	5.47	3.38	0.2
19	3.35	1.83	4.70	4.36	4.25	1.2
20	NA[a]	NA[a]	NA[a]	NA[a]	NA[a]	0.5

[a] Compound cannot be fitted to pharmacophoric models because they only have two pharmacophoric groups.

Table 3. Correlation of TD with RBP values

Set of compounds Used	Compounds used	Correlation of TD with RBP, r^2 values				
		Model A	Model B	Model C	Model D	Model E
Training set	**1-5**	0.80	0.82	0.43	0.85	0.70
All	**1-14**	0.34	0.18	0.41	0.55	0.39
Charged nitrogen	**1-7**	0.83	0.73	0.46	0.73	0.55
Uncharged nitrogen	**8-14**	0.56	0.41	0.57	0.55	0.59

would be inversely correlated. TD values were correlated with their RBP values for each of the pharmacophoric models (**Table 3**).

The first step was to validate using compounds in the training set. The r^2 values of the five pharmacophoric models ranged from 0.43 to 0.85. Other than model C, the other models had good r^2 values, which indicated that the pharmacophoric models were well correlated with the RBP values of compounds in the training set. This was expected as compounds in the training set have high affinity for the sodium channel receptor, and thus tend to satisfy well all receptor-binding requirements. In other words, the correlation was not confounded by interference from unfavourable parameters, such as steric hindrance of pharmacophoric groups. Model C had a low r^2 value of 0.43 and was deemed not to be the correct model. It was difficult to isolate the best model from the others based on the correlation of the TD with RBP values of the training set.

Compounds **15** to **20** were omitted from the correlations due to reasons such as steric hindrance, electron withdrawing effects, or lack of pharmacophoric elements. When a correlation study was carried out on compounds **1** to **14**, the results yielded low r^2 values of 0.18 to 0.55. Upon careful inspection of the 14 compounds, it was found that 7 of the

compounds (compounds **1**-**7**) would be ionised with a positive charge at physiological pH while the rest of the compounds would not. It was also observed that compounds with a chargeable nitrogen atom as one of their pharmacophoric elements were usually more active than those without. When the 14 compounds were separated and correlation studies carried out independently, better r^2 values for both the positively charged compounds and non-chargeable compounds were obtained. Correlation of the models using the charged nitrogen group of compounds yielded r^2 values, for the five pharmacophoric models, of a range from 0.46 to 0.83. It became more obvious that models C and E were less credible. Further correlation of the models using the compounds having uncharged nitrogen group resulted in r^2 values of 0.41 to 0.59. The poorer correlations with compounds having the uncharged nitrogen group were expected as these compounds were of low to moderate binding affinity to the receptor, and the correlations were confounded by interference from unfavourable parameters, such as steric hindrance of pharmacophoric groups. The results of the correlation studies in the group of compounds having uncharged nitrogen suggested that model B would not be a good model, due to the lowest r^2 value obtained. From the correlation studies of both groups of compounds, that has or do not have the charged nitrogen group, the three models: B, C and E were eliminated from the list of possible pharmacophoric models. The choice was left between model A and model D, as the r^2 values of the correlation in these two models were similar.

When the tolerance values (**Table 1**) of these two models were compared, it seemed that model A was the better pharmacophoric model. A high tolerance value in the model meant that the compounds in the training set fitted onto vinpocetine with a large margin of error. In other words, the ranges of inter-pharmacophoric distances in model D were larger, and it was thus a less precise model. The tolerance in the model was expected

to be low because the compounds used in the training set had high binding affinities to the receptor and should be similar in their inter-pharmacophoric distances. Furthermore, model A had better r^2 values in the correlation studies of both groups of compounds that have or do not have the charged nitrogen group (**Figure 3** to **5**).

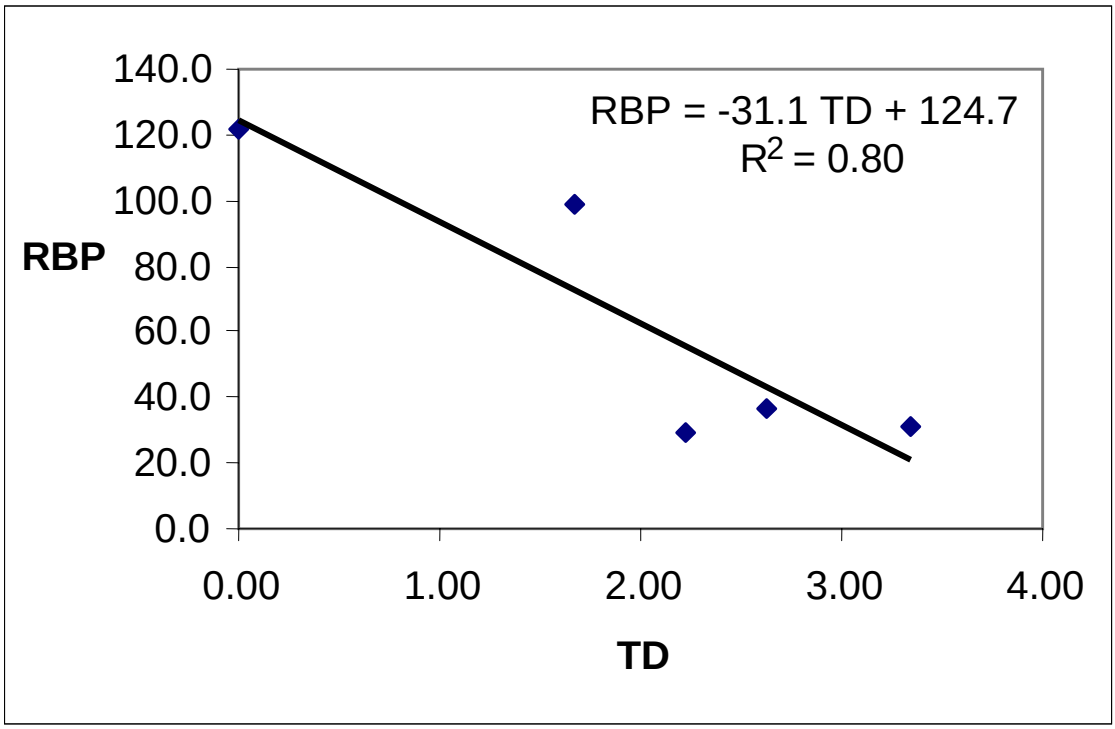

Figure 3. Correlation plot of RBP vs. TD (from model A) using compounds in the training set

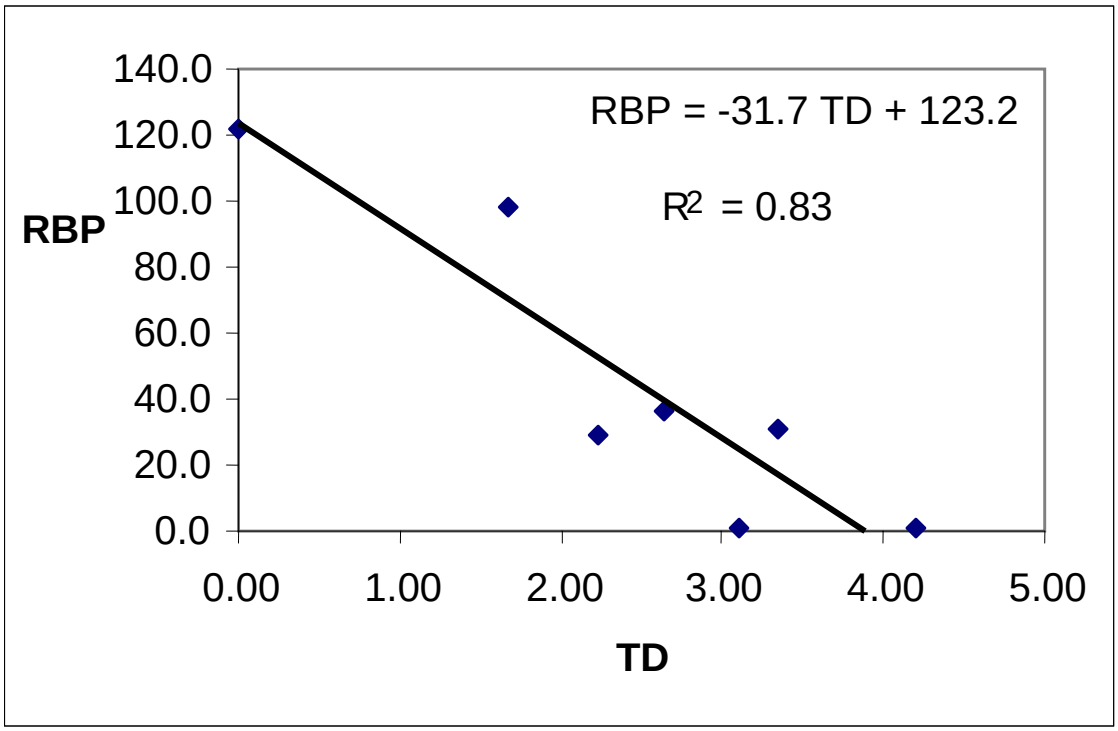

Figure 4. Correlation plot of RBP vs. TD (from model A) using compounds **1** to **7** (compounds with a charged nitrogen at physiological pH)

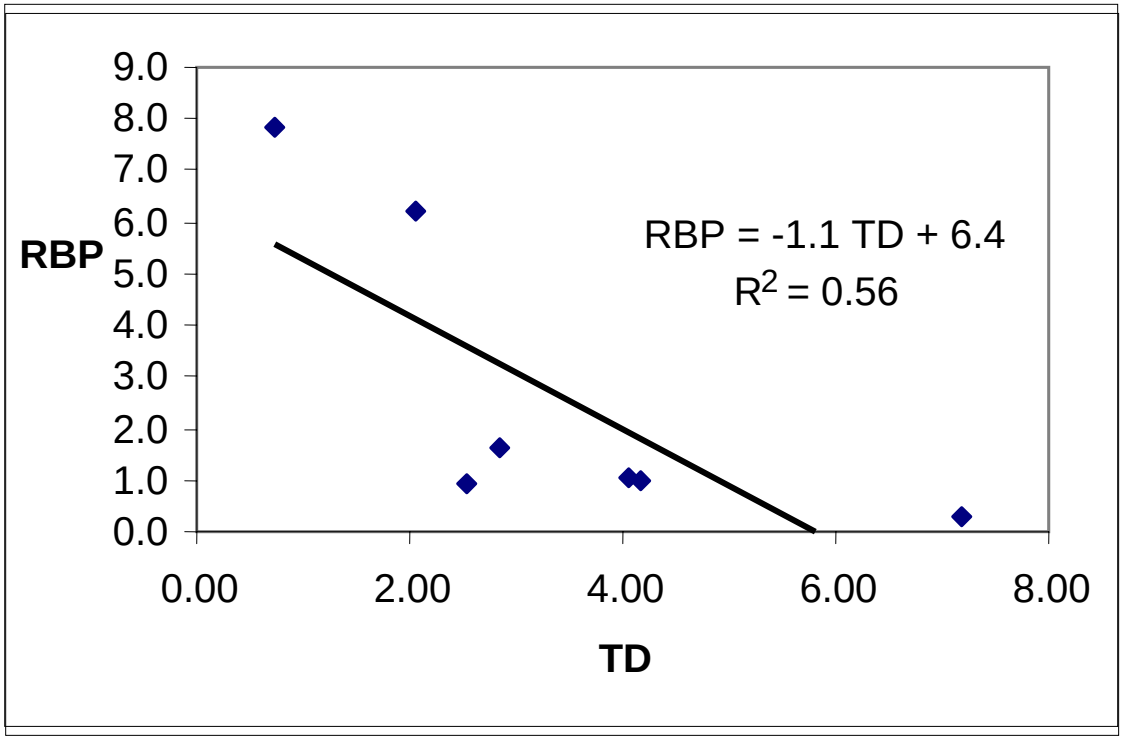

Figure 5. Correlation plot of RBP vs. TD (from model A) using compounds **8** to **14** (compounds that do not have a charged nitrogen at physiological pH)

From the above observations that compounds having the charged nitrogen group have higher RBP values than those having the uncharged nitrogen group, it was therefore inferred that charged nitrogen in the pharmacophoric elements of the compound is good for activity, but is not essential for its binding to the receptor. A possible situation would be that compounds in the charged nitrogen group are able to participate in long distance ion-ion interactions with negatively charged groups at the receptor site and/or along the channel leading to the receptor site. Another explanation is that the receptor site has a negatively charge group as its H-bond acceptor, which binds more tightly with a charged H-bond donor (e.g. a charged nitrogen).

Compounds **15** to **20,** from the uncharged nitrogen group were not included for correlation of TD and RBP. Corey-Pauling-Koltun (CPK) view of compound **17** (**Figure 6**) showed that the two phenyl rings sterically hinder the H-bond donor atom (the secondary amide in the ureido functional group). It was not possible to find an unhindered pharmacophoric triangle; thus the interaction between the receptor and compound **17** was weak despite having a good TD value. Similarly in compound **18**, its ester group sterically hinders the hydrophobic group, thus its RBP is low despite its low TD. Riluzole **(19)** has a trifluoro-methyl group attached to its oxygen atom (H-bond acceptor), which withdraws electrons from the oxygen atom inductively, thus its activity was lower than what was suggested by its TD value. Compound **15** and Kavain **(20)** only have two of the three pharmacophoric groups, thus they do not have TD values and cannot be correlated to RBP values. Compound **16** is a derivative of carbamazepine **(9)**, with compounds **9** and **16** having RBP values of 0.31 and 0.58, respectively, while their TD values were very different in the model. There was insignificant difference between their RBP values whereas there was a very sharp contrast between the TD values of the two compounds.

The difference in TD values could be attributed to the additional H-bond acceptor in compound **16**. However, observation from the RBP values suggested that the two compounds would bind to the receptor site in a similar fashion, as their structures and binding affinities were very similar. It was thus suggested that compound **16** did not utilise its acetyl group as an H-bond acceptor. Therefore its TD value should not be correlated to its RBP value, since it was calculated by assigning the acetyl group as the H-bond acceptor.

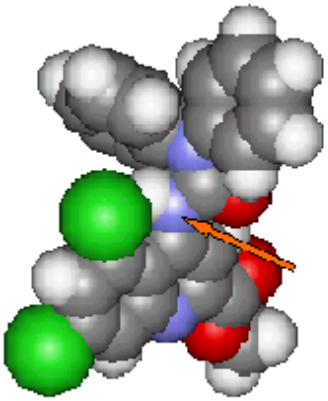

Figure 6. Compound **(17)** is shown with an arrow indicating the H-bond donor atom. It can be seen that the two phenyl rings sterically hinder the interaction of the H-bond donor atom with the receptor site.

All the conformations used for analysis in DISCO were in their GMECs, except for lidocaine **(6)**. For lidocaine, the two ethyl groups attached on the nitrogen atom sterically hindered the charged nitrogen. In the GMEC of lidocaine, neither the charged nitrogen nor the uncharged nitrogen was able to present an unhindered pharmacophore in the CPK view. In other words, the GMEC was not likely to be the active conformation in

which lidocaine would adopt when interacting with the receptor site. The LMEC of lidocaine did not utilize its charged nitrogen to bind to the receptor site, but instead used its uncharged nitrogen to form a pharmacophoric triangle.

4.6 Proposed Pharmacophoric Model for Neuronal (Type II) Sodium Channels

This study generated a new pharmacophoric model (**Figure 7**) for blockers of the sodium channel receptor, as represented by model A. The proposed pharmacophoric model A is a triangle formed by three pharmacophoric elements: 1 hydrogen bond donor atom (H-bond donor), 1 hydrogen bond acceptor atom (H-bond acceptor) and 1 hydrophobic group. The dimensions of the pharmacophoric triangle are as follows. The H-bond acceptor to hydrophobic group distance (A-H distance) is 4.02±1.26Å, H-bond acceptor to donor distance (A-D distance) is 5.65±1.26Å, and the H-bond donor to hydrophobic group distance (D-H distance) is 3.27±1.26Å. It was observed that compounds with a charged nitrogen at physiological pH will have better binding affinity to the sodium channels. Correlation studies of the seven compounds having a charged nitrogen gave rise to an equation, RBP = -31.7 TD + 123.2, with a r^2 value of 0.83.

Figure 7. Proposed pharmacophoric model

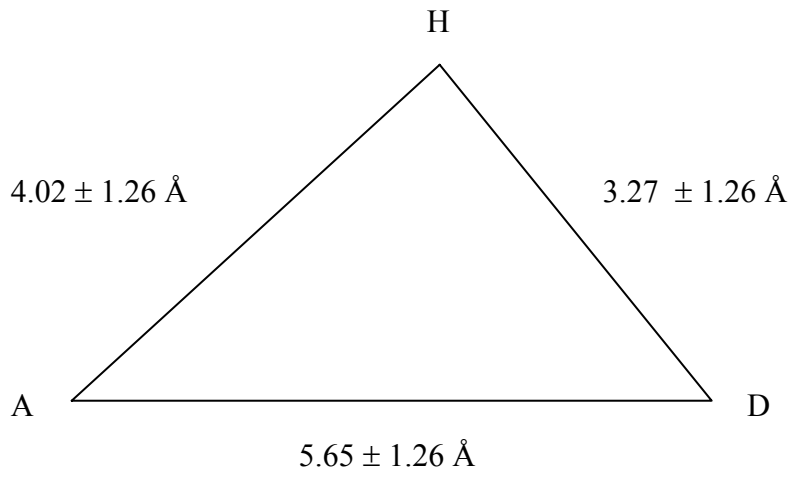

The model proposed by the current study was derived from structurally diverse compounds and could be related to compounds from other chemical classes acting at the rat brain neuronal sodium channel receptors. Unverferth *et. al*. [10] also used five structurally diverse compounds to generate a pharmacophoric model for anticonvulsants that are sodium channel blockers. Their model had different pharmacophoric elements from the current study, which consist of an electron donor, an aryl ring and a hydrogen bond acceptor/donor unit. However, the author concluded that the model had three essential pharmacophoric elements, which were a hydrogen bond donor, and two other essential structural elements, namely the aryl ring and the electron donor. Their essential pharmacophoric elements are similar to those proposed by the current study. The current study's H-bond acceptor, H-bond donor and hydrophobic group are similar to their model's electron donor, hydrogen bond donor part of the HAD unit and aryl ring respectively. The similarity of pharmacophoric elements in the two models suggest that these are the essential features needed in a compound for binding to the sodium channels.

However the dimensions of the pharmacophoric triangles in the two models are different, as the compounds used for the two models were selected based on different criteria. In addition, the current study also considered the ionisation of compounds in physiological pH, and was thus able to show that compounds with a charged nitrogen as the H-bond donor were more active as sodium channel blockers than those which were uncharged. Thus it was suggested that a possible lead for sodium channel blockers should fit the proposed pharmacophoric model and should preferably have a charged nitrogen as its H-bond donor.

The proposed model had pharmacophoric elements which differed from those proposed by Tasso *et. al*. [115] Tasso's group proposed that the pharmacophoric model includes a polar group comprising of two negative atoms and one positive atom, and a hydrophobic group that should be no smaller than three atoms. The two negative atoms and one positive atom in the polar group are local density charges and not formal charges. The pharmacophoric model in the current study is inherently different from that of Tasso's model, because the model in the current study is based on formal charges.

The proposed pharmacophoric model was derived from a training set of compounds that were selected based on their binding affinity to the sodium channels, as measured in the BTX assay. Thus the pharmacophoric model in the current study is different from the models proposed by Unverferth and Tasso, as their models were derived using anticonvulsants that act via sodium channel blockade. In other words, the focus of the current pharmacophoric model is to find a common pharmacophore for neuronal sodium channel blockers, and not only for anticonvulsants. The main advantage of the current study is that it can be useful for predicting the binding affinity of potential sodium

channel blockers in the BTX assay due to the derived linear correlations between RBP and TD values. The model can be used to predict the sodium channel blockade activity of new compounds, or to screen existing compounds in the literature for sodium channel blockade activity.

5. ADAPTATION OF THE PHARMACOPHORIC MODEL FOR IDENTIFYING POTENTIAL SODIUM CHANNEL BLOCKERS

The current study has derived a pharmacophoric model for neuronal (type II) sodium channels, based on 3D conformations and binding affinity profiles of known sodium channel blockers. It must be emphasized that the binding affinity profiles of the compounds have been measured using the BTX assay, thus the pharmacophoric model can be viewed as a computational model that can be used to predict the binding affinity of compounds in the BTX assay. In other words, the pharmacophoric model can be adapted to identify ligands that have high binding affinity to the neuronal (type II) sodium channel receptors. Such a screening process is advantageous as the displacement of tritiated BTX has been widely used as a rapid *in vitro* assay for the screening of potential sodium channel blockers. As a high throughput and non wet lab-based screening procedure, it can reduce screening time and save costs during lead identification.

5.1 Criteria of a Screening Process for Potential Sodium Channel Blockers

The pharmacophoric model suggested that a good sodium channel blocker should ideally have the three stipulated pharmacophoric elements, a charged nitrogen at physiological pH and a good fit to the pharmacophoric model. The first and second criteria can be fulfilled by the requisite functional groups, but a range needs to be defined for the goodness of fit of compounds to the model in order to use it to screen for potential sodium channel blockers. The objective of the screening process is to identify compounds with good binding affinity, as such; the compounds in the training set can be used as a

guide to determine the range of TD values that a potential sodium channel blocker should possess. The training set of compounds had a range of TD values from 0.00 to 3.34, therefore a TD value of less than 3.50 was chosen as the range of TD values for the screening process. The equation, RBP = -31.7 TD + 123.2, which was derived from the correlation study of the seven compounds having a charged nitrogen at physiological pH, will be used to predict the RBP of the potential sodium channel blocker.

In summary, active sodium channel blockers should have the three stipulated pharmacophoric elements, a TD value less than 3.50, and a charged nitrogen at physiological pH. The equation, RBP = -31.7 TD + 123.2, will be used to predict the RBP values of compounds that satisfy the three criteria. A potential ligand can be identified using a flowchart (**Figure 8**).

Figure 8. Flowchart for the screening process.

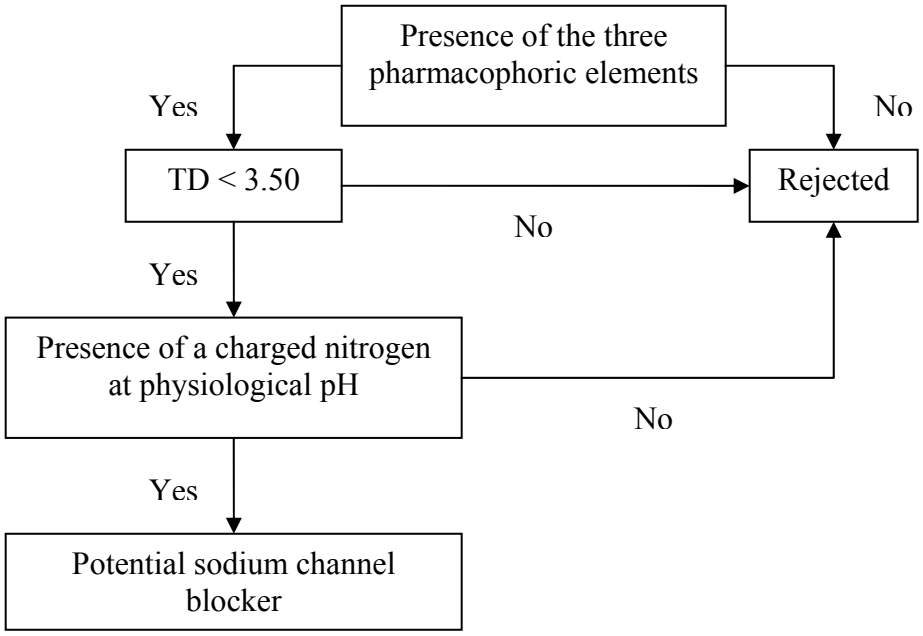

5.2 Limitations of the Screening Process

Other than the three criteria outlined above, the binding affinity of a sodium channel blocker is also governed by another major factor that was not incorporated into the pharmacophoric model. Compounds that are charged and possess low TD values need not necessarily have good binding affinity to the sodium channels, as their ability to interact with the receptor is not solely based on its pharmacophoric elements, but is also dependent on other parts of the molecule. In other words, non-pharmacophoric elements will modulate the binding affinity of a compound. For example, if a compound has a very bulky substitution next to its H-bond donor that hinders receptor-ligand interaction, then its RBP value would be much lower than predicted. As mentioned, only the most potent compound in each chemical class was chosen for computer modelling, so as to reduce confounding factors such as steric hindrance from interfering with the analysis of the pharmacophoric model. In such situations, it means that the compounds already have 'optimized' non-pharmacophoric elements present in their structure. For example, compound **2** had the best binding affinity in a series of 2-aminopropanamides, that had IC_{50} values ranging from 1.1 to 150.8 μM. [116] This series of compounds had the same prerequisites (charge and TD value) when assessed by the screening process, but their binding affinity to the sodium channel receptors differed up to 150 times. Such observations suggest that although both charge and TD value are important parameters, the substitutions that do not form part of the pharmacophoric elements can significantly alter the binding affinity of the compound. The screening process has a limitation as it is based on distances between pharmacophoric elements, and cannot detect whether compounds possess 'optimized' non-pharmacophoric elements.

In view of the limitation of the screening process, a lead compound that is predicted to be a good sodium channel blocker should not be discarded if it is subsequently found to possess only weak binding affinity in the BTX assay. Instead, structural modifications to the lead compound should be attempted in order to find the compound with the elusive 'optimised' non-pharmacophoric elements. The rationale behind this approach is that a lead compound that had been predicted to possess good binding affinity possesses the basic chemical structure for good affinity, and thus should be explored further to optimise the binding affinity of the compounds from the same chemical class.

Another limitation of the screening process is that it cannot be used for compounds that do not have a charged nitrogen. A separate screening process for such compounds was not derived because compounds that do not possess a charged nitrogen in their structure are inherently weaker and thus not desirable as lead compounds. Another reason was that the correlation study involving compounds that do not have a charged nitrogen yielded a r^2 value of 0.56. In other words, the predictive power of such a screening process will be weak.

6. VERIFICATION OF PREDICTIONS THROUGH CHEMICAL SYNTHESIS AND *IN VITRO* TESTING

6.1 Identification of Potential Sodium Channel Blockers

Compounds from two chemical classes were selected to verify the ability of the pharmacophoric model to discern good sodium channel blockers from the poor blockers. The compounds in one of the chemical classes possess a charged nitrogen at physiological pH and have low TD values, while the compounds in the other chemical class do not possess a charged nitrogen and have high TD values. The former chemical class was chosen to show that the screening process would be able to identify compounds that possess good binding affinity for the neuronal sodium channels. The latter chemical class was used to show that the screening process was able to differentiate the poor sodium channel blockers from the good ones.

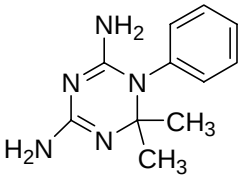

Compound **21**

Intuitively, it can be rationalised that 4,6-diamino-1,2-dihydro-2,2-dimethyl-1-phenyl-1,3,5-triazine (compound **21**), possesses the 3 pharmacophoric elements delineated in the derived pharmacophoric model, and its structure closely resembles the sodium channel blocker, lamotrigine. In addition, compound **21** possesses a charged nitrogen at physiological pH. Compound **21** was identified for further investigation, and was

subsequently modelled using the computer software and superimposed onto the pharmacophoric model, yielding a TD value of 1.87. In short, compound **21** satisfied the two parameters set by the screening process and was predicted to have good binding affinity to the sodium channels.

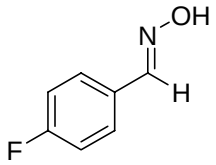

Compound **22**

4'-Fluoro benzyloxime (compound **22**) possesses the three pharmacophoric elements that were stipulated in the pharmacophoric model. However, compound **22** does not have a charged nitrogen at physiological pH and has a high TD value of 7.9, and is therefore expected to have low binding affinity to the neuronal sodium channels.

6.2 Chemical Synthesis and *In Vitro* Testing of Compounds

6.2.1 Chemistry

Compound **21** was synthesized using a general synthetic pathway for the phenyldihydro-1,3,5-triazines, which involves the condensation of molecular equivalents of the arylammonium chloride salt, cyanoguanidine, and acetone or cyclohexanone, with loss of one molecule of water (**Figure 9**). One equivalent of HCl was used and the reaction was carried out in 96% ethanol, with heating at reflux. The reaction mixture becomes a clear solution, from which the product crystallizes directly in pure form. The crystals were then re-crystallized with ethanol/water mixture.

Figure 9. Chemistry of phenyldihydro-1,3,5-triazines. (R_1=H, Cl, CH_3 or CH_3O and R_2=CH_3 or R_2-R_2 = C_4H_8 or C_5H_{10})

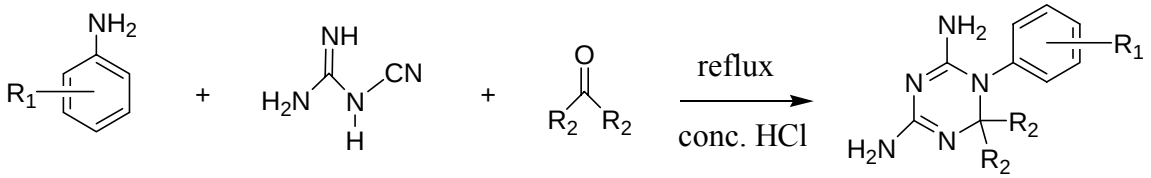

substituted aniline cyanoguanidine ketone phenyldihydro-1,3,5-triazines

Compound **22** was synthesized by a general procedure for benzyloximes, in which a Schiff-base reaction was carried out between the corresponding aldehyde/ketone and hydroxylamine hydrochloride, with sodium acetate as a base catalyst (**Figure 10**). The reaction was carried out in aqueous ethanol with stirring at room temperature.

Figure 10. Chemistry of benzyloximes (R_1= 4-F, 4-CF_3, 4-OCH_3, 2, 3-di-OCH_3, 4-OC_4H_9, 4-CN, 4-NO_2, 3-NH_2, 4-NH_2 or H and R_2=H, CH_3 or C_2H_5)

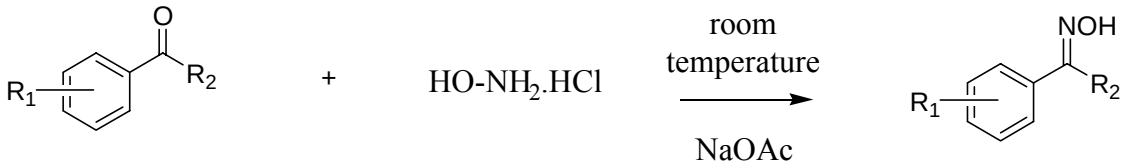

substituted carbonyl benzyloximes

6.2.2 BTX Radioligand Binding Assay

The BTX assay is a well established radio-ligand binding assay used for screening neuronal (type II) sodium channel blockers pioneered mainly by William A. Catterall and his co-workers. [27] The current study made use of an assay method modified from that reported by Brown *et. al.* [43] Synaptosomes has been used in the assay because they have

the same properties as those in neuroblastoma cells with respect to neurotoxin binding and action. [120] Furthermore the number of sodium channels per milligram of protein is much greater in synaptosomes, thus making it suitable for high throughput sodium channel binding assay. Synaptosomes are obtained from rat cerebral cortex because autoradiographic localization of the BTX binding sites shows that the highest density of the receptors are concentrated in the grey matter and lower in the white matter. [121] In the preparation of the receptors for the study, the brain tissue was first disrupted by homogenization to increase access of the radio-ligand to the receptor population. A series of manipulations with centrifugation and filtration were carried out to obtain the desired fraction of protein that contained the sodium channel receptors. This fraction was subsequently stored frozen in isotonic sucrose solution and thawed before use.

Since the BTX assay is a competitive binding assay, the isolated receptors were incubated with increasing concentrations of the drug being tested, together with a fixed concentration of tritiated BTX. Scorpion venom was used to increase the specific binding of tritiated BTX by approximately 15 fold. [27] At equilibrium, the proportion of unbound and bound tritiated BTX depended on the ability of the drug to displace BTX from its binding site. As most of the tritiated BTX remained unbound at the end of the binding reaction, an efficient method for its removal, without the loss or dissociation of the receptor-ligand complex, was necessary to accurately quantify the amount of bound tritiated BTX. Separation was carried out at 0°C in order to reduce the ligand dissociation rate. Filtration was employed as it was an efficient and convenient method of separating free from bound tritiated BTX, because it required less handling and manipulation of samples compared to the centrifugation method.

In radio-ligand binding assays, there will always be a certain amount of nonspecific binding, which is not saturated by radio-ligand and therefore continues to increase as a function of radio-ligand. Thus, non specific binding must be quantitated at every concentration of receptor and radio-ligand by including assay tubes that had high concentration of veratridine. Since veratridine was present in such a concentration which was sufficient to occupy more than 99% of the receptors, it prevented the tritiated BTX from binding to the receptors; therefore the remaining bound radioactivity that was measured represented the nonspecific binding. The specific binding of the tritiated BTX can therefore be calculated by subtracting nonspecific binding from the total binding.

6.3 Results of CADD and *In Vitro* Testing of 4,6-Diamino-1,2-dihydro-2,2-substituted-1-phenyl-1,3,5-triazines (Phenyldihydro-1,3,5-triazines)

6.3.1 *In Vitro* Testing of 4,6-Diamino-1,2-dihydro-2,2-dimethyl-1-phenyl-1,3,5-triazines (Series (I))

In order to verify the prediction of the pharmacophoric model, compound **21** was synthesized and tested for its binding affinity for the neuronal sodium channels using the BTX assay, and was found to have a IC_{50} value of 195.1 ±10.8 μM. The screening process predicted, through equation RBP = -31.7 TD + 123.2, that compound **21** should have a RBP value of 63.9. However, on comparing the K_i values of compound **21** and phenytoin, compound **21** was found to have a RBP value of 0.8.

As iterated in the limitations of the screening process, if a potential lead compound was found to have weak *in vitro* activity, it should not be discarded immediately. Different substitution to the basic chemical structure should be attempted in order to improve its

binding affinity, as it is believed that a lead compound that satisfies the screening process's criteria should possess the prerequisites that are needed to bind strongly to the receptor. Thus a series of 4,6-diamino-1,2-dihydro-2,2-dimethyl-1-phenyl-1,3,5-triazines, series (**I**), was synthesized and tested in the BTX assay (**Figure 11**). This series of compounds explored the effects of phenyl substitutions. Attempts to use more electron-withdrawing substituents (such as *para*-nitro) were not successful.

Figure 11. Binding affinity of compounds in series (**I)** in the BTX assay

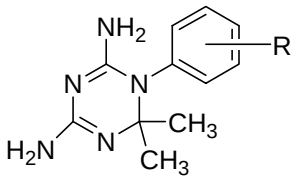

Compound	R	BTX IC_{50} (μM)	SEM	RBP
21	H	195.1	10.8	0.8
23	*o*-Cl	123.4	4.7	1.3
24	*m*-Cl	44.0	3.6	3.6
25	*p*-Cl	48.3	7.4	3.3
26	*o*-CH_3	81.2	9.7	2.0
27	*m*-CH_3	38.7	1.7	4.1
28	*p*-CH_3	48.3	5.2	3.3
29	*o*-OCH_3	180.7	15.9	0.9
30	*m*-OCH_3	71.5	11.8	2.2
31	*p*-OCH_3	97.6	10.8	1.6
Phenytoin		159.5	7.8	1.0

All the compounds in series (**I)** showed moderate binding affinity to the neuronal sodium channels, with compound **27** having the lowest IC_{50} value of 38.7 ± 1.7 μM, which translated to an RBP value of 4.1. In other words, the *meta*-methyl substitution (compound **27**) improved the binding affinity of the unsubstituted compound (compound **21**) by about 5 times.

The results showed that, the presence of a substituent on the phenyl ring, has a positive effect on the binding of the compounds in the phenyldihydro-1,3,5-triazines series with the receptor site on the sodium channel. This is inferred from the significantly lower IC_{50} values of the compounds with substitutions introduced at the *meta* and *para* position compared to the unsubstituted compound.

The *ortho*-substituted compounds have similar IC_{50} values to the unsubstituted compound. The lower binding affinities of these compounds are likely to be due to the steric interaction between the *ortho*-substitution and the heterocyclic ring. The electron donating or electron withdrawing characteristics of the phenyl-substitutions does not have significant impact on the BTX activity of the compounds, as can be seen from the similar results between the chloro-substituted and methyl substituted compounds.

6.3.2 *In Vitro* Testing of 4,6-Diamino-1,2-dihydro-2,2-cyclohexyl-1-phenyl-1,3,5-triazines (Series (II))

Although the *in vitro* testing of the compounds in series (**I**) showed that compound **27** had a RBP value of 4.1, its binding affinity was still considered too weak compared to the predicted RBP value of 63.9 by the screening process. Therefore further modifications

had to be made in order to unearth the potential of the phenyldihydro-1,3,5-triazines. A further attempt to improve compound **21** as a sodium channel blocker was made by the Computer-aided Drug Refinement (CADR) approach.

Figure 12. Compound **21** overlapped onto the pharmacophoric triangle

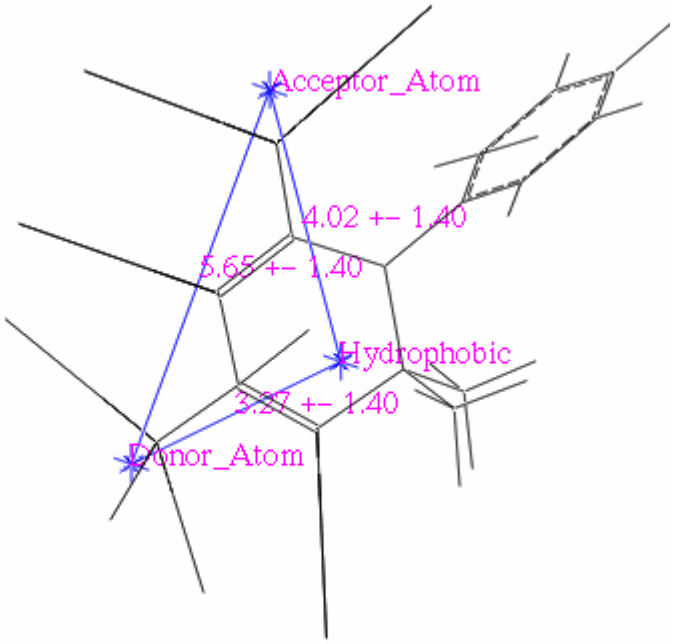

Compound **21** was superimposed on the pharmacophoric model and examined in detail (**Figure 12**). For compound **21**, DISCO assigned the 4-NH_2 group as **D** (H-bond donor), its 6-NH_2 group as **A** (H-bond acceptor) and its heterocyclic ring as **H** (hydrophobic site). It can be seen from the figure that the 'epicentre' of the hydrophobic group, as depicted by the pharmacophoric model, is near to the 2-position. Thus the dimethyl group at the 2-position has an important contribution to the hydrophobic pharmacophoric element of the compound. An increase in hydrophobicity at the 2-position should theoretically increase the binding affinity of compound **21**, and it was proposed to

change the dimethyl group at the 2-position to a cyclohexyl group. With this information, compound **32** was synthesized and tested in the BTX assay, and was found to have an IC_{50} value of 14.7 ± 1.3 μM. Compound **32** has a RBP value of 10.9 and is approximately 13 times more active than compound **21** in the BTX assay. In other words, the CADR approach was accurate in predicting, that increasing the hydrophobicity at the 2-position, will improve binding affinity.

As it was observed that phenyl substitutions in series (**I**) improved binding affinities of the compounds, the same phenyl substitutions were used to form series (**II**) (**Figure 13**). The phenyldihydro-1,3,5-triazine compounds in series (**II**) generally exhibited good sodium channel inhibitory activity based on the IC_{50} values obtained from the BTX binding assay. In particular compound **34** (IC_{50} of 4.0 ± 0.5 μM) has a RBP value of 39.9. The high binding affinity of compound **34** suggested that the screening process was able to identify potential sodium channel blockers that have high affinity to the neuronal sodium channels. Emphasis must be placed on the fact that 4,6-diamino-1,2-dihydro-2,2-substituted-1-(substituted)-phenyl-1,3,5-triazines were never before reported as sodium channel blockers. The trend in the binding affinities of the compounds in series (**II**) is similar to that of series (**I**), as it was observed that compounds with substitutions introduced at the *meta* and *para* positions have significantly lower IC_{50} values compared to the unsubstituted compound. The *ortho*-substituted compounds in series (**II**) have similar IC_{50} values as compound **32,** which is unsubstituted.

Figure 13. Binding affinity of compounds in series (**II)** in the BTX assay

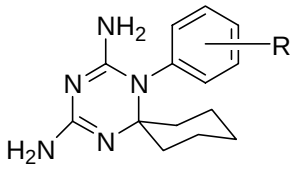

Compound	R	BTX IC_{50} (μM)	SEM	RBP
32	H	14.7	1.3	10.9
33	*o*-Cl	13.0	0.6	12.3
34	*m*-Cl	4.0	0.5	39.9
35	*p*-Cl	4.4	0.3	36.3
36	*o*-CH_3	9.1	1.2	17.5
37	*m*-CH_3	4.7	0.1	33.9
38	*p*-CH_3	4.2	0.6	38.0
39	*o*-OCH_3	12.3	2.1	13.0
40	*m*-OCH_3	5.1	0.3	31.3
41	*p*-OCH_3	7.8	0.8	20.4

Although compound **21** had a RBP value of only 0.8, the phenyldihydro-1,3,5-triazines were explored further based on the belief that this chemical class of compounds possess the prerequisites required for good binding affinity to the neuronal sodium channel receptors. The use of the CADR approach and variation of the phenyl substitutions had improved the RBP value to 39.9 in compound **34**. It must be emphasized that the TD values of compound **21** and **34** are the same, thus reinforcing the belief that a

compound with a good TD value need not necessarily possess good binding affinity to the sodium channels, but with structural modifications and functional group substitutions (without changing the TD value), it is possible to improve its activity. The RBP of compound **34** is 39.9, still lower than the predicted RBP value of 63.9. A margin of error is expected in the prediction of the TD value of compound **34**, especially since only seven compounds were used for formulating the equation. Furthermore, it is possible that the RBP values of phenyldihydro-1,3,5-triazines can still be increased through further structural changes.

The screening process had been shown to be able to identify a potential sodium channel blocker, based on the criteria set for the process and through the use of the flowchart in **figure 8**. Future experiments can be done using the derived screening process to identify new compounds with potential sodium channel blockade activities. The activities of existing compounds can be improved using the pharmacophoric model, through the application of the CADR approach, where subtle modifications can be performed on existing compounds in the literature, to generate derivative compounds with improved binding affinity. Since only small changes are being made, the resulting compounds are more likely to have favourable activity in the BTX assay. The best compounds can then be synthesized and tested in the BTX assay to verify the accuracy of the modifications.

6.3.3 Structural Activity Relationships of Phenyldihydro-1,3,5-triazines and PLS Analysis

In order to get a better understanding of the factors that are important for binding of the compounds to the receptor, a partial least squares (PLS) analysis, using SIMCA version 8.0, of the BTX activity (as the y variable) and physical parameters (8 x variables) of the phenyldihydro-1,3,5-triazines compounds in series (**I**) and (**II**) was performed (**Table 4**). The x variables selected were Log P, molecular refractivity (MR), solvent accessibility surface (SAS), dipole moment, lowest unoccupied molecular orbital (LUMO) energy, highest occupied molecular orbital (HOMO) energy, electron affinity and dielectric energy. A 3-component principal component analysis (PCA) of the x variables gave a r^2 of 0.973. The scores scatter plot (**Figure 14**) showed a good scatter of the observations in all the four quadrants, with no outliers as seen by the Hotelling's t^2 eclipse on the same plot.

With this information, a partial least squares (PLS) analysis was carried out, yielding a 2-component model, with r^2 of 0.749 and validated r^2 (q^2) of 0.528. The scores scatter plot (**Figure 15**), showed two prominent clusters, namely the 2,2-dimethyl series in the upper right quadrant, and the 2,2-cyclohexyl series in the lower left quadrant. In other words, the PLS model was able to differentiate, based on the physicochemical properties of the compounds, the active and less active compounds into two different clusters. It was noted that BTX IC_{50} values were used for the analysis, thus the smaller the value, the more active the compound. Therefore the active compounds are in the lower left quadrant of the scores scatter plot while the BTX variable is in the upper right quadrant of the loadings scatter plot (**Figure 16**).

Together, the loadings scatter plot and the variable importance plot (VIP, **Figure 17**) clearly identified Log P, MR and SAS as the most important parameters that contributed significantly to the binding affinity of the compounds. This is consistent with major forces that are important in biochemical ligand binding are hydrophobic, dispersive and electrostatic interactions. Log P and MR are related respectively to hydrophobicity and dispersive forces, while SAS is related to electrostatic interactions. SAS was measured *in silico* by conductor-like screening model (COSMO), a dielectric continuum model.[26] The solute molecule was embedded in a dielectric continuum of permittivity and formed a cavity within the dielectric. The interface between the cavity and the dielectric is called the SAS. The importance of hydrophobicity, as shown in the PLS analysis, further supports the CADR approach's deduction on the improvement of compound **21**'s activity. The PLS model also suggested that dipole moment, LUMO energy, HOMO energy, electron affinity and dielectric energy are of less importance to BTX activity. This conclusion was in agreement with the observation of this study that electronic factor was less important, because the activities of chloro-substituted and methyl substituted compounds were similar.

Table 4. Physical parameters of Phenyldihydro-1,3,5-triazines as calculated *in silico*

Compound	Log P	HOMO Energy (eV)	LUMO Energy (eV)	Molar Refractivity	Solvent Accessibility Surface Area (angstrom square)	Dipole Moment (debye)	Dielectric Energy (kcal/mole)	Electron Affinity (eV)
21	2.320	-12.508	-4.575	63.958	233.225	8.640	-3.075	4.575
22	3.349	-12.408	-4.509	75.694	264.981	8.812	-3.021	4.509
23	2.838	-12.402	-4.580	68.762	244.683	8.886	-3.092	4.580
24	2.838	-12.226	-4.641	68.762	251.358	12.198	-3.167	4.641
25	2.838	-12.156	-4.643	68.762	251.362	13.410	-3.187	4.643
26	2.787	-12.195	-4.548	68.999	243.317	9.034	-3.049	4.548
27	2.787	-12.117	-4.543	68.999	250.038	9.387	-3.052	4.543
28	2.787	-12.064	-4.532	68.999	250.589	9.501	-3.053	4.532
29	2.067	-11.905	-4.425	70.421	253.568	8.187	-3.071	4.425
30	2.067	-11.700	-4.535	70.421	260.353	9.741	-3.199	4.535
31	2.067	-11.660	-4.539	70.421	261.500	11.226	-3.239	4.539
32	3.867	-12.360	-4.509	80.499	275.682	8.320	-3.014	4.509
33	3.867	-12.196	-4.573	80.499	283.089	11.724	-3.098	4.573
34	3.867	-12.120	-4.576	80.499	283.623	12.774	-3.147	4.576
25	3.816	-12.161	-4.483	80.735	275.187	9.075	-2.995	4.483
36	3.816	-12.086	-4.478	80.735	283.487	9.298	-3.001	4.478
37	3.816	-12.026	-4.468	80.735	283.492	9.349	-2.994	4.468
38	3.096	-11.873	-4.365	82.157	286.087	8.183	-3.026	4.365
39	3.096	-11.674	-4.469	82.157	292.771	9.409	-3.141	4.469
40	3.096	-11.629	-4.475	82.157	293.132	10.718	-3.182	4.475

Figure 14. PCA scores scatter plot

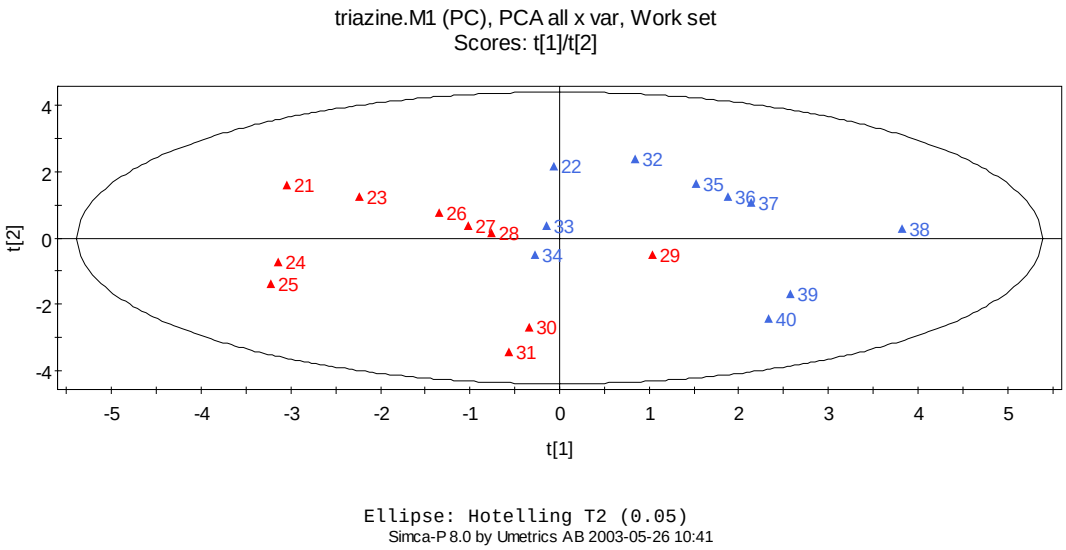

Figure 15. PLS scores scatter plot

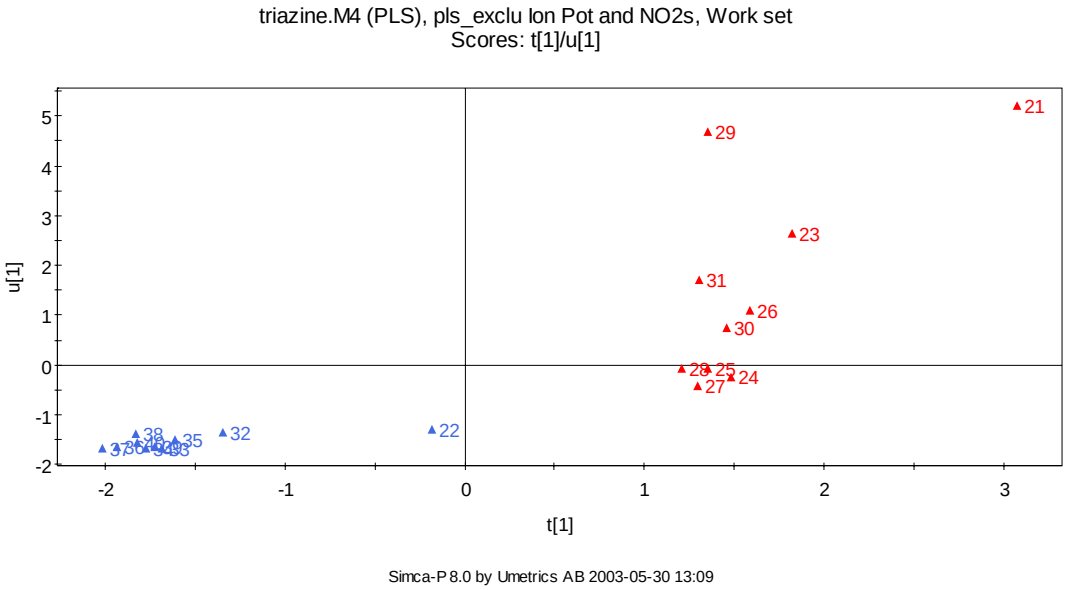

Figure 16. PLS loadings plot

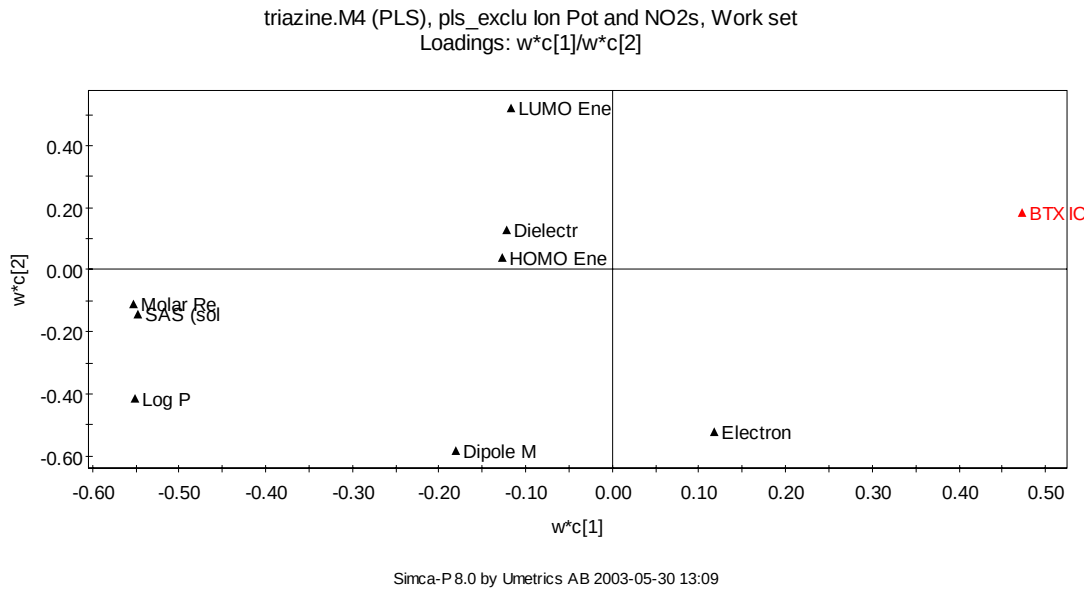

Figure 17. PLS Variable Importance Plot (VIP)

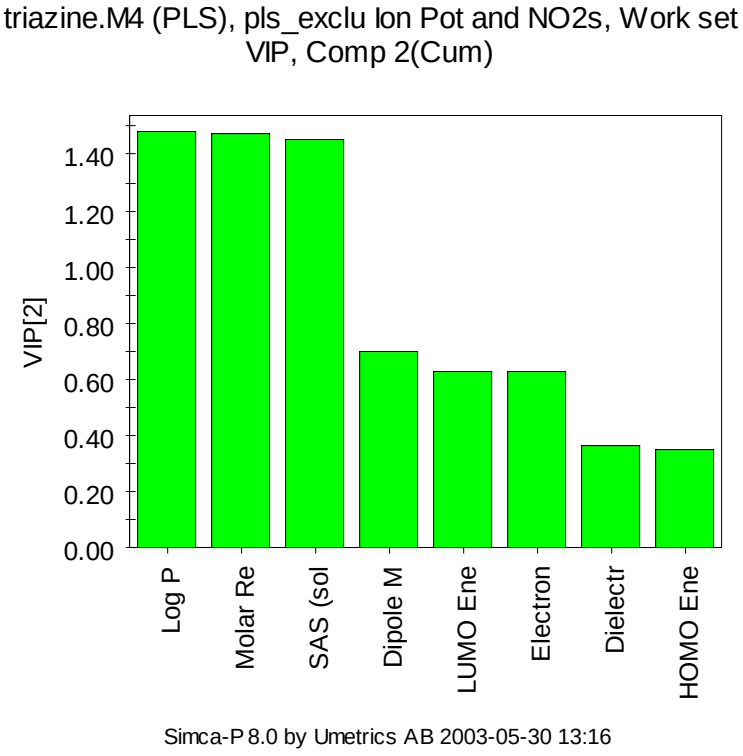

6.4 Results of CADD and *In Vitro* Testing of Benzyloximes

In a separate study, benzyloximes were used as the investigative molecules. Upon analysis of the oxime functional group, it was noted that benzyloximes possessed the three pharmacophoric elements needed for binding to the sodium channel receptor. Compound **22**, 4'-fluoro benzyloxime, was modeled *in silico* and superimposed onto the pharmacophoric model, and it was found to have a TD value of 7.9. The high TD value, and the absence of a charged nitrogen at physiological pH, suggested that compound **22** was likely to be a weak sodium channel blocker. Therefore a series of benzyloximes was synthesized and tested in the BTX assay to verify this prediction.

All the 11 compounds in the series were screened for biological activity at concentrations of 100 and 1000 μM, and only six were further investigated to obtain IC_{50} values (**Figure 18**) based on the preliminary screening. The five compounds that were not tested further consisted of three compounds which were found to be insufficiently soluble, and two others that had low binding affinity for the receptor. In general, all the 11 benzyloximes synthesized exhibited poor sodium channel blockade activity, which suggested that the pharmacophoric model's prediction, that the benzyloximes being weak sodium channel blockers, was accurate and the model is able to discern between good blockers from the poor blockers.

Figure 18. Binding affinity of compounds in the benzyloximes series

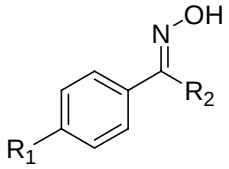

Compound	R_1	R_2	Percentage Inhibition (%)		IC_{50} (mM)	RBP
			100 μM	1000 μM		
22	4-F	H	3.2 (6.0)	43.1 (3.2)	1.45 (0.24)	0.11
42	4-CF_3	H	16.8 (1.3)	NS	NS	NA
43	4-OCH_3	H	1.9 (2.8)	32.2 (5.7)	2.67 (0.59)	0.06
44	2,3-di-OCH_3	H	0.0	30.4 (0.8)	2.60 (0.03)	0.06
45	4-OC_4H_9	H	24.9 (4.0)	NS	NS	NA
46	4-CN	H	1.2(1.3)	NS	NS	NA
47	4-NO_2	H	3.9 (1.8)	44.2 (2.2)	1.43 (0.13)	0.11
48	3-NH_2	CH_3	0.6 (3.0)	16.5 (1.1)	ND	NA
49	4-NH_2	CH_3	2.7 (5.9)	15.0 (5.0)	ND	NA
50	4-NH_2	C_2H_5	3.8 (1.5)	31.3 (1.9)	2.36 (0.23)	0.07
51	H	C_2H_5	10.1 (0.7)	80.1 (1.1)	0.44 (0.02)	0.36

Values in parentheses are SEM values; NS are compounds not tested as it was insoluble in the incubation mixture; ND are compounds not tested due to low binding affinity.

Of the six compounds that were tested further for IC_{50} values, compound **51** had the best binding affinity with an IC_{50} value of 0.44 ± 0.02 mM (RBP = 0.36), which was approximately three times weaker than phenytoin. The results showed that electron-donating substitution on the benzene ring decreased binding affinity for the receptor, as observed from the comparison of compounds **50** and **51**. An increase in hydrophobicity of the substitution at R_2 increased binding affinity, which was reflected in the percentage inhibition values of compounds **49** and **50**. The results of compounds **43** and **45** also suggested that an increase in hydrophobicity of the substitution at R_1 will improve binding affinity. Compounds **42** and **45** were not sufficiently soluble in the incubation buffer, thus they were only screened in the BTX assay at a concentration of 100 μM. From these preliminary results, it would be expected that these two compounds had the best binding affinity in the benzyloxime series of compounds for the sodium channel receptors.

In summary, electron-withdrawing substitution at R_1 and hydrophobic substitutions at R_1 and R_2 showed better binding affinity of the benzyloximes. It was postulated that electron-withdrawing substitution at R_1 can improve binding affinity by increasing the overall electron-withdrawing effects on the oxime group, thus facilitating the formation of a partially charged nitrogen atom, through mesomeric interactions between the oxime and benzene functional groups. This observation agreed with the results of the pharmacophoric model, which suggested that a charged nitrogen in the compound will improve binding affinity to the sodium channel receptors.

7. POTENTIAL PHARMACOLOGICAL ACTIONS RELATED TO SODIUM CHANNEL BLOCKADE

The ultimate aim of CADD is to develop new lead compounds with specific pharmacological actions that have clinical utility. Blockers of the neuronal (type II) sodium channels are known to be anticonvulsants, analgesics and neuroprotective agents. The most logical path to assume after the compounds have been shown to be active sodium channel blockers in the BTX assay was to carry out *in vivo* screening of these compounds.

7.1 Choice of Pharmacological Assays

Anticonvulsant screening can be done using the MES, s. c. Met (PTZ) and TTE tests. The MES and TTE tests are based on electrically-induced convulsions, while the s.c. Met test utilizes chemically-induced convulsions. Although it has been claimed that the different assay methods can be used to differentiate the compounds' potential clinical use, it has been observed that most articles in the literature only reported MES test results. As a preliminary screening test for protection against convulsion, only the MES test was performed.

Antinociceptive screening can be performed using the hot-plate, tail-flick and writhing syndrome tests. The hot-plate and writhing syndrome tests are behavioural tests, while the tail-flick test is mainly a test of pain reflex. The most commonly performed tests were the hot-plate and tail-flick tests. Both tests were equally easy to perform, and the hot-plate test was chosen as the screening assay for antinociceptives.

Cerebral ischemia involves very complex neurochemical sequelae, and it is generally agreed that neuroprotection requires a multi-prong approach in order to be effective. Thus it is not feasible to target cerebral ischemia with a drug that has a single mechanism of action, as stopping a single mechanism will only mean that the effects of ischemia will emerge through another pathway. This view is supported by the fact that riluzole, a clinically used neuroprotectant for amyotrophic lateral sclerosis, and many compounds that are still in clinical trials, such as AM-36, had been reported to possess multiple mechanisms of action. [24, 69] Furthermore, the MCAO assay is technically difficult to carry out, as it requires a lot of skill to perform the surgery. In view of the point that the compounds were not expected to be effective neuroprotective agents, coupled with the difficulty in operations, this screening assay was not attempted.

Phenyldihydro-1,3,5-triazines are known to be dihydrofolate reductase (DHFR) inhibitors, and some of them are used as antineoplastic, antimalarial and antiparasitic agents. [122] As such, DHFR inhibition is considered a potential side effect of the compounds if they are to be used as sodium channel blockers. Therefore, the abilities of the phenyldihydro-1,3,5-triazines in inhibiting DHFR were explored. It was postulated that the phenyldihydro-1,3,5-triazines with rigid and bulky substitutions at the 2-position of the triazine ring would have weak inhibitory activity on DHFR. [122] In addition to compounds in series (**I**) and (**II**), another series of compounds, with 2,2-cyclopentyl substitution, was included for DHFR inhibitory assays to better ascertain the change in inhibitory activity with respect to the increase in the rigidity and bulkiness of the substitution at the 2-position.

7.2 Anticonvulsant and Sedative Effects of the Phenyldihydro-1,3,5-triazines and Benzyloximes in the MES and Rotarod Assays

The MES test was carried out to screen and evaluate the anticonvulsant activity of the compounds. Chemical entities that abolished the tonic extension of maximal seizures in the MES test would most likely show clinical efficacy in the treatment of generalized tonic-clonic seizures. The MES test used a supra maximal current (four to five times threshold) to elicit threshold limb tonic extension, and the anticonvulsant activity of the test compound was graded upon the limb tonic extensor component. In other words, arbitrary grades were given based on the ability to abolish the extension of either hind limbs, or both forelimbs and hind limbs extension. The higher the MES score, the better the protection of the compounds against electrically-induced seizures.

The mice were subjected to rotarod screening, which was basically an assay to assess the sedative and CNS impairment effects of the compounds on the mice. The mice were subjected to the rotarod test before injecting the test compounds and those that were unable to stay on the rotarod for 300 seconds were rejected and not used for the assay. This pre-screening of the mice ensured that the inability to stay on the rotarod after injection of the test compounds could be attributed to the sedative effects of the compounds. Mice injected with test compounds that had lower CNS impairment effects would stay longer on the rotarod.

The MES scores and rotarod values for the phenyldihydro-1,3,5-triazines are listed in **Figure 19**. MES scores for all of the phenyldihydro-1,3,5-triazines at both 25 mg/Kg and 50 mg/Kg were 1.00. Hence it was apparent that none of the compounds exhibited any anticonvulsant activity. Increasing the dose from 25 mg/kg to 50 mg/kg resulted in toxicity for compounds **33** to **37,** and compound **39**. When the mice were injected with

these test compounds at the dose of 50 mg/Kg, some, if not all, of the mice died shortly after drug administration. All the phenyldihydro-1,3,5-triazines tested were lethal at 100 mg/Kg. The lack of anticonvulsant activity in the phenyldihydro-1,3,5-triazines in the MES test could be partly attributed to the high toxicity of the compounds, which prevented testing at higher doses. The results in **Figure 20** showed that compound **51**, the most potent of the benzyloximes tested, was also not active in the MES assay at the dose of 50 mg/Kg. Another possibility was that the phenyldihydro-1,3,5-triazines were unable to adequately transverse the blood brain barrier to exert their effects on the sodium channel receptors in the brain. The average rotarod values (**Figure 19)** at the dose of 25 mg/kg were generally at the maximum of 300 seconds whilst there was reduction in the values when the dose was doubled to 50 mg/kg. However, compounds **38** and **41** only exhibited slight sedative effects at 50 mg/kg. The sedative effect of the compounds therefore manifested at higher doses but at 25 mg/kg it was absent, except for compound **36,** which was highly sedative at this dose.

Figure 19. MES scores and Rotarod values of phenyldihydro-1,3,5-triazines

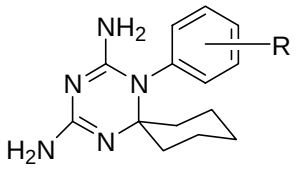

(**II**)

Compound	R	50 mg/Kg		25 mg/Kg	
		MES score	Rotarod (sec)	MES score	Rotarod (sec)
32	H	1.00(0.00)	39.0	1.00(0.00)	300(0)
33	*o*-Cl	1.00(0.00)[b]	168.5[b]	1.00(0.00)	300(0)
34	*m*-Cl	--	--	1.00(0.00)	300(0)
35	*p*-Cl	1.00[c]	29.0[c]	1.00(0.00)	300(0)
36	*o*-CH_3	--	--	1.00(0.00)	25
37	*m*-CH_3	1.00[c]	110.3[c] (95.2)	1.00(0.00)	300(0)
38	*p*-CH_3	1.00(0.00)	231.0 (38.0)	1.00(0.00)	300(0)
39	*o*-OCH_3	1.00[c]	134.0[c]	1.00(0.00)	300(0)
40	*m*-OCH_3	1.00(0.00)	165.3 (16.8)	1.00(0.00)	300(0)
41	*p*-OCH_3	1.00(0.00)	223.0 (27.1)	1.00(0.00)	281

[a] all the mice died after drug administration; [b] 1 mouse died after drug administration; [c] 2 mice died after drug administration; values in parentheses are SEM values

The toxicity profile of the benzyloximes was better than the phenyldihydro-1,3,5-triazines, thus they were tested at doses up to 200 mg/Kg. Only the six compounds, which had their IC_{50} values determined in the BTX assay, were tested in the MES and rotarod

tests. The most potent compound of the benzyloxime series was compound **51**, which had a MES score of 4 at 150 mg/Kg. It was noted that compound **51** was also the most potent compound of benzyloxime series in the BTX assay. On comparison of the data from **Figure 18** and **Figure 20**, it was observed that the test compounds with better affinity for the receptor in the BTX assay generally had better MES scores, with compound **47** as the only exception. The results suggested that in a single chemical class of compounds, the compounds with better binding affinity for the sodium channel receptors in the BTX assay are more likely to have better anticonvulsant effects in the MES assay.

The results showed that an electron-donating substituent on the benzene ring decreased the MES score, as was observed from the comparison of compounds **50** and **51**. The benzyloximes ranged from non-sedative to absolute sedation at the dose of 100 mg/Kg in the rotarod test. The rotarod test results (**Figure 20)** seemed to suggest that electron-withdrawing groups in the phenyl ring tend to cause sedation, as can be seen in compounds **22**, **43** and **47**. On the other hand, compound **50**, with an electron-donating group in the phenyl ring, had low sedative effects. Compound **44** (2',3'-dimethoxy) was non-sedative, while mice injected with compound **43** (*para*-methoxy) were too sedated to be put on the rotarod apparatus. It was interesting to note that these two compounds had similar substitutions, thus it was suggested that electron-withdrawing effects was not the only factor in determining the sedative effects of the compounds, and that an *ortho* substitution may abolish sedative effects completely.

Figure 20. MES scores and Rotarod values of benzyloximes

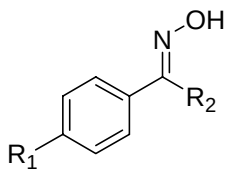

Compound	R_1	R_2	200 mg/Kg		150 mg/Kg		100 mg/Kg		50 mg/Kg	
			MES score	Rotarod (sec)	MES score	Rotarod (sec)	MES score	Rotarod (sec)	MES score	Rotarod (sec)
22	4-F	H			2.75(0.25)	0[a]	1.50(0.34)	60(28)		
43	4-OCH_3	H	-----	-----			1.25(0.25)	0		
44	2,3-di-OCH_3	H	1.25(0.25)	154(79)			1.00(0.00)	300(0)		
47	4NO_2	H			-----	-----	1.00(0.00)	110(55)		
50	4-NH_2	CH_2 CH_3	2.00(0.00)	101(15)			1.5(0.29)	222(46)		
51	H	CH_2 CH_3			4.00(0.00)	0	3.00(0.00)	117(29)	1.00(0.00)	177(71)

[a] mice too sedated to be put on rotarod apparatus; ----- mice too sick; values in parentheses are SEM values.

7.3 Antinociceptive Effects of the Phenyldihydro-1,3,5-triazines and Benzyloximes in the Hot-plate Assay

The hot-plate assay is a behavioural test that measures the response of the mouse to heat as a noxious stimulus. Each mouse was placed on a heated surface maintained at a temperature which caused pain to be felt at the paws of the animal. Latency time, the interval between the placement of the mouse on the hot-plate and the reaction of heat, was recorded. Reaction to heat can be licking of front paws or jumping from the hot-plate surface. Hind paw-licking was not used as a reaction criterion as the action was usually performed a long time after the mouse was placed on the hotplate. The hot-plate assay measures a behavioural reaction to heat, and thus cannot be performed on mice which are sedated. Therefore, for the phenyldihydro-1,3,5-triazines, only compounds **38** and **41** were tested in the hot-plate assay, as they had the lowest sedative effects in the whole series of compounds. In order reduce the number of mice used, compound **51** was the only compound from the benzyloxime series that was tested, as it had the best binding affinity for the sodium channel receptor in the BTX assay.

From the results listed in **Table 5**, it can be seen that the two phenyldihydro-1,3,5-triazines showed insignificant antinociceptive effects at 25 mg/Kg, but displayed weak antinociceptive effects at 50 mg/kg. Due to the toxicity of the phenyldihydro-1,3,5-triazines, tests at 100 mg/kg were not carried out. From the results, it was estimated that compounds **38** and **41** were approximately 10 times weaker than morphine as an antinociceptive.

Table 5. Mean hot-plate latency values of selected phenyldihydro-1,3,5-triazines and benzyloxime

Compound	**Mean hot-plate latency (sec) and amount of drug injected**				
	0 mg/Kg	**5 mg/Kg**	**25 mg/Kg**	**50 mg/Kg**	**100 mg/Kg**
Control	6.5				
Morphine		13.9 (2.9×10^{-5})[a]			
38			8.4 (0.12)	13.6 (3.9×10^{-5})	
41			8.5 (0.04)	13.1 (6.8×10^{-6})	
51				7.0 (0.52)	9.3 (5.5×10^{-3})

[a] *p* value from ANOVA (single factor) analysis.

The benzyloxime, compound **51**, had insignificant antinociceptive effects at the dose of 50 mg/Kg, but had slight antinociceptive effects at 100 mg/Kg. Since compound **51** displayed weak antinociceptive activity, further hot-plate tests were not performed on the other benzyloximes in order to reduce the number of mice used.

Emphasis had to be placed on the fact that antinociceptive effects measured in the hot-plate assay did not necessarily mean that the compounds gained access to the brain through the blood brain barrier. Antinociceptive can either work by binding to the neuronal sodium channel receptors in the brain or by binding to the neuronal sodium

channel receptors in the peripheral nerves. The preliminary screening of the compounds in the hot-plate assay only served to highlight their potential as antinociceptives, and more work need to be done to ascertain their site of action.

7.4 Inhibitory Activity of the Phenyldihydro-1,3,5-triazines against DHFR

As iterated above, the phenyldihydro-1,3,5-triazines had been known to be DHFR inhibitors, thus the DHFR inhibitory activity of three series of phenyldihydro-1,3,5-triazines was explored. In view of the need to increase bulkiness at the 2-position to reduce DHFR inhibitory activity, cyclopentyl and cyclohexyl substitutions were utilized. Although a tertiary-butyl substitution at the 2-position could further increase bulkiness, it was not attempted as the synthesis of such compounds was of low yield due to steric hindrance of the ketones. [123]

The DHFR enzyme assay is an Ultra Violet (UV) spectrophotometric assay which measures the change in UV absorbance over time. DHFR catalyzes the NADPH-dependent reduction of dihydrofolate (DHF) to tetrahydrofolate (THF). NADPH is oxidized to $NADP^+$ in the process. NADPH absorbs maximally at 340 nm whereas $NADP^+$ does not. Therefore, the rate of decrease in absorbance at 340 nm over time is an indication of the rate of enzyme reaction. In the presence of a DHFR inhibitor, this decrease in absorbance will occur at a slower rate and if there is 100% inhibition of DHFR activity, no reduction in absorbance will be observed.

During the enzyme assay, DHFR was allowed to equilibrate with NADPH in phosphate buffer at 37°C. A fixed amount of DHF was then added and the UV absorbance at 340 nm was monitored automatically by the spectrophotometer to generate the absorbance versus time graph and the gradient of the slope was calculated. If an inhibitor

was present, the enzyme would be allowed to incubate with the inhibitor at 37 ^{o}C before the addition of DHF. Different concentrations of the inhibitor were used and the percentage of DHFR inhibition at each concentration was calculated. A graph of the percentage of inhibition against the logarithmic concentrations of the inhibitor was then plotted using Prism 3.0. The concentration of the inhibitor which inhibited 50% of DHFR activity (IC_{50}) was found from the graph. 4,6-Diamino-1-(4'-chloro-3'-nitrophenyl)-1,2-dihydro-2,2-dimethyl-s-triazine was used as a positive control (IC_{50} = 0.083 μM).

There was a trend of decreasing DHFR inhibitory activity with increasing bulkiness of the substitution at the 2-position, which was evident in the *meta*-methyl (compounds **27**, **37** and **57**), *para*-methyl (compounds **28**, **38** and **58**) and *para*-methoxy (compounds **31**, **41** and **61**) substitutions in the three series of compounds (**Figure 21**). However, it was observed that some compounds in the cyclopentyl series, such as compounds **54**, **55** and **57**, had good DHFR inhibitory activity. On comparison, the compounds in the cyclohexyl series were at least a thousand fold weaker in their inhibitory activity than the positive control; 4,6-diamino-1-(4'-chloro-3'-nitrophenyl)-1,2-dihydro-2,2-dimethyl-s-triazine (IC_{50} = 0.083 μM). From these results, it was suggested that only the compounds in the cyclohexyl series should be considered for further pharmacological exploration, as the low DHFR inhibitory activity in this series means lesser side effects.

It should be highlighted that the compounds with the *ortho* substituted phenyl rings had markedly higher IC_{50} values than the *meta* and *para* substituted compounds in all the three series of compounds. It was initially proposed by Modest *et. al.* that the reduced activity in triazines with *ortho* substitutions in the phenyl ring was due to the steric interference of

the substitution that manifests in certain conformational changes of the molecule. It was suggested that tendency towards coplanarity between the phenyl ring and the triazine ring led to an increase in biological activity of the phenyldihydro-1,3,5-triazines. [122] Matthews *et. al.*, however, found that the two rings were out of plane with respect to each other in the active conformation. [127] Hence, the low activity of the *ortho* substituted compounds could be due to the inability of the molecule to fit the receptor pocket as a consequence of the sterically-induced restrained freedom of rotation of the phenyl ring by the *ortho* substitution. On the other hand, the *meta* and *para* substituted compounds in all the three series generally had similar DHFR inhibitory activity.

Figure 21. DHFR inhibitory activity of phenyldihydro-1,3,5-triazines

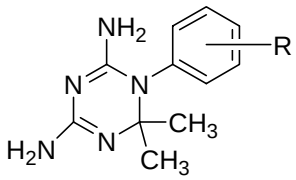

(**I**)

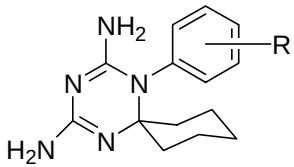

(**II**)

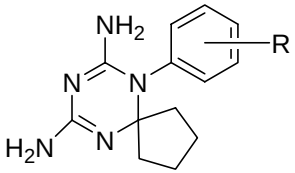

(**III**)

	(I)			(II)			(III)	
Compound	**R**	**DHFR IC_{50} (μM)** [a]	**Compound**	**R**	**DHFR IC_{50} (μM)**	**Compound**	**R**	**DHFR IC_{50} (μM)**
21	H	0.18	**32**	H	146.20	**52**	H	ND
23	*o*-Cl	6.46	**33**	*o*-Cl	> 1000 [b]	**53**	*o*-Cl	> 1000 [b]
24	*m*-Cl	0.08	**34**	*m*-Cl	7.95	**54**	*m*-Cl	0.08
25	*p*-Cl	NA	**35**	*p*-Cl	73.78	**55**	*p*-Cl	1.06
26	*o*-CH_3	5.89	**36**	*o*-CH_3	> 500 [b]	**56**	*o*-CH_3	1009.00
27	*m*-CH_3	0.08	**37**	*m*-CH_3	15.54	**57**	*m*-CH_3	0.71
28	*p*-CH_3	0.09	**38**	*p*-CH_3	12.99	**58**	*p*-CH_3	3.75
29	*o*-OCH_3	91.20	**39**	*o*-OCH_3	> 500 [b]	**59**	*o*-OCH_3	> 1000 [b]
30	*m*-OCH_3	0.29	**40**	*m*-OCH_3	217.10	**60**	*m*-OCH_3	ND
31	*p*-OCH_3	0.13	**41**	*p*-OCH_3	252.10	**61**	*p*-OCH_3	14.15

[a] data from references [124-126]; [b] exact IC_{50} not determined due to solubility problems.

7.5 Pharmacological Profile of Phenyldihydro-1,3,5-triazines and Benzyloximes

The phenyldihydro-1,3,5-triazines in series (**I**) and (**II**) had good binding affinity for the sodium channel receptor in the BTX assay. The compounds in the cyclohexyl series had higher binding affinity, with compound **34** being approximately 40 times more potent than phenytoin. However, on screening for *in vivo* pharmacological actions, none of the phenyldihydro-1,3,5-triazines have anticonvulsant activity in the MES test, but instead were found to be toxic in mice; all the compounds were lethal at 100 mg/Kg. Compounds **38** and **41**, with the lowest sedative effects as measured in the rotarod test were further tested in the hot-plate test. The results showed that both the compounds displayed antinociceptive effects at 50 mg/Kg, and were both approximately 10 times weaker than morphine as an antinociceptive. As these two compounds exhibited antinociceptive potential, it was interesting to find out whether they also exhibit DHFR inhibitory activity as phenyldihydro-1,3,5-triazines are traditionally recognized as DHFR inhibitors. An additional series of phenyldihydro-1,3,5-triazines, the cyclopentyl series of compounds, were synthesized and the DHFR inhibitory activity of the phenyldihydro-1,3,5-triazines were elucidated. The results showed that an increase in bulkiness of the substitution at the 2-position decreased DHFR inhibitory activity. However, compound **37** still possessed considerable DHFR inhibitory activity, with an IC_{50} value of 13.0 μM. On the other hand, compound **41** had much weaker DHFR inhibitory activity, with an IC_{50} value of 252.1 μM. Therefore it was proposed that compound **41** was the most suitable candidate to be developed as a potential antinociceptive which acts at the sodium channel receptors.

The benzyloximes had weak binding affinity to the sodium channel receptors, and were synthesized mainly to provide data for the validation of the screening process. One of the compounds in the benzyloxime series, compound **51**, had moderate binding affinity for the sodium channel receptor, with an IC_{50} value of 0.44 ± 0.02 mM and was approximately 3 times weaker than phenytoin. MES scores of compound **51** showed that it had excellent and good anticonvulsant activity at 150 mg/Kg and 100mg/Kg, respectively. However, this compound only displayed weak antinociceptive effects even at 100 mg/Kg.

8. CONCLUSIONS AND FUTURE WORK

8.1 CADD and its Application in the Development of a Pharmacophoric model for Sodium Channel Blockers

Lead compound identification for neuronal (type II) sodium channel blockers has been mainly focused on analogues and derivatives of hydantoins or other first generation sodium channel blockers such as carbamazepine and lidocaine. Furthermore, the traditional method of screening compounds for sodium channel blockade activity is tedious and costly. The use of CADD, a rational drug design approach, will potentially save both time and cost of discovering new lead compounds.

The current study focused on the derivation of a pharmacological model for sodium channel blockers. Five structurally diverse compounds having good blocking activity against the sodium channel receptor were selected for DISCO study, and a new pharmacophoric model for neuronal (type II) sodium channel blockers was derived. The dimensions of the pharmacophoric triangle are as follows. The H-bond acceptor to hydrophobic group distance (A-H distance) is 4.02±1.26Å, H-bond acceptor to donor distance (A-D distance) is 5.65±1.26Å, and the H-bond donor to hydrophobic group distance (D-H distance) is 3.27±1.26Å.

The pharmacophoric model was subsequently validated with 20 compounds from the literature, by correlating TD against RBP. Through correlation studies, the pharmacophoric model was found to have r^2 values of 0.83 and 0.56 for the charged nitrogen set and uncharged nitrogen set of compounds respectively. The current study took into account the charge status of the compounds at physiological pH and the observations of the RBP of the charged nitrogen set and the uncharged nitrogen set of compounds suggested that in addition to the pharmacophoric triangle, a positively charged nitrogen would give better blocking effect.

The major strength of the pharmacophoric model in the current study is the selection of compounds from different chemical classes for derivation of the model. Due to the diversity of the compounds used for its derivation, the model is robust enough to be used to analyse compounds from different chemical classes. If a single chemical class of compounds was used, then the resulting pharmacophoric model can only be used for analyzing that particular class of compounds.

Another advantage of the current study is the use of *in vitro* binding affinity data of the compounds, both for the selection of the training set of compounds and for the validation of the pharmacophoric model. The use of *in vitro* data allows the selection of compounds that has the highest binding affinity to the receptor for use as the training set. If the training set consists of compounds, with weak to moderate binding affinity to the receptor, the resulting pharmacophoric model will be inaccurate. Choosing compounds for the training set using *in vivo* data is not advisable, because *in vivo* data cannot give accurate information regarding the abilities of the compounds to bind to the receptor, due to confounding factors such as pharmacokinetic profiles of the compounds. The use of *in vitro* data for validation of the pharmacophoric model is also preferred over *in vivo* data.

8.2 Adaptation of the Pharmacophoric Model into a Screening Process for Potential Neuronal Sodium Channel Blockers

The pharmacophoric model was adapted into a high throughput screening process for the identification of potential neuronal sodium channel blockers. The screening process is based on three criteria; the presence of the three pharmacophoric elements, the presence of a charge nitrogen at physiological pH, and a TD value of less than 3.50. The equation, RBP = -31.7 TD + 123.2, is used to predict the RBP values of

compounds that satisfy the three criteria. Compounds that do not satisfy the three criteria are not recommended for further investigation.

The screening process was carried out using two series of compounds, which have not been tested in the BTX assay before. The two series of compounds, the phenyldihydro-1,3,5-triazines and the benzyloximes, were selected because of their *in-silico* ability, and inability respectively, to fulfil the criteria of the screening process. The screening process predicted that the phenyldihydro-1,3,5-triazines will have good binding affinity to the neuronal sodium channels, while the benzyloximes will have poor binding affinity. As expected from the prediction of the screening process, the phenyldihydro-1,3,5-triazines generally have good binding affinity, as measured by the BTX assay, with the most potent phenyldihydro-1,3,5-triazine (compound **34**) having an IC_{50} value of 4.0 ± 0.5 μM. The benzyloximes tested generally have poor binding affinity, with the most potent compound (compound **51)**, having an IC_{50} value of 0.44 ± 0.02 mM.

A screening process capable of identifying potent neuronal sodium channel blockers had been derived in the current study. Since the displacement of tritiated BTX has been widely used as a rapid *in vitro* assay for screening potential blockers of neuronal sodium channels, such an *in silico* screening process can potentially reduce costs of lead identification. However, the screening process does not have an equation for predicting the RBP values of compounds without a charged nitrogen at physiological pH as the linear correlation studies done on these compounds yielded a r^2 value of only 0.56.

8.3 Screening of Pharmacological Activities

Since the ultimate purpose of developing a pharmacophoric model is to use it to identify new lead compounds with pharmacological properties that have therapeutic interests, the compounds synthesized were screened for their pharmacological activities. Knowing that neuronal sodium channel blockers were potential anticonvulsants, antinociceptives and neuroprotective agents, these compounds were screened in the MES and hot-plate assays. The rotarod assay was conducted in tandem with the MES assay to assess the sedative effects of the compounds. Neuroprotective potential of the compounds was not explored as it was deemed that neuroprotective agents would be more likely to be active if they possessed multiple mechanisms of actions.

The animal studies showed that the phenyldihydro-1,3,5-triazines did not possess any anticonvulsant activity in the MES assay at 50 mg/Kg and were lethal at 100 mg/Kg. Since rotarod assay results showed that only compounds **38** and **41** from this series of compounds had low sedative effects, these two compounds were further tested in the hot-plate assay. Compounds **38** and **41** displayed antinociceptive effects at a dose of 50 mg/Kg and were approximately ten times weaker than morphine as an antinociceptive in the hot-plate assay. Since the phenyldihydro-1,3,5-triazines had been known traditionally as DHFR inhibitors, the compounds were tested in the DHFR inhibition assay. An additional series of compounds, the cyclopentyl series of phenyldihydro-1,3,5-triazines, was also synthesized and tested in this assay to help determine how an increase in bulkiness of the substitution at the 2-position of the molecule would affect its DHFR inhibitory activity. From the results, it was observed that an increase in bulkiness in the substitution at the 2-position decreased the DHFR inhibitory activity of the compounds. However, it was noted that the extent of decrease

in DHFR inhibitory activity was more prominent in the cyclohexyl series, but less significant in the cyclopentyl series of compounds. Compound **38** had been found to possess significant DHFR inhibitory activity, while compound **41** was much weaker as a DHFR inhibitor. The current study identified a suitable candidate, compound **41,** for future exploration as a potential antinociceptive.

MES assay results showed that the benzyloximes had varied potency as anticonvulsants, and that the MES scores were generally higher in those compounds that had better binding affinity in the BTX assay. For example, of the compounds in the benzyloxime series, compound **51** had the highest binding affinity in the BTX assay and the highest anticonvulsive potential in the MES assay. Compound **51** was tested in the hot-plate assay and had slight antinociceptive effects at the dose of 100 mg/Kg, and since compound **51** did not display potential as an antinociceptive, the benzyloximes were not tested further in this assay.

The current study identified a potential lead compound for the treatment of pain (compound **41**). However, the major contribution of the current study, to the discovery of new sodium channel blockers, lies in the development of a general procedure; for the *in silico* screening of potential sodium channel blockers, verification of the binding affinity of the compounds to the neuronal sodium channels and the *in vivo* screening of the compounds for anticonvulsant and antinociceptive effects.

8.4 Future Work

Future experiments can be done using the derived screening process to identify new compounds with potential sodium channel blockade. Compounds predicted to have good binding affinity in the screening processes can be synthesized and tested in the BTX assay. Compounds with good binding affinity in the BTX assay can then be

put through *in vivo* pharmacological screening assays. Another alternative is to use Unity, a module in the Sybyl program, which allows a three-dimensional search of databases for compounds that fit the pharmacophoric model. The pharmacophoric model can also be used to improve the activities of existing compounds using CADR. Subtle modifications can be performed on existing compounds in the literature, based on the pharmacophoric model, to generate derivative compounds with improved binding affinity. Since only small changes are being made, the resulting compounds are more likely to have favourable activity in the BTX assay. The best compounds can then be synthesized and tested in the BTX assay to verify the accuracy of the modifications.

The pharmacophoric model can be used to predict the mechanism of actions of antinociceptives and anticonvulsants. For example, a novel compound with an unknown mechanism of action can be tested *in silico* for its potential to block sodium channel receptors, and if the compound fits the model well, it is highly likely that the compound acts via sodium channel blockade. Then the mechanism of action can be further elucidated by either the BTX assay or patch-clamp technique. This idea can be taken a step further by introducing screening processes for therapeutic compounds that have different mechanisms of action. For example, a pharmacophoric model for anticonvulsants that act via N-methyl-*D*-aspartate antagonism can be developed. Then compounds can be screened to determine whether they are likely to act via N-methyl-*D*-aspartate antagonism. Screening compounds using pharmacophoric models for different mechanisms can determine whether the compounds have multiple mechanisms of action.

The structural similarities between the sodium, potassium and calcium voltage-gated ion channels meant that selectivity of the compounds between the receptors of

these channels would determine the extent of side effects. Many compounds that block sodium channels are also calcium channel blockers. For example, lubeluzole's ability to block sodium channels contributed to its neuroprotective effects, but its ability to block calcium channel currents caused its side effects. [84] Therefore, it was suggested to derive pharmacophoric models of the potassium and calcium channel, and the results can be analyzed in order to find the area of the pharmacophoric models which are overlapping. The overlapped area can be avoided when designing new compounds in order to attain selectivity for only one type of voltage-gated ion channels.

9 MATERIALS AND METHODS

9.1 Computer-aided Drug Design

9.1.1 Systematic Conformational Search

The structures of the compounds were modelled using Sybyl6.6 by Tripos. The computer system used was Indigo 2 from Silicon Graphics. Structures were then built according to their net charge status at physiological pH and minimized to their global minimum energy conformation (GMEC) using grid search, at rotatable single bonds with steps of 30° or 60°. The conjugate-gradient optimization and MMFF94s force field were utilized. The global minimum energy conformation (GMEC) of each compound, which is the conformation with the lowest energy value, was then selected for further work in DISCO. Ideally, all the conformations near the GMEC should be used to derive possible pharmacophoric models, however the GMEC of each compound was used due to limited computational resources.

9.1.2 Distance Comparison (DISCO)

DISCO is a molecular superimposition program (Sybyl6.6 from Tripos), which used the least-squares superimposition of pharmacophore elements represented as ligand points or site points. The DISCO program was set to overlap the compounds according to 3 main ‘functional classes’. The functional class can be an H-bond acceptor, an H-bond donor or a hydrophobic group. The three functional classes had been used in various combinations, and only the combination with one H-bond acceptor, one H-bond donor and one hydrophobic group gave a viable pharmacophore. All the other combinations did not result in any pharmacophore. When using DISCO, a reference compound had to be chosen as a template for the rest of the compounds to

superimpose upon. Vinpocetine was chosen as the reference compound as it is the most potent sodium channel blocker, according to BTX radio-ligand binding assays.

9.1.3 Quantitative Structure-Activity Relationship (QSAR)

QSAR of the 4,6-diamino-1,2-dihydro-1-phenyl-1,3,5-triazines were carried out using Principal Component Analysis (PCA) and Partial Least Squares (PLS) modelling in SIMCA version 8.0. All physical parameters were calculated with BioMedCaChe version 5.1 by the CAChe Group, Fujitsu. All compounds were first minimized using gridsearch for single bonds, at 30° steps, employing PM5 geometry minimization. Log P and molecular refractivity (MR) was done using the program's atom typing parameters. Solvent accessibility surface (SAS) and dielectric energy was done using COSMO in PM5 geometry. Dipole moment, LUMO energy, HOMO energy, dielectric energy and electron affinity were measured in PM5 geometry.

9.2 Chemical Synthesis

9.2.1 Materials and Equipments

The chemicals used in the synthesis were obtained from Aldrich Chemical Company (USA) and Tokyo Kasei Organic Chemicals (TCI, Japan). Melting points were determined using a Gallenkamp Melting Point Apparatus without correction. Maximum UV absorption wavelengths of the compounds were determined by a Shimadzu UV-160A UV-visible Recording Spectrophotometer. Infrared (IR) spectra were recorded using KBr discs *via* a Jasco FT/IR-430 Fourier Transform Infrared Spectrophotometer. ^{1}H NMR spectra were recorded on a Bruker ACF 300MHz NMR Spectrometer. Chemical shifts (δ) were expressed in parts per million (ppm) relative to tetramethylsilane (TMS), the internal standard.

9.2.2 General Three-component Synthesis of 4,6-Diamino-1-(substituted)phenyl-1,2-dihydro-2,2-substituted-1,3,5-triazine HCl.

Compound **21,** compounds **23** to **41** and compounds **52** to **61** were synthesized by the three-component synthesis developed by Modest *et al*. [123] A mixture of the substituted aniline (0.05 mole), cyanoguanidine (0.055 mole), concentrated hydrochloric acid (0.05 mole), ketone (0.05 mole) and 96% ethanol (15 ml) was refluxed with stirring for 3 to 24 hours, depending on the type of aniline used. The reaction mixture became clear within 10 to 20 minutes, followed by the precipitation of the product during reflux. Progress of the reaction was monitored by TLC. The absence of arylbiguanide in the reaction mixture was ascertained by carrying out the biguanide test. For all of the compounds, precipitation of the product occurred during the reaction process. Upon completion of the reaction, the reaction mixture was vacuum filtered and washed with cold ethanol. The product obtained was then oven dried and purification was achieved by recrystallisation using admixtures of ethanol and water. The filtrate was kept in the refrigerator for a few days and the crystalline products harvested by vacuum filtration. The final product was dried in a vacuum oven at 50°C for at least 24 hours before further characterization.

4,6-Diamino-1,2-dihydro-2,2-dimethyl-1-phenyl-1,3,5-triazine HCl (21)

Yield 32.9 %; mp 198-200 ^{o}C (200-203 ^{o}C) [123] ; λ_{max} (methanol) = 240.6 nm; IR (KBr disc) 3304 (ν_{N-H}); 3133 ($\nu_{C-H,\ aromatic}$); 2991 ($\nu_{C-H,\ aliphatic}$); 1648 ($\nu_{C=N}$); 1546 ($\nu_{C\cdots C,\ aromatic}$) cm^{-1}; ^{1}H NMR (DMSO-d$_6$) δ 9.25 (2H, br s, NH_2, ex) 7.55-7.54 (3H, m, ArH) 7.38-7.36 (2H, m, ArH) 6.26 (2H, br s, NH_2, ex) 1.34 (6H, s, CH_3) ppm.

1-(*o*-Chlorophenyl)-4,6-diamino-1,2-dihydro-2,2-dimethyl-1,3,5-triazine HCl (23)

Yield 35.4 %; mp 217 ^{o}C (222-225 ^{o}C) [128] ; λ_{max} (methanol) = 239.8 nm; IR (KBr disc) 3262 (ν_{N-H}); 3125 ($\nu_{C-H, aromatic}$); 2968 ($\nu_{C-H, aliphatic}$); 1645 ($\nu_{C=N}$); 1589 ($\nu_{C\cdots C, aromatic}$) cm^{-1}; ^{1}H NMR (DMSO-d$_6$) δ 9.11 (2H, br s, NH$_2$, ex) 7.72-7.69 (1H, m, Ar-H) 7.60-7.50 (3H, m, Ar-H) 6.64 (2H, br S, NH$_2$) 1.56 (3H, s, CH$_3$) 1.20 (3H, s, CH$_3$) ppm.

1-(*m*-Chlorophenyl)-4,6-diamino-1,2-dihydro-2,2-dimethyl-1,3,5-triazine HCl (24)

Yield 27.7 %; mp 190-193 ^{o}C (196.5-197.5 ^{o}C) [129] ; λ_{max} (methanol) = 241.0 nm; IR (KBr disc) 3294 (ν_{N-H}); 3142 ($\nu_{C-H, aromatic}$); 2967 ($\nu_{C-H, aliphatic}$); 1645 ($\nu_{C=N}$); 1591 ($\nu_{C\cdots C, aromatic}$) cm^{-1}; ^{1}H NMR (DMSO-d$_6$) δ 9.08 (2H, br s, NH$_2$, ex) 7.62-7.53 (3H, m, ArH) 7.38-7.36 (1H, m, ArH) 6.51 (2H, br s, NH$_2$, ex) 1.36 (6H, s, CH$_3$) ppm.

1-(*p*-Chlorophenyl)-4,6-diamino-1,2-dihydro-2,2-dimethyl-1,3,5-triazine HCl (25)

Yield 35.7 %; mp 205-207 ^{o}C (210-215 ^{o}C) [123] ; λ_{max} (methanol) = 240.8 nm; IR (KBr disc) 3303 (ν_{N-H}); 3141 ($\nu_{C-H, aromatic}$); 2979 ($\nu_{C-H, aliphatic}$); 1646 ($\nu_{C=N}$); 1598 ($\nu_{C\cdots C, aromatic}$) cm^{-1}; ^{1}H NMR (DMSO-d$_6$) δ 9.20 (2H, br s, NH$_2$, ex) 7.60(2H, d, J = 8.7, ArH) 7.42 (2H, d, J = 8.3 ArH) 6.47 (2H, br s, NH$_2$, ex) 1.35 (6H, s, CH$_3$) ppm.

4,6-Diamino-1,2-dihydro-2,2-dimethyl-1-(*o*-methylphenyl)-1,3,5-triazine HCl (26)

Yield 33.7 %; mp 211-214 ^{o}C (223-224 ^{o}C) [128] ; λ_{max} (methanol) = 244.0 nm; IR (KBr disc) 3300 (ν_{N-H}); 3132 ($\nu_{C-H, aromatic}$); 2970 ($\nu_{C-H\ aliphatic}$); 1643 ($\nu_{C=N}$); 1590 ($\nu_{C\cdots C, aromatic}$) cm^{-1}; ^{1}H NMR (DMSO-d$_6$) δ 8.90 (2H, br s, NH$_2$, ex) 7.33-7.43 (4H, m, ArH) 6.35 (2H, br s, NH$_2$, ex) 2.17 (3H, s, Ar-CH$_3$) 1.55 (3H, s, CH$_3$) 1.12 (3H, s, CH$_3$) ppm.

4,6-Diamino-1,2-dihydro-2,2-dimethyl-1-(*m*-methylphenyl)-1,3,5-triazine HCl (27)

Yield 45.0 %; mp 196-198 ^{o}C (204.5-205.5 ^{o}C) [129] ; λ_{max} (methanol) = 246.8 nm; IR (KBr disc) 3305 (ν_{N-H}); 3142 ($\nu_{C-H, aromatic}$); 2975 ($\nu_{C-H, aliphatic}$); 1644 ($\nu_{C=N}$); 1591 ($\nu_{C\cdots C, aromatic}$) cm^{-1}; ^{1}H NMR (DMSO-d$_6$) δ 8.76 (2H, br s, NH$_2$, ex) 7.45-7.32 (2H, m, ArH) 7.18-7.14 (2H, m, ArH) 6.25 (2H, br s, NH$_2$, ex) 2.37 (3H, s, Ar-CH$_3$) 1.35 (6H, s, CH$_3$) ppm.

4,6-Diamino-1,2-dihydro-2,2-dimethyl-1-(*p*-methylphenyl)-1,3,5-triazine HCl (28)

Yield 39.1 %; mp 199-201 ^{o}C (206-208 ^{o}C) [123] ; λ_{max} (methanol) = 245.2 nm; IR (KBr disc) 3314 (ν_{N-H}); 3147 ($\nu_{C-H, aromatic}$); 2977 ($\nu_{C-H, aliphatic}$); 1643 ($\nu_{C=N}$); 1593 ($\nu_{C\cdots C, aromatic}$) cm^{-1}; ^{1}H NMR (DMSO-d$_6$) δ 8.99 (2H, br s, NH$_2$, ex) 7.30 (4H, q, J = 7.9, ArH) 6.25 (2H, br s, NH$_2$, ex) 2.37 (3H, s, CH$_3$) 1.33 (6H, s, CH$_3$) ppm.

4,6-Diamino-1,2-dihydro-2,2-dimethyl-1-(*o*-methoxyphenyl)-1,3,5-triazine HCl (29)

Yield 33.1 %; mp 193-195 ^{o}C (198-201 ^{o}C) [128] ; λ_{max} (methanol) = 243.2 nm; IR (KBr disc) 3314 (ν_{N-H}); 3138 ($\nu_{C-H, aromatic}$); 2973 ($\nu_{C-H, aliphatic}$); 1646 ($\nu_{C=N}$); 1591 ($\nu_{C\cdots C, aromatic}$); 1278 ($\nu_{C-O}$) cm^{-1}; ^{1}H NMR (DMSO-d$_6$) δ 8.98 (2H, br s, NH$_2$, ex) 7.52-7.46 (1H, t, J = 7.9, ArH) 7.31-7.22 (2H, q, J = 7.9, ArH) 7.09-7.04 (1H, t, J = 7.6, ArH) 6.35 (1H, br s, NH$_2$, ex) 3.82 (3H, s, Ar-OCH$_3$) 1.41 (3H, s, CH$_3$) 1.21 (3H, s, CH$_3$) ppm.

4,6-Diamino-1,2-dihydro-2,2-dimethyl-1-(*m*-methoxyphenyl)-1,3,5-triazine HCl (30)

Yield 55.6 %; mp 192-194 ^{o}C (200-203 ^{o}C) [129] ; λ_{max} (methanol) = 244.6 nm; IR (KBr disc) 3375 (ν_{N-H}); 3172 ($\nu_{C-H,\ aromatic}$); 2920 ($\nu_{C-H,\ aliphatic}$); 1630 ($\nu_{C=N}$); 1568 ($\nu_{C\cdots C,\ aromatic}$); 1327 ($\nu_{C-O}$) cm^{-1}; ^{1}H NMR (DMSO-d$_6$) δ 8.93 (2H, br s, NH$_2$, ex) 7.47-7.42 (1H, t, J = 8.3, ArH) 7.10 (1H, d, J = 9.1, ArH) 6.91 (2H, s, ArH) 6.32 (2H, br s, NH$_2$, ex) 3.80 (3H, s, Ar-OCH$_3$) 1.36 (6H, s, CH$_3$) ppm.

4,6-Diamino-1,2-dihydro-2,2-dimethyl-1-(*p*-methoxyphenyl)-1,3,5-triazine HCl (31)

Yield 35.6 %; mp 200-203 ^{o}C (210 ^{o}C) [130] ; λ_{max} (methanol) = 242.6 nm; IR (KBr disc) 3399 (ν_{N-H}); 3162 ($\nu_{C-H,\ aromatic}$); 2948 ($\nu_{C-H,\ aliphatic}$); 1632 ($\nu_{C=N}$); 1592 ($\nu_{C\cdots C,\ aromatic}$); 1250 ($\nu_{C-O}$) cm^{-1}; ^{1}H NMR (DMSO-d$_6$) δ 8.84 (2H, br s, NH$_2$, ex) 7.17 (4H, q, J = 8.7, ArH) 6.27 (2H, br s, NH$_2$, ex) 3.81 (3H, s, Ar-OCH$_3$) 1.33 (6H, s, CH$_3$) ppm.

2,2-Cyclohexyl-4,6-diamino-1,2-dihydro-1-phenyl-1,3,5-triazine HCl (32)

Yield 56.4 %; mp 217-219 ^{o}C ; λ_{max} (methanol) = 245.2 nm; IR (KBr disc) 3297 (ν_{N-H}); 3132 ($\nu_{C-H,\ aromatic}$); 2945 ($\nu_{C-H,\ aliphatic}$); 1637 ($\nu_{C=N}$); 1591 ($\nu_{C\cdots C,\ aromatic}$) cm^{-1}; ^{1}H NMR (DMSO-d$_6$) δ 9.18 (2H, br s, NH$_2$, ex) 7.57-7.53(3H, m, ArH) 7.37-7.33 (1H, m, ArH) 6.22 (2H, br s, NH$_2$, ex) 1.89-0.82 (m, 10H, (CH$_2$)$_5$) ppm; $C_{14}H_{19}N_5$.HCl, (Found C, 57.32; H, 6.85; N, 23.58); M-H$^+$ 257.9.

1-(*o*-Chlorophenyl)-2,2-cyclohexyl-4,6-diamino-1,2-dihydro-1,3,5-triazine HCl (33)

Yield 25.7%; mp 217-219 ^{o}C; λ_{max} (methanol) = 244.8 nm; IR (KBr disc) 3296 (ν_{N-H}); 3136 ($\nu_{C-H,\ aromatic}$); 2928 ($\nu_{C-H,\ aliphatic}$); 1643 ($\nu_{C=N}$); 1590 ($\nu_{C\cdots C,\ aromatic}$) cm^{-}1; ^{1}H NMR (DMSO-d$_6$) δ 9.16 (2H, br s, NH$_2$, ex) 7.72-7.52 (4H, m, Ar-H) 6.57 (2H, br s, NH$_2$) 1.77-1.04 (10H, m, (CH$_2$)$_5$) ppm; $C_{14}H_{18}N_5Cl.HCl$, (Found C, 51.17; H, 6.01; N, 20.89); M-H$^+$ 291.9 [293.8] (3:1).

1-(*m*-Chlorophenyl)-2,2-cyclohexyl-4,6-diamino-1,2-dihydro-1,3,5-triazine HCl (34)

Yield 25.9 %; mp 234-237 ^{o}C; λ_{max} (methanol) = 245.2 nm; IR (KBr disc) 3220 (ν_{N-H}); 3130 ($\nu_{C-H,\ aromatic}$); 2947 ($\nu_{C-H\ aliphatic}$); 1647 ($\nu_{C=N}$); 1607 ($\nu_{C\cdots C,\ aromatic}$) cm^{-1}; ^{1}H NMR (DMSO-d$_6$) δ 9.22 (2H, br s, NH$_2$, ex) 7.64-7.51 (3H, m, ArH) 7.37-7.27 (1H, m, ArH) 6.45 (2H, br s, NH$_2$, ex) 1.89-0.93 (m, 10H, (CH$_2$)$_5$) ppm; $C_{14}H_{18}N_5Cl.HCl$, (Found C, 51.24; H, 5.82; N, 20.99); M-H$^+$ 291.9 [293.8] (3:1).

1-(*p*-Chlorophenyl)-2,2-cyclohexyl-4,6-diamino-1,2-dihydro-1,3,5-triazine HCl (35)

Yield 28.0 %; mp 242-244 ^{o}C; λ_{max} (methanol) = 244.8 nm; IR (KBr disc) 3300 (ν_{N-H}); 3134 ($\nu_{C-H,\ aromatic}$); 2936 ($\nu_{C-H,\ aliphatic}$); 1666 ($\nu_{C=N}$); 1601 ($\nu_{C\cdots C,\ aromatic}$) cm^{-1}; ^{1}H NMR (DMSO-d$_6$) δ 9.23 (2H, br s, NH$_2$, ex) 7.68-7.57 (2H, m, ArH) 7.40 (2H, d, J = 8.7, ArH) 6.41 (2H, br s, NH$_2$, ex) 1.89-0.91 (m, 10H, (CH$_2$)$_5$) ppm; $C_{14}H_{18}N_5Cl.HCl.(H_2O)_{0.5}$, (Found C, 45.22; H, 5.23; N, 18.31); M-H$^+$ 291.9 [293.8] (3:1).

2,2-Cyclohexyl-4,6-diamino-1,2-dihydro-1-(*o*-methylphenyl)-1,3,5-triazine HCl (36)

Yield 26.1 %; mp 250-252.5 ^{o}C; λ_{max} (methanol) = 244.4 nm; IR (KBr disc) 3298 (ν_{N-H}); 3133 ($\nu_{C-H, aromatic}$); 2928 ($\nu_{C-H, aliphatic}$); 1667 ($\nu_{C=N}$); 1590 ($\nu_{C\cdots C, aromatic}$) cm^{-1}; ^{1}H NMR (DMSO-d$_6$) δ 9.05 (2H, br s, NH$_2$, ex) 7.68-7.35 (4H, m, ArH) 6.40 (2H, br s, NH$_2$, ex) 2.17 (3H, s, CH$_3$) 1.72-1.03 (m, 10H, (CH$_2$)$_5$) ppm; $C_{15}H_{21}N_5$.HCl, (Found C, 58.51; H, 7.26; N, 22.25); M-H$^+$ 271.9.

2,2-Cyclohexyl-4,6-diamino-1,2-dihydro-1-(*m*-methylphenyl)-1,3,5-triazine HCl (37)

Yield 20.6 %; mp 234-235 ^{o}C; λ_{max} (methanol) = 245.0 nm; IR (KBr disc) 3304 (ν_{N-H}); 3136 ($\nu_{C-H, aromatic}$); 2925 ($\nu_{C-H, aliphatic}$); 1664 ($\nu_{C=N}$); 1599 ($\nu_{C\cdots C, aromatic}$) cm^{-1}; ^{1}H NMR (DMSO-d$_6$) δ 9.10 (2H, br s, NH$_2$, ex) 7.45-7.39 (1H, t, J = 7.5, ArH) 7.33 (1H, d, J = 7.5, ArH) 7.16-7.11 (2H, t, J = 6.4, ArH) 6.16 (2H, br s, NH$_2$, ex) 2.37 (3H, s, CH$_3$) 1.89-0.89 (m, 10H, (CH$_2$)$_5$) ppm; $C_{15}H_{21}N_5$.HCl, (Found C, 58.58; H, 6.89; N, 22.50); M-H$^+$ 271.8.

2,2-Cyclohexyl-4,6-diamino-1,2-dihydro-1-(*p*-methylphenyl)-1,3,5-triazine HCl (38)

Yield 25.0 %; mp 234-235 ^{o}C; λ_{max} (methanol) = 244.8 nm; IR (KBr disc) 3296 (ν_{N-H}); 3135 ($\nu_{C-H, aromatic}$); 2936 ($\nu_{C-H, aliphatic}$); 1646 ($\nu_{C=N}$); 1593 ($\nu_{C\cdots C, aromatic}$) cm^{-1}; ^{1}H NMR (DMSO-d$_6$) δ 9.14 (2H, br s, NH$_2$, ex) 7.37 (2H, d, J = 7.9, ArH) 7.21 (2H, d, J = 8.3, ArH) 6.16 (2H, br s, NH$_2$, ex) 2.37 (3H, s, CH$_3$) 1.88-0.88 (m, 10H, (CH$_2$)$_5$) ppm; $C_{15}H_{21}N_5$.HCl, (Found C, 57.59; H, 7.00; N, 22.01); M-H$^+$ 271.9.

2,2-Cyclohexyl-4,6-diamino-1,2-dihydro-1-(*o*-methoxyphenyl)-1,3,5-triazine HCl (39)

Yield 30.6 %; mp 248.250 ^{o}C; λ_{max} (methanol) = 243.4 nm; IR (KBr disc) 3298 (ν_{N-H}); 3140 ($\nu_{C-H,\ aromatic}$); 2932 ($\nu_{C-H,\ aliphatic}$); 1640 ($\nu_{C=N}$); 1555 ($\nu_{C\cdots C,\ aromatic}$);1278 ($\nu_{C-O}$) cm^{-1}; 1H NMR (DMSO-d$_6$) δ 9.00 (2H, br s, NH_2, ex) 7.53-7.49 (1H, t, J = 8.6, ArH) 7.26 (2H, q, J = 7.9, ArH) 7.11-7.09 (1H, t, J = 7.5, ArH) 6.29 (2H, br s, NH_2, ex) 3.80 (3H, s, Ar-OCH_3) 1.99-0.95 (m, 10H, $(CH_2)_5$) ppm; $C_{15}H_{21}N_5O.HCl$, (Found C, 55.71; H, 6.40; N, 21.05); M-H$^+$ 287.9.

2,2-Cyclohexyl-4,6-diamino-1,2-dihydro-1-(*m*-methoxyphenyl)-1,3,5-triazine HCl (40)

Yield 31.6 %; mp 231-233 ^{o}C; λ_{max} (methanol) = 244.6 nm; IR (KBr disc) 3312 (ν_{N-H}); 3141 ($\nu_{C-H,\ aromatic}$); 2826 ($\nu_{C-H,\ aliphatic}$); 1665 ($\nu_{C=N}$); 1553 ($\nu_{C\cdots C,\ aromatic}$); 1270 ($\nu_{C-O}$) cm^{-1}; ^{1}H NMR (DMSO-d$_6$) δ 9.22 (2H, br s, NH_2, ex) 7.47-7.42 (1H, t, J = 8.7, ArH) 7.10 (1H, d, J = 9.0, ArH) 6.86 (2H, d, J = 7.2, ArH) 6.25 (2H, br s, NH_2, ex) 3.80 (3H, s, Ar-OCH_3) 1.92-0.91 (m, 10H, $(CH_2)_5$) ppm; $C_{15}H_{21}N_5O.HCl$, (Found C, 54.99; H, 6.17; N, 20.78); M-H$^+$ 287.9.

2,2-Cyclohexyl-4,6-diamino-1,2-dihydro-1-(*p*-methoxyphenyl)-1,3,5-triazine HCl (41)

Yield 45.5 %; mp 288-289 ^{o}C; λ_{max} (methanol) = 244.4 nm; IR (KBr disc) 3293 (ν_{N-H}); 3144 ($\nu_{C-H,\ aromatic}$); 2938 ($\nu_{C-H,\ aliphatic}$); 1640 ($\nu_{C=N}$); 1557 ($\nu_{C\cdots C,\ aromatic}$); 1249 ($\nu_{C-O}$) cm^{-1}; ^{1}H NMR (DMSO-d$_6$) δ 9.14 (2H, br s, NH_2, ex) 7.25 (2H, d, J = 8.6, ArH) 7.06 (2H, d, J = 8.3, ArH) 6.21 (2H, br s, NH_2, ex) 3.80 (3H, s, Ar-OCH_3) 1.88-1.24 (m, 10H, $(CH_2)_5$) ppm; $C_{15}H_{21}N_5O.HCl$, (Found C, 55.75; H, 6.61; N, 21.14); M-H$^+$ 288.3.

1-(*o*-Chlorophenyl)-2,2-cyclopentyl-4,6-diamino-1,2-dihydro-1,3,5-triazine HCl (53)

Yield: 25.1%; mp: 219–220.8 °C; λ_{max} (methanol): 243.8 nm; IR (KBr disc): 3298 ($\nu_{N–H}$), 3139 ($\nu_{C–H, aromatic}$), 2970 ($\nu_{C–H, cyclopentane}$), 1645 ($\nu_{C=N}$), 1600 ($\nu_{C\cdots C, aromatic}$) cm^{-1}; ^1H NMR (DMSO-d_6): δ 9.36 (2H, br s, NH_2), 7.80–7.33 (4H, m, ArH), 6.64 (2H, br s, NH_2), 2.01–1.24 (8H, m, Cyclopentyl) ppm; $C_{13}H_{16}N_5Cl.HCl$, (Found C, 49.74; H, 5.17; N, 22.37); M-H^+ 277.9 [279.7] (3:1).

1-(*m*-Chlorophenyl)-2,2-cyclopentyl-4,6-diamino-1,2-dihydro-1,3,5-triazine HCl (54)

Yield: 5.6%; mp: 201.2–203.1 °C; λ_{max} (methanol): 245.2 nm; IR (KBr disc): 3301 ($\nu_{N–H}$), 3143 ($\nu_{C–H, aromatic}$), 2967 ($\nu_{C–H, cyclopentane}$), 1647 ($\nu_{C=N}$), 1604($\nu_{C\cdots C, aromatic}$) cm^{-1}; ^1H NMR (DMSO-d_6): δ 9.39 (2H, br s, NH_2), 7.61–7.07 (4H, m, ArH), 6.57 (2H, br s, NH_2), 1.83–1.49 (8H, m, Cyclopentyl) ppm; $C_{13}H_{16}N_5Cl.HCl.(H_2O)_{0.5}$, (Found C, 48.62; H, 5.37; N, 22.11); M-H^+ 277.9 [279.7] (3:1).

1-(*p*-Chlorophenyl)-2,2-cyclopentyl-4,6-diamino-1,2-dihydro-1,3,5-triazine HCl (55)

Yield: 34.7%; mp: 222.8–224.3 °C; λ_{max} (methanol): 245.2 nm; IR (KBr disc): 3293 ($\nu_{N–H}$), 3131 ($\nu_{C–H, aromatic}$), 2972 ($\nu_{C–H, cyclopentane}$), 1640 ($\nu_{C=N}$), 1599 ($\nu_{C\cdots C, aromatic}$) cm^{-1}; ^1H NMR (DMSO-d_6): δ 9.39 (2H, br s, NH_2), 7.61–7.41 (4H, m, ArH), 6.53 (2H, br s, NH_2), 1.82–1.48 (8H, m, Cyclopentyl) ppm; $C_{13}H_{16}N_5Cl.HCl$, (Found C, 49.88; H, 6.06; N, 22.07); M-H^+ 278.3 [280.1] (3:1).

2,2-Cyclopentyl-4,6-diamino-1,2-dihydro-1-(*o*-methylphenyl)-1,3,5-triazine HCl (56)

Yield: 27.4%; mp: 221.7–223.5 °C; λ_{max} (methanol): 244.0 nm; IR (KBr disc): 3297 ($\nu_{N–H}$), 3135 ($\nu_{C–H, aromatic}$), 2968 ($\nu_{C–H, cyclopentane}$), 1644 ($\nu_{C=N}$), 1596 ($\nu_{C\cdots C, aromatic}$) cm^{-1}; ^1H NMR (DMSO-d_6): δ 9.28 (2H, br s, NH_2), 7.46–7.32 (4H, m, ArH), 6.34 (2H, br s, NH_2), 2.22 (s, 3H, CH_3), 1.67–1.28 (8H, m, Cyclopentyl) ppm; $C_{14}H_{19}N_5$.HCl, (Found C, 57.26; H, 6.16; N, 23.41); M-H^+ 257.9.

2,2-Cyclopentyl-4,6-diamino-1,2-dihydro-1-(*m*-methylphenyl)-1,3,5-triazine HCl (57)

Yield: 8.6%; mp: 213.3–213.9 °C; λ_{max} (methanol): 245.0 nm; IR (KBr disc): 3301 ($\nu_{N–H}$), 3138 ($\nu_{C–H, aromatic}$), 2975 ($\nu_{C–H, cyclopentane}$), 1643 ($\nu_{C=N}$), 1597 ($\nu_{C\cdots C, aromatic}$) cm^{-1}; ^1H NMR (DMSO-d_6): δ 9.34 (2H, br s, NH_2), 7.45–7.13 (4H, m, ArH), 6.28 (2H, br s, NH_2), 2.37 (s, 3H, CH_3), 1.83–1.50 (8H, m, Cyclopentyl) ppm; $C_{14}H_{19}N_5$.HCl, (Found C, 57.26; H, 6.44; N, 23.42); M-H^+ 257.9.

2,2-Cyclopentyl-4,6-diamino-1,2-dihydro-1-(*p*-methylphenyl)-1,3,5-triazine HCl (58)

Yield: 19.0%; mp: 208.9–211.0 °C; λ_{max} (methanol): 245.2 nm; IR (KBr disc): 3292 ($\nu_{N–H}$), 3134 ($\nu_{C–H, aromatic}$), 2971 ($\nu_{C–H, cyclopentane}$), 1638 ($\nu_{C=N}$), 1593 ($\nu_{C\cdots C, aromatic}$) cm^{-1}; ^1H NMR (DMSO-d_6): δ 9.21 (2H, br s, NH_2), 7.66–7.23 (4H, m, ArH), 6.29 (2H, br s, NH_2), 2.37 (s, 3H, CH_3), 1.81–1.47 (8H, m, Cyclopentyl) ppm; $C_{14}H_{19}N_5$.HCl, (Found C, 57.25; H, 6.34; N, 23.48); M-H^+ 258.3.

2,2-Cyclopentyl-4,6-diamino-1,2-dihydro-1-(*o*-methoxyphenyl)-1,3,5-triazine HCl (59)

Yield: 14.5%; mp: 221.1–222.3 °C; λ_{max} (methanol): 243.2 nm; IR (KBr disc): 3292 ($\nu_{N–H}$), 3162 ($\nu_{C–H, aromatic}$), 2962 ($\nu_{C–H, cyclopentane}$), 1637 ($\nu_{C=N}$), 1586 ($\nu_{C\cdots C, aromatic}$), 1236 ($\nu_{C-O}$) cm^{-1}; ^1H NMR (DMSO-d_6): δ 9.31 (2H, br s, NH_2), 7.52–7.04 (4H, m, ArH), 6.39 (2H, br s, NH_2), 3.84 (3H, s, OCH_3), 1.86–1.49 (8H, m, Cyclopentyl) ppm; $C_{14}H_{19}N_5O.HCl$, (Found C, 54.44; H, 6.52; N, 22.38); $M-H^+$ 273.9.

2,2-Cyclopentyl-4,6-diamino-1,2-dihydro-1-(*p*-methoxyphenyl)-1,3,5-triazine HCl (61)

Yield: 16.5%; mp: 215.4–216.7 °C; λ_{max} (methanol): 242.2 nm; IR (KBr disc): 3293 ($\nu_{N–H}$), 3135 ($\nu_{C–H, aromatic}$), 2968 ($\nu_{C–H, cyclopentane}$), 1639 ($\nu_{C=N}$), 1595 ($\nu_{C\cdots C, aromatic}$), 1255 ($\nu_{C-O}$) cm^{-1}; ^1H NMR (DMSO-d_6): δ 9.33 (2H, br s, NH_2), 7.67–7.05 (4H, m, ArH), 6.30 (2H, br s, NH_2), 3.81 (3H, s, OCH_3), 1.80 – 1.46 (8H, m, Cyclopentyl) ppm $C_{14}H_{19}N_5O.HCl$, (Found C, 54.17; H, 6.16; N, 22.09); $M-H^+$ 274.3.

9.2.3 General Synthesis of Benzyloximes. [131]

Compound **22** and compounds **42** to **51** were synthesized from the corresponding aryl aldehydes/ketones using modified standard procedure for preparing oximes. 0.02 moles of the aryl aldehyde/ketone was reacted with two equivalents of hydroxylamine hydrochloride in the presence of 4 equivalents of sodium acetate in alcoholic solution at room temperature with stirring. The carbonyl compound was first dissolved in 96% ethanol while hydroxylamine hydrochloride and sodium acetate were dissolved in water and ethanol solution (2:1). The hydroxylamine hydrochloride solution was then added drop wise to the solution of aryl aldehyde/ketone with

continued stirring, and the reaction was monitored using Thin Layer Chromatography (TLC).Except for compounds **46**, **48**, **49** and **50**,where the products precipitated out from the reaction mixture, the products were extracted with ether. Anhydrous sodium sulphate was used to dry the combined ether layers. The products remained as liquid after evaporation of ether under vacuum and solidified after being kept in the fridge for at least one day. Recrystallisation was carried out using 96% ethanol and/or distilled water. All crystals were collected by suction filtration, washed with ice-cold ethanol/water (1:9) solution and dried in the vacuum oven. Compound **45** was purified by passing through a flash column.

4'-Fluoro benzyloxime (22)

Yield 41.1%; mp 88-90 ^{o}C (88.5 ^{o}C) [132] ; λ_{max} (methanol) = 251.8 nm; IR (KBr disc) 3263 (ν_{OH}, str); 1596 ($\nu_{C=N}$, str) cm^{-1}; ^{1}H NMR (DMSO-d$_6$) δ 11.24 (1H, s, NOH, ex) 8.15 (1H, s, C(NOH)H) 7.68-7.20 (4H, m, ArH) ppm; M-H^{+} 140.1.

4'-Trifluoromethyl benzyloxime (42)

Yield 60.2 %; mp 103-104 ^{o}C (100-101.5 ^{o}C) [133] ; λ_{max} (methanol) = 256.2 nm; IR (KBr disc) 3295 (ν_{OH}, str); 1618 ($\nu_{C=N}$, str) cm^{-1}; ^{1}H NMR (DMSO-d$_6$) δ 11.62 (1H, s, NOH, ex) 8.26 (1H, s, C(NOH)H) 7.82 (2H, d, J = 8.3, ArH) 7.76 (2H, d, J = 8.3, ArH) ppm; M-H^{+} 174.1.

4'-Methoxy benzyloxime (43)

Yield 43.5 %; mp 62-64 ^{o}C (63-64 ^{o}C) [134] ; λ_{max} (methanol) = 267.0 nm; IR (KBr disc) 3212 (ν_{OH}, str); 1608 ($\nu_{C=N}$, str) cm^{-1}; ^{1}H NMR (DMSO-d$_6$) δ 10.95 (1H, s, NOH, ex)

8.06 (1H, s, C(NOH)H) 7.52 (2H, d, J = 9.0, ArH) 6.96 (2H, d, J = 8.7, ArH) 3.78 (3H, s, OCH_3) ppm; M-H^+ 152.1.

2',3'-Dimethoxy benzyloxime (44)

Yield 80.1 %; mp 97-99 ^oC (98-99 ^oC) [132] ; λ_{max} (methanol) = 300 nm; IR (KBr disc) 3219 (ν_{OH}, str); 1577 ($\nu_{C=N}$, str) cm^{-1}; ^1H NMR ($CDCl_3$) δ 8.65 (1H, s, NOH, ex) 8.5 (1H, s, C(NOH)H) 7.35-6.92 (3H, m, ArH) 3.86 (6H, s, OCH_3) ppm; M-H^+ 182.1.

4'-Buthoxy benzyloxime (45)

Yield 32.4 %; mp 57-60 ^oC; λ_{max} (methanol) = 267.0 nm; IR (KBr disc) 3256 (ν_{OH}, str); 1605 ($\nu_{C=N}$, str) cm^{-1}; ^1H NMR (DMSO-d_6) δ 10.94 (1H, s, NOH, ex) 8.05 (1H, s, C(NOH)H) 7.50 (2H, d, J = 8.7, ArH) 6.94 (2H, d, J = 8.7, ArH) 4.00-3.96 (2H, t, CH_2) 1.74-1.65 (2H, m, CH_2) 1.49-1.37 (2H, m, CH_2) 0.96-0.91 (3H, t, CH_3) ppm; $C_{11}H_{15}NO_2$, (Found C, 68.51; H, 7.97; N, 7.26); M-H^+ 194.1.

4'-Cyano benzyloxime (46)

Yield 41.2 %; mp 162-164 ^oC; λ_{max} (methanol) = 272.0 nm; IR (KBr disc) 3249 (ν_{OH}, str); 1605 ($\nu_{C=N}$, str) cm^{-1}; ^1H NMR (DMSO-d_6) δ 11.73 (1H, s, NOH, ex) 8.24 (1H, s, C(NOH)H) 7.86 (2H, d, J = 8.3, ArH) 7.72 (2H, d, J = 8.3, ArH) ppm; $C_8H_6N_2O$, (Found C, 65.75; H, 4.05; N, 19.21); M-H^+ 131.1.

4'-Nitro benzyloxime (47)

Yield 56.4 %; mp 128-131^oC (133 ^oC) [132] ; λ_{max} (methanol) = 304.0 nm; IR (KBr disc) 3304 (ν_{OH}, str); 1538 ($\nu_{C=N}$, str) cm^{-1}; ^1H NMR (DMSO-d_6) δ 11.85 (1H, s, NOH, ex)

8.31 (1H, s, C(NOH)H) 8.26 (2H, d, J = 7.1, ArH) 7.86 (2H, d, J = 7.2, ArH) ppm; M-H^+ 165.1.

3'-Aminophenyl-methyl ketoxime (48)

Yield 75.6 %; mp 148-151 ^oC (149-151 ^oC) [135] ; λ_{max} (methanol) = 305.6 nm; IR (KBr disc) 3361 (ν_{OH}, str); 1580 ($\nu_{C=N}$, str) cm^{-1}; ^1H NMR (DMSO-d_6) δ 10.97 (1H, s, NOH, ex) 7.03-6.53 (4H, m, ArH) 5.08 (2H, br, NH_2, ex) 2.07 (3H, s, CH_3) ppm; M-H^+ 151.1.

4'-Aminophenyl-methyl ketoxime (49)

Yield 81.6 %; mp 144-147 ^oC (150-152 ^oC) [136] ; λ_{max} (methanol) = 277.4 nm; IR (KBr disc) 3350 (ν_{OH}, str); 1605 ($\nu_{C=N}$, str) cm^{-1}; ^1H NMR (DMSO-d_6) δ 10.60 (1H, s, NOH, ex) 7.32 (2H, d, J = 8.7, ArH) 6.53 (2H, d, J = 8.6, ArH) 5.26 (2H, br, NH_2, ex) 2.04 (3H, s, CH_3) ppm; M-H^+ 151.1.

4'-Aminophenyl-ethyl ketoxime (50)

Yield 78.2 %; mp 83-86 ^oC; λ_{max} (methanol) = 278.4 nm; IR (KBr disc) 3396 (ν_{OH}, str); 1604 ($\nu_{C=N}$, str) cm^{-1}; ^1H NMR (DMSO-d_6) δ 10.54 (1H, s, NOH, ex) 7.32 (2H, d, J = 8.6, ArH) 6.53 (2H, d, J = 8.7, ArH) 5.26 (2H, br, NH_2, ex) 2.64-2.59 (2H, q, J=7.53, CH_2) 1.03-0.98 (3H, t, CH_3) (2H, t, CH_2) (3H, d, CH_2) ppm; $C_9H_{12}N_2O$, (Found C, 65.81; H, 7.48; N, 17.35); M-H^+ 165.1.

Phenylethyl ketoxime (51)

Yield 46.0 %; mp 53-55 ^oC (53 ^oC) [137] ; λ_{max} (methanol) = 244.5 nm; IR (KBr disc) 3204 (ν_{OH}, str); 1466 ($\nu_{C=N}$, str) cm^{-1}; ^1H NMR (DMSO-d_6) δ 11.11 (1H, s, NOH, ex)

7.65-7.37 (5H, m, ArH) 2.75-2.68 (2H, q, J=7.53, CH_2) 1.07-1.02 (3H, t, CH_3) ppm; M-H^+ 150.1.

9.3 Pharmacological Assays

9.3.1 Sodium Channel Binding Assay

The assay method was modified from that reported by Brown *et. al.*[43] Synaptoneurosomes for the assay were obtained from Sprague-Dawley rat cerebral cortex. These experiments were carried out within the appropriate institutional guidelines for animal experiments. The cerebral cortex (grey matter) was extracted from the rat brain by separating the white matter and other subcortical structures. The tissue (about 1 g) was then homogenized in 2 ml of incubation buffer using 10 full strokes of a low-speed Teflon-glass homogeniser. The incubation buffer was made up of 130 mM choline chloride, 50 mM HEPES, 5.5 mM glucose, 0.8 mM $MgSO_4$ and 5.4 mM KCl adjusted to pH 7.4 using Tris base. The tissue preparation was then centrifuged at 1000 g for 30 minutes at 4 ^oC. The pellet was resuspended in a total volume of 20 ml of the incubation buffer and homogenised. The suspension was gently filtered through a 160 μm stainless steel mesh and then through a Whatman #4 filter paper using house vacuum. The filtrate was centrifuged at 1000 g for 30 minutes at 4 ^oC. The pellet was then resuspended with 2 ml of isotonic sucrose solution, which contained 10 mM NaH_2PO_4 and 0.32 mM sucrose at pH 7.4 (Tris base). The isotonic solution was stored in a freezer at -70 ^oC until the assay was performed. Prior to the binding assay, the tissue was thawed, the suspension centrifuged at 1000 g for 30 minutes at 4 ^oC and the pellet resuspended in the incubation buffer. The compounds were tested at 5 different concentrations to obtain the IC_{50} value. The appropriate amount of test drug was dissolved in DMSO and topped up with incubation buffer. 50

μl of this drug solution contained 45 μl of buffer. The incubation mixture consisted of 10 nM [^{3}H] BTX, 50 μg /ml scorpion venom, 100 μl of synaptoneurosomes from rat cerebral cortex (approximately 1 mg of protein), 5 μl of DMSO, and top up with incubation buffer to 300 μl.

The mixture was incubated for 30 minutes at 37 ^{o}C. The incubation was terminated by dilution with 3 ml of ice-cold wash buffer, which contained 130 mM choline chloride, 1.8 mM $CaCl_2$, 0.8mM $MgSO_4$, 1 mg/mL of bovine serum albumin, and 5 mM of HEPES at pH 7.4 (using Tris base). The mixture was then filtered through Whatman GF/B filter paper and the filters washed 2 times with ice-cold wash buffer (2 x 3 ml). The filters were left to stand overnight with liquid scintillant (NBCS104 from BCS) and were counted in a Beckman scintillation counter. Specific binding was determined by subtracting the nonspecific binding, which was measured in the presence of 300 μM veratridine, from the total binding of [^{3}H]-BTX. The IC_{50} values were determined from *Prism 3*, using one-site competition non-linear regression.

9.3.2 MES and Rotarod Test

The MES test was carried out using the UGO BASILE ECT Unit 7801. Neurotoxicity was assessed using the UGO BASILE Accelerating Rota-Rod (Jones and Roberts) 7650. Animals used in the test were adult male and female Swiss albino mice (20-28 g). These experiments were carried out within the appropriate institutional guidelines for animal experiments.

The mice were subjected to rotarod screening before the tests were commenced. They were placed on the accelerating rotarod treadmill, which was accelerated from 4 to 40 rpm over 5 minutes. Mice which were able to stay on the rotating rod for at least 5 minutes passed the screening test and were subsequently used for the MES test.

Since most of the compounds were sparingly soluble in water, dimethylsulphoxide (DMSO) was used as solvent. The drug solutions were injected intraperitoneally (IP) at 5 ml/kg body weight of the mice. The phenyldihydro-1,3,5-triazines were tested at dose levels of 25 mg/kg and 50 mg/kg, while the benzyloximes were tested from 50 mg/Kg to 200mg/Kg.

The mice were subjected to the rotarod test to assess the neurotoxicity of the drugs 15 minutes after injection. Measurements were reported as the time (in seconds) at which the mice fell from the rotating rod with 300 seconds (5 minutes) as the cut-off time. 15 minutes after the rotarod test (i.e. 30 minutes after drug administration), the mice were shocked with auricle electrodes using a 100 Hz alternating current at 45 mA, 0.2 ms in width, delivered for 0.4 s. The anticonvulsant protection was evaluated by an arbitrary scoring system of 1 to 4, where 1 = no protection; 2 = tonic extension of the hind limbs was abolished; 3 = both hind limbs extension and tonic flexor stage were abolished; 4 = full protection with no apparent seizure activity. For each drug substance at each dose level, 4 mice were used for the animal testing.

9.3.3 Hot-plate assay [138]

Adult, male Swiss albino mice (20-28 g) were used for this study. These experiments were carried out within the appropriate institutional guidelines for animal experiments. The mice were randomly divided into groups of eight animals each. One group of mice was used as a control, and was injected (via the i.p. route) with the drug vehicle (DMSO), while the other groups were injected (via the i.p. route) with the test compounds at a specified dose. Each animal was placed on a heated surface that was maintained at 55 ± 0.5 °C, and monitored until it either licked it front paws or jumped. Latency time, the time interval between the placement of the animal on the hotplate

and the reaction to heat, was recorded. Tissue damage was prevented by setting the cut-off time of 45 seconds for the test duration. Data analysis was performed using one-way analysis of variance (ANOVA).

9.3.4 DHFR Inhibition Assay

Phosphate buffer (0.15 M, pH 7) was used for all of the DHFR assays and was prepared by dissolving potassium dihydrogen orthophosphate (10.21 g) in distilled water (*ca* 300 ml) adjusting the solution to pH 7 with potassium hydroxide (2 M) and diluting to 500 ml with distilled water. The buffer was kept at 4 ^{o}C and discarded after 3 days. 2- Mercaptoethanol solution (0.25 M) was prepared by dissolving 2-mercaptoethanol (1.75 ml) in distilled water to 100 ml. The solution was stored in a tinted bottle at 4 ^{o}C prior to use. An aqueous solution of NADPH (2 mg/ml, 2 mM) was prepared immediately prior to use by dissolving 2 mg in 1 ml of the phosphate buffer. A solution of dihydrofolate (DHF) (1mg/ml, 2 mM) was also prepared immediately before use by suspending 1 mg of DHF in about 0.8 ml of the 2-mercaptoethanol solution and adding 0.2 ml of sodium hydroxide (2 M) solution drop wise until dissolution had occurred. The solution was protected from light and maintained at 0°C.

The assay was performed in the Shimadzu UV-160A UV-visible Recording Spectrophotometer using the kinetics mode. The assay was conducted by mixing the appropriate volumes of phosphate buffer, NADPH, DHF, bovine liver DHFR and inhibitor in the quartz cuvette (**Table 6**). The temperature of the phosphate buffer was maintained at 37 ^{o}C using a water bath. Rate of consumption of NADPH at 340 nm during the conversion of dihydrofolic acid to tetrahydrofolic acid was monitored by the reduction in the absorbance of the reaction mixture. The kinetics mode of the

spectrophotometer automatically generates the absorbance *versus* time graph and calculates the gradient of the slope (a measure of enzyme activity). Each run time was 4 minutes and the absorbance was recorded at 10 second intervals by the software. Total inhibition of DHFR was indicated by an insignificant change in the rate of consumption of NADPH and no inhibition would be seen when the rate of consumption of NADPH was equal to that of the uninhibited enzyme. The percentage activity of each inhibitor was calculated by the following formulae:-

(i) $$\text{Activity} = \frac{\text{Slope of inhibited enzyme}}{\text{Slope of uninhibited enzyme}} \times 100\ \%$$

(ii) Inhibition = 100 % - % Activity

For each inhibitor, the assay was first carried out at an inhibitor concentration of 1000 μM. A 30 mM solution of the inhibitor was prepared by dissolving 3×10^{-2} moles of the inhibitor in 1 ml of distilled water. 0.1 ml of this solution was used for the assay. Thus the inhibitor concentration in the assay mixture was 1000 μM. Subsequent assays were carried out with serial dilution (10-100x dilution) of the inhibitor solution until an inhibition of less than 40% was achieved. 3 to 4 different inhibitor concentrations were tested to provide sufficient data points for the percentage inhibition against logarithmic concentration graph. IC_{50} values for the different compounds were derived from *Prism 3*.

Table 6. Volume of reagents, enzyme and inhibitors used in the DHFR enzyme assay

Nature of assay	NADPH (ml)	Enzyme (ml)	DHF (ml)	Buffer (ml)	Inhibitor (ml)	Final vol (ml)
Uninhibited enzyme	0.1	0.1	0.1	2.7	-	3.0
Inhibited enzyme	0.1	0.1	0.1	2.6	0.1	3.0

1. DiMasi, J. A.; Hansen, R. W.; Grabowski, H. G. The price of innovation: new estimates of drug development costs. *J. Health Econ*. **2003**, *835*, 1-35.
2. Mustata, G. I.; Briggs, J. M. A structure-based design approach for the identification of novel inhibitors: application to an alanine racemase. *J. Comput. Aided Mol. Des.* **2003**, *16(12)*, 935-953.
3. Niwas, S.; Chand, P.; Pathak, V. P.; Montgomery, J. A. Structure-based design of inhibitors of purine nucleoside phosphorylase. 5. 9-Deazahypoxanthines. *J. Med. Chem.* **1994**, *37*, 2477-2480.
4. Tantillo, C.; Ding, J. P.; Jacobo-Molina, A.; Nanni, R. G.; Boyer, P. L.; Hughes, S. H.; Pauwels, R. Andries, K.; Janssen, P. A.; Arnold, E. Locations of anti-AIDS drug binding sites and resistance mutations in the three-dimensional structure of HIV-1 reverse transcriptase-implications for mechanisms of drug inhibition and resistance. *J. Mol. Biol.* **1994**, *243*, 369-387.
5. Tollinger, M.; Eichmuller, C.; Konrat, R.; Huhta, M. S.; Marsh, E. N. G.; Krautler, B. The B12-Binding Subunit of Glutamate Mutase from Clostridium Tetanomorphum Traps the Nucleotide Moiety of Coenzyme B12. *J.Mol.Biol.* **2001**, 309, 777-791.
6. Spadola, L.; Novellino, E.; Folkers, G.; Scapozza, L. Homology modelling and docking studies on Varicella Zoster Virus Thymidine kinase. *Eur. J. Med. Chem.* **2003**, 38(4), 413-419.
7. Lewis, D. F. V.; Lake, B. G.; Bird, M. G.; Loizou, G. D.; Dickins, M.; Goldfarb, P. S. Homology modelling of human CYP2E1 based on the CYP2C5 crystal structure: investigation of enzyme-substrate and enzyme-inhibitor interactions. *Tox. In.Vitro*. **2003**, *17(1)*, 93-105.

8. Shoichet, B. K.; Bodian, D. L.; Kuntz, I. D. Molecular docking using shape descriptors. *J. Comp. Chem.* **1992**, *13(4)*, 505-524.
9. Oshiro, C. M.; Kuntz, I. D.; Dixon, J. S. Flexible ligand docking using a genetic algorithm. *J. Comput. Aided. Mol. Des.* **1995**, *9(2)*, 113-130.
10. Jones, G.; Willet, P. Glen, R. C. Molecular recognition of receptor sites using a genetic algorithm with a description of solvation. *J. Mol. Biol.* **1995**, *245*, 43-53.
11. Gehlhaar, D. K.; Moerder, K. E.; Zichi, D.; Sherman, C. J.; Ogden, R. C.; Freer, S. T. *De novo* design of enzyme inhibitors by Monte Carlo ligand generation. *J. Med. Chem.* **1995**, *38*, 466-472.
12. Marshall, G. R. Computer-aided drug design. *Ann. Rev. Pharmacol. Toxicol*. **1987**, *27*, 193-213.
13. Naruto, S.; Motoc, I., Marshall, G. R. Computer-assisted analysis of bioactivity. I. Active conformation of histamine H1 receptor antagonists. *Eur. J. Med. Chem*. **1985**, *20(6)*, 529-532.
14. Sheridan, R. P.; Nilakantan, R.; Dixon, J. S.; Venkataraghavan, R. The ensemble approach to distance geometry: application to the nicotinic pharmacophore. *J. Med. Chem.* **1986**, *29(6)*, 899-906.
15. Poulsen, A.; Liljefors, T.; Gundertofte, K.; Bjornholm, B. A pharmacophore model for NK2 antagonist comprising compounds from several structurally diverse classes. *J. Comput. Aided Mol. Des.* **2002**, *16(4)*, 273-286.
16. Tsakovska, I. M. QSAR and 3D-QSAR of phenothiazine type multidrug resistance modulators in P388/ADR cells. *Bioorg. Med. Chem*. **2003**, *11(13)*, 2889-2899.
17. Paier, J.; Stockner, T.; Steinreiber, A.; Faber, K.; Fabian, W. M. F. Enantioselectivity of epoxide hydrolase catalysed oxirane ring opening: a 3D QSAR Study. *J. Comput. Aided Mol. Des.* **2003**, *17(1)*, 1-11.

18. Parrill, A. L. Evolutionary algorithms in computer-aided molecular design. *Drug Discovery Today*. **1996**, *1(12)*, 514-521.

19. Hou, T.; Xu, X. A new molecular simulation software package - Peking University Drug Design System (PKUDDS) for structure-based drug design. *J. Mol. Graphics Modell*. **2001**, *19(5)*, 455-465.

20. Gogonea, V. The QM/MM method. An overview. *Internet Electron. J. Mol. Des.* **2002**, *1*, 173-184, http://www.biochempress.com.

21. Morgan, K.; Stevens, E. B.; Shah, B.; Cox, P. J.; Dixon, A. K.; Lee, K.; Pinnock, R. D.; Hughes, J.; Richardson, P. J.; Mizuguchi, K.; Jackson, A. P. β3: An additional auxiliary subunit of the voltage-sensitive sodium channel that modulates channel gating with distinct kinetics. *Proc. Natl. Acad. Sci. U. S. A.* **2000**, *97*, 2308-2313.

22. Wann, K. T. Neuronal sodium and potassium channels: structure and function. *Br. J. Anaesth*. **1993**, *71(1)*, 2-14.

23. Catterall, W. A. Structure and function of voltage-gated ion channels. *Annu. Rev. Biochem*. **1995**, 64, 493-531.

24. Anger, T.; Madge, D. J.; Mulla, M.; Riddall, D. Medicinal chemistry of neuronal voltage-gated sodium channel blockers. *J. Med. Chem*. **2001**, 44(2), 115-137.

25. McPhee, J. C.; Ragsdale, D. S.; Scheuer, T.; Catterall, W. A. A mutation in segment IVS6 disrupts fast inactivation of sodium channels. *Proc. Natl. Acad. Sci. U.S.A.* **1994**, 91, 12346-12350.

26. Linford, N. J.; Catterall, A. R.; Qu, Y. S.; Scheuer, T.; Catterall, W. A. Interaction of batrachotoxin with the local anesthetic receptor site in transmembrane segment IVS6 of the voltage-gated sodium channel. *Proc. Natl. Acad. Sci. U.S.A.* **1998**, 95, 13947-13952.

27. Willow, M.; Catterall, W. A. Inhibition of binding of [^{3}H]batrachotoxinin A 20-α-benzoate to sodium channels by the anticonvulsant drugs diphenylhydantoin and carbamazepine. *Mol. Pharmacol*. **1982**, *22*, 627-635.

28. Maillard, M. C.; Perlman, M. E.; Amitay, O.; Baxter, D.; Berlove, D.; Connaughton, S.; Fischer, J. B.; Guo, J. Q.; Hu, L.; McBurney, R. N.; Nagy, P. I.; Subbarao, K.; Yost, E. A.; Zhang, L.; Durant, G. J. Design, Synthesis, and Pharmacological evaluation of conformationally constrained analogs of N,N'-Diaryl- and N-Aryl-N-aralkylguanidines as potent inhibitors of neuronal Na+ channels. *J. Med. Chem*. **1998**, *41(16)*, 3048-3061.

29. Leong, D.; Bloomquist, J. R.; Bempong, J.; Dybas, J. A.; Kinne, L. P.; Lyga, J. W.; Marek, F. L.; Nicholson, R. A. Insecticidal arylalkylbenzhydrolpiperidines: novel inhibitors of voltage-sensitive sodium and calcium channels in mammalian brain. *Pest Manag. Sci*. **2001**, *57(10)*, 889-895.

30. Deffois, A.; Fage, D.; Carter, C. Inhibition of synaptosomal veratridine-induced sodium influx by antidepressants and neuroleptics used in chronic pain. *Neurosci. Lett.* **1996**, *220(2)*, 117-120.

31. Haeseler, G.; Tetzlaff, D.; Bufler, J.; Dengler, R.; Munte, S.; Hecker, H.; Leuwer, M. Blockade of voltage-operated neuronal and skeletal muscle sodium channels by S(+)- and R(-)-ketamine. *Anesth. Analg.* **2003**, *96(4)*, 1019-26,

32. Grolleau, F; Gamelin, L; Boisdron-Celle, M; Lapied, B; Pelhate, M; Gamelin, E. A possible explanation for a neurotoxic effect of the anticancer agent oxaliplatin on neuronal voltage-gated sodium channels. *J. Neurophysiol*. **2001**, *85(5)*, 2293-7.

33. White, H. S.; Woodhead, J. H.; Franklin, M. R.; Swinyard, E. A.; Wolf, H. H. In *Antiepileptic Drugs*, 4th ed.; Levy, R. H., Mattson, R. H., Meldrum, B. S., Eds; Raven Press Ltd: New York, 1995; pp99-110.

34. Porreca, F.; Mosberg, H. I.; Omnaas, J. R.; Burks, T. F.; Cowan, A. Supraspinal and spinal potency of selective opioid agonists in the mouse writhing test. *J. Pharmacol. Exp. Ther.* **1987**, *240(3),* 890-4.

35. Steinlein, O. K. Channelopathies can cause epilepsy in man. *Eur. J. Pain.* **2002***, 6 Suppl*, A27-34.

36. Wallace, R. H.; Wang, D. W.; Singh, R.; Scheffer, I. E.; George, A. L.; Phillips, H. A.; Saar, K.; Reis, A.; Johnson, E. W.; Sutherland, G. R.; Berkovic, S. F.; Mulley, J. C. Febrile seizures and generalised epilepsy associated with a mutation in the Na+ channel,1 subunit gene *SCN1B*. *Nat. Genet.* **1998**, *19*, 366-370.

37. Escayg, A.; Macdonald, B. T.; Meisler, M. H.; Baulac, S.; Huberfeld, G.; An-Gourfinkel, I.; Brice, A.; LeGuern, E.; Moulard, B.; Chaigne, D.; Buresi, C.; Malafosse, A. Mutations of *SCN1A*, encoding a neuronal sodium channel, in two families with GEFS+. *Nat. Genet.* **2000**, *24*, 343-345.

38. Brouilette, W. J.; Brown, G. B.; DeLorey, T. M.; Liang, G. Sodium channel binding and anticonvulsant activities of hydantoins containing conformationally constrained 5-phenyl substituents. *J. Pharm. Sciences* **1990**, 79(10), 871-874.

39. Brouilette, W. J.; Brown, G. B.; DeLorey, T. M.; Shirali, S. S.; Grunewald, G. L. Anticonvulsant activities of phenyl-substituted bicyclic 2,4-oxazolidinediones and monocyclic models. Comparison with binding to the neuronal voltage-dependent sodium channel. *J. Med. Chem.* **1988**, 31, 2218-2221.

40. Brouillette, W. J.; Jestkov, V. P.; Brown, M. L.; Akhtar, M. S.; DeLorey, T. M.; Brown, G. B. Bicyclic hydantoins with a bridgehead nitrogen. Comparison of anticonvulsant activities with binding to the neuronal voltage-dependent sodium channel. *J. Med. Chem*. **1994**. 37, 3289-3293.

41. Scholl, S.; Koch, A.; Henning, D; Kempter, G.; Kleinpeter, E. The influence of structure and lipophilicity of hydantoins derivatives on anticonvulsant activity. *Struct. Chem*. **1999**, 10(5), 355-366.

42. Boucher, B. A. Fosphenytoin: a novel phenytoin prodrug. *Pharmacotherapy* **1996**, 16(5), 777-91.

43. Brown, M. L.; Zha, C. C.; Van Dyke, C. C.; Brown, G. B.; Brouillette, W. J. Comparative Molecular Field Analysis of hydantoins Binding to the neuronal voltage-dependent sodium channel. *J. Med. Chem*. **1999**, 42, 1537-1545.

44. Benes, J.; Parada, A.; Figueiredo, A. A.; Alves, P. C.; Freitas, A.P.; Learmonth, D. A.; Cunha, R. A.; Garrett, J.; Soares-da-Silva, P. Anticonvulsant and sodium channel-blocking properties of novel 10,11-dihydro-5H-dibenz[b,f]azepine-5-carboxamide derivative. *J. Med. Chem*. **1999**, 42, 2582-2587.

45. Sun, L.; Lin, S. S. The anticonvulsant SGB-017 (ADCI) blocks voltage-gated sodium channels in rat and human neurons: comparison with carbamazepine. *Epilepsia* **2000**, 41(3), 263-270.

46. Lang, D. G.; Wang, C. M.; Cooper, B. R. Lamotrigine, Phenytoin and carbamazepine interactions on the sodium current present in N4TG1 mouse neuroblastoma cells. *J. Pharmacol. Exp. Ther*. **1993**, 266(2), 829-835.

47. Southam, E.; Kirkby, D.; Higgins, G. A.; Hagan, R. M. Lamotrigine inhibits monoamine uptake *in vitro* and modulates 5-hydroxytryptamine uptake in rats. *Eur. J. Pharmacol*. **1998**, 358, 19-24.

48. Oommen, K. J.; Mathews, S. Zonisamide: a new antiepileptic drug. *Clin. Neurophamacol.* **1999**, 22(4), 192-200.

49. Taverna, S.; Sancini, G.; Mantegazza, M.; Franceschetti, S.; Avanzini, G. Inhibition of transient and persistent Na^+ current fractions by the new anticonvulsant topiramate. *J. Pharmacol. Exp. Ther*. **1999**, 288(3), 960-968.

50. McLean, M. J.; Bukhari, A. A.; Wamil, A. W. Effects of topiramate on sodium-dependent action-potential firing by mouse spinal cord neurons in cell culture. *Epilepsia*, **2000**, 41(suppl. 1), S21-S24.

51. Patsalos, P. N. The mechanism of topiramate. *Rev. Contemp. Pharmaco*. **1999**, *10(3)*, 147-153.

52. Rock, D. M.; McLean, M. J.; Macdonald, R. L.; Catterall, W. A.; Taylor, C. P. Ralitoline (CI-946) and CI-953 block sustained repetitive sodium action potentials in cultured mouse spinal cord neurons and displace batrachotoxin A 20-α-benzoate binding *in vitro*. *Epilepsy Res*. **1991**, 8, 197-203.

53. Zhu, Y.; Im, W.; Lewis, R. A.; Althaus, J. S.; Cazers, A. R.; Nielsen, J. W.; Palmer, J. R.; VonVoigtlander, P. F. Two metabolites of U-54494A: their anticonvulsant activity and interaction with sodium channel. *Brain Res*. **1993**, 606, 50-55.

54. Edafiogho, I. O.; Hinko, C. N.; Chang, H.; Moore, J. A.; Mulsac, D.; Nicholson, J. M.; Scott, K. R. Synthesis and anticonvulsant activity of enaminones. *J. Med. Chem*. **1992**, 35(15), 2798-2805.

55. Scott, K. R.; Rankin, G. O.; Stables, J. P.; Alexander, M. S.; Edafiogho, I. O.; Farrar, V. A.; Kolen, K. R.; Moore, J. A.; Sims, L. D.; Tonnu, A. D. Synthesis and anticonvulsant activity of enaminones. 3. Investigations on 4'-, 3'-, and 2'-substituted and polysubstituted anilino compounds, sodium channel binding studies, and toxicity evaluations. *J. Med. Chem*. **1995**, 38, 4033-4043.

56. Erdõ, S. L.; Molnár, P.; Lakics, V.; Bence, J. Z.; Tömösközi, Z. Vincamime and vincanol are potent blockers of voltage-gated Na^+ channels. *Eur. J. Pharmacol.* **1997**. 314, 69-73.

57. Clark, C. R.; Davenport, T. W. Synthesis and anticonvulsant activity of analogs of 4-amino-N-(1-phenylethyl)benzamide. *J. Med. Chem*. **1987**, 30(7), 1214-18.

58. Vamecq, J.; Lambert, D.; Poupaert, J. H.; Masereel, B.; Stables, J. P. Anticonvulsant activity and interactions with neuronal voltage-dependent sodium channel of analogues of ameltolide. *J. Med. Chem*.**1998,** 41(18), 3307-3313.

59. Vamecq, J.; Bac, P.; Herrenknecht, C.; Maurois, P.; Delcourt, P.; Stables, J. P. Synthesis and anticonvulsant and neurotoxic properties of substituted N-phenyl derivatives of the phthalimide pharmacophore. *J. Med. Chem*. **2000**, 43(7), 1311-1319.

60. Unverferth, K.; Engel, J.; Höfgen, N.; Rostock, A.; Günther, R.;Lankau, H.; Menzer, M.; Rolfs, A.; Liebscher, J.; Müller, B.; Hofmann, H. Synthesis, anticonvulsant activity, and structure-activity relationships of sodium channel blocking 3-aminopyrroles. *J. Med. Chem*. **1998**, 41(1), 63-73.

61. Reddy, N. L.; Fan, W.; Magar, S. S.; Perlman, M. E.; Yost, E.; Zhang, L.; Berlove, D.; Fischer, J. B.; Burke-Howie, K.; Wolcott, T.; Durant, G. J. Synthesis and pharmacological evaluation of N, N'-diarylguanidines as potent sodium channel blockers and anticonvulsant agents. *J. Med. Chem*. **1998**, 41(17), 3298-3302.

62. Hill, M. W.; Reddy, P. A.; Covey, D. F.; Rothman, S. M. Inhibition of voltage-dependent sodium channels by the anticonvulsant γ-Aminobutyric acid type A receptor modulator, 3-benzyl-3-ethyl-2-piperidinone. *J. Pharmacol. Ther.* **1998**, 285(3), 1303-1309.

63. Weiser, T.; Brenner, M.; Palluk, R.; Bechtel, W. D.; Ceci, A.; Brambilla, A.; Ensinger, H. A.; Sagrada, A.; Weinrich, M. BIIR 561 CL: A novel combined antagonist of α-amino-3-hydroxy-5-methyl-4-isoxazolepropionic acid receptors and voltage-dependent sodium channels with anticonvulsive and neuroprotective properties. *J. Pharmacol. Exp. Ther.* **1999**, 289(3), 1343-1349.

64. Kuo, C.; Huang, R.; Lou, B. Inhibition of Na^+ current by diphenhydramine and other diphenyl compounds: molecular determinants of selective binding to the inactivated channels. *Am. Soc. Pharmacol. Exp. Ther*. **2000**, 57, 135-143.

65. Kelly, J. L.; Koble, C. S.; Davis, R. G.; McLean, E. W.; Soroko, F. E.; Cooper, B. R. 1-(Fluorobenzyl)-4-amino-1*H*-1, 2, 3-triazolo-[4, 5-c]pyridines: Synthesis and anticonvulsant activity. *J. Med Chem*. **1995**, 38, 4131-4134.

66. Rundfeldt, C. The novel anticonvulsant AWD 140-190 acts as a highly use-dependent sodium channel blocker in neuronal cell preparations. *Epilepsy Res.* **1999**, 34, 57-64.

67. Salvati, P.; Maj. R.; Caccia, C.; Cervini, M. A.; Fornaretto, M. G.; Lamberti, E.; Pevarello, P.; Skeen, G. A.; White, H. S.; Wolf, H. H.; Faravelli, L.; Mazzanti, M.; Mancinelli, E.; Varasi, M.; Fariello, R. G. Biochemical and electrophysiological studies on the mechanism of action of PNU-151774E, a novel antiepileptic compound. *J. Pharmacol. Exp. Ther.* **1999**, 288(3), 1151-1159.

68. Snell, L. D.; Claffey, D. J.; Ruth, J. A.; Valenzuela, C. F.; Cardoso, R.; Wang, Z.; Levinson, S. R.; Sather, W. A.; Williamson, A. V.; Ingersoll, N. C.; Ovchinnikova, L.; Bhave, S. V.; Hoffman, P. L.; Tabakoff, B. Novel structure having antagonist actions at both the glycine site of the N-methyl-*D*-aspartate receptor and neuronal voltage-sensitive sodium channels: biochemical, electrophysiological, and behavioural characterization. *J. Pharmacol. Exp. Ther.* **2000**, 292(1), 215-221.

69. Callaway, J. K. Investigation of AM-36: a novel neuroprotective agent. *Clin. Exp. Pharmacol. Physiol*. **2001**, *28(11)*, 913-918.

70. Dirnagl, U.; Iadecola, C; Moskowitz, M. A. Pathobiology of ischemic stroke: an integrated view. *Trends Neurosci.* **1999**, *22*, 391-397.

71. Fisher, M.; Garcia, J. H. Evolving stroke and the ischemic penumbra. *Neurology*. **1996**, *47*, 884-888.

72. Niedergaard, M.; Hansen, A. J. Characterization of cortical depolarizations evoked in focal cerebral ischemia. *J. Cereb. Blood Flow Metab*. **1993**, 13, 568-574.

73. Lipton, P. Ischemic cell death in brain neurons. *Physiol. Rev.* **1999**, *79*, 1431-1568.

74. Taylor, C. P.; Narasimhan, L. S. Sodium Channels and Therapy of Central Nervous System Diseases. *Adv. Pharmacol.* **1997**, *39*, 447-98.

75. Fung, M. Role of voltage-gated Na+ channels in hypoxia-induced neuronal injuries. *Clin. Exp. Pharmacol. Physiol.* **2000**, *27(8)*, 569-574.

76. Pratt, J.; Rataud, J.; Bardot, F.; Roux, M.; Blanchard, J. C.; Laduron, P. M.; Stutzmann, J. M. Neuroprotective actions of riluzole in rodent models of global and focal cerebral ischemia. *Neurosci. Lett.* **1992**, 140(2), 225-230.

77. Hebert, T.; Drapeau, P.; Pradier, L.; Dunn, R. J. Block of the rat brain IIA sodium channel α subunit by the neuroprotective drug riluzole. *Mol. Pharmacol.* **1994**, 45(5), 1055-1060.

78. Ashton, D.; Willems, R.; Wynants, J.; Van Reempts, J.; Marrannes, R.; Clincke, G. Altered Na+-channel function as an *in vitro* model of the ischemic penumbra: action of lubeluzole and other neuroprotective drugs. *Brain Res.* **1997**, 745(1,2), 210-221.

79. De Ryck, M.; Keersmaekers, R.; Duytschaever, H.; Claes, C.; Clincke, G.; Janssen, M.; Van Reet, G. Lubeluzole protects sensorimotor function and reduces infarct

size in a photochemical stroke model in rats. J. *Pharmacol. Exp. Thera.* **1996**, 279(2), 748-58.

80. Aronowski, J.; Strong, R.; Grotta, J. C. Treatment of experimental focal ischemia in rats with lubeluzole. *Neuropharmacology* **1996**, 35(6), 689-693.
81. Maiese, K.; TenBroeke, M.; Kue, I. Neuroprotection of lubeluzole is mediated through the signal transduction pathways of nitric oxide. *J. Neurochem*. **1997**, 68(2), 710-4.
82. Ashton, D.; Willems, R.; Wynants, J.; Van Reempts, J.; Marrannes, R.; Clincke, G. Altered Na+-channel function as an *in vitro* model of the ischemic penumbra: action of lubeluzole and other neuroprotective drugs. *Brain Res*. **1997**, 745(1,2), 210-221.
83. Koinig, H.; Vornik, V.; Rueda, C.; Zornow, M. H. Lubeluzole inhibits accumulation of extracellular glutamate in the hippocampus during transient global cerebral ischemia. *Brain Res.* **2001**, 898(2), 297-302.
84. Gandolfo, C.; Sandercock, P.; Conti, M. Lubeluzole for acute ischaemic stroke. *Cochrane Database Syst. Rev.* **2002**, 1, CD001924.
85. Hainsworth, A. H.; Stefani, A.; Calabresi, P.; Smith, T. W.; Leach, M. J. Sipatrigine (BW 619C89) is a neuroprotective agent and a sodium channel and calcium channel inhibitor. *CNS Drug Rev.* **2000**, 6(2), 111-134.
86. Schachter, S. C.; Tarsy, D. Remacemide: current status and clinical applications. *Expert Opin. Invest. Drugs.* **2000**, 9(4), 871-83.
87. McGivern, J. G.; Patmore, L.; Sheridan, R. D. Actions of the novel neuroprotective agent, lifarizine (RS-87476-190), on voltage-dependent sodium currents in the neuroblastoma cell line, N1E-115. *Br. J. Pharmacol.* **1995**, 114(8), 1738-44.

88. Budd, D. C.; May, G. R.; Nicholls, D. G.; McCormack, J. G. Inhibition by lifarizine of intracellular Ca2+ rises and glutamate exocytosis in depolarized rat cerebrocortical synaptosomes and cultured neurons. *Br. J. Pharmacol.* **1996**, 118(1), 162-166.

89. McBean, D. E.; Winters, V.; Wilson, A. D.; Oswald, C. B.; Alps, B. J.; Armstrong, J. M. Neuroprotective efficacy of lifarizine (RS-87476) in a simplified rat survival model of 2 vessel occlusion. *Br. J. Pharmacol.* **1995**, 116(8), 3093-8.

90. Brown, C. M.; Calder, C.; Linton, C.; Small, C.; Kenny, B. A.; Spedding, M.; Patmore, L. Neuroprotective properties of lifarizine compared with those of other agents in a mouse model of focal cerebral ischemia. *Br. J. Pharmacol.* **1995**, 115(8), 1425-32.

91. McGivern, J. G.; Patmore, L.; Sheridan, R. D. Effects of the neuroprotective agent, KB-2796, on the voltage-dependent sodium current in mouse neuroblastoma, N1E-115. *Br. J. Pharmacol. (Proc. Suppl.)* **1995**, 137P.

92. Pauwels, P. J.; Van Assouw, J. P.; Peeters, L.; Leysen, J. E. Neurotoxic action of veratridine in rat brain neuronal cultures: mechanism of neuroprotection by Ca^{2+} antagonists nonselective for slow Ca^{2+} channels. *J. Pharmacol. Exp. Ther.***1990**, *255*, 1117-1122.

93. Carter, A. J.; Grauert, M.; Pschorn, U.; Bechtel, W. D.; Bartmann-Lindholm, C.; Qu, Y.; Scheuer, T.; Catterall, W. A.; Weiser, T. Potent blockade of sodium channels and protection of brain tissue from ischemia by BIII 890 CL. *Proc. Natl. Acad. Sci. U. S. A.* **2000**, 97(9), 4944-9.

94. Owen, A. J.; Ijaz, S.; Miyashita, H.; Wishart, T.; Howlett, W.; Shuaib, A. Zonisamide as a neuroprotective agent in an adult gerbil model of global forebrain

ischemia: a histological, *in vivo* microdialysis and behavioural study. *Brain Res*. **1997**, *770(1,2)*, 115-122.

95. Lee, S. R.; Kim, S. P.; Kim, J. E. Protective effect of topiramate against hippocampal neuronal damage after global ischemia in the gerbils. *Neurosci. Lett*. **2000**, *281(2,3)*, 183-186.

96. Okuyama, K.; Kiuchi, S.; Okamoto, M.; Narita, H.; Kudo, Y. T-477, a novel Ca2+- and Na+ channel blocker, prevents veratridine-induced neuronal injury. *Eur. J. Pharmacol.* **2000**, *398(2)*, 209-216.

97. Waxman, S. G. The molecular pathophysiology of pain: abnormal expression of sodium channel genes and its contributions to hyperexcitability of primary sensory neurons. *Pain*. **1999**, *Suppl. 6*, S133-S140.

98. Rush, A. M.; Elliott, J. R. Phenytoin and carbamazepine: differential inhibition of sodium currents in small cells from adult rat dorsal root ganglia. *Neurosci. Lett*., **1997**, 226(2), 95-98.

99. Chapman, V.; Dickenson, A. H. Inflammation reveals inhibition of noxious responses of rat spinal neurons by carbamazepine. *NeuroReport* **1997**, 8(6), 1399-1404.

100. Troels, S. J. Anticonvulsants in neuropathic pain: rationale and clinical evidence. *Eur. J. Pain.* **2002**, *6 (Suppl. A)*, 61-68.

101. Pevarello, P.; Varasi, M.; Salvati, P.; Post, C. Substituted 2-benzylamino-2-phenylacetamide compounds useful as sodium channel blockers. *PCT Int. Appl. WO 9935123 A1*, 15 Jul 1999, 20 pp.

102. Lan, N. C.; Wang, Y.; Cai, S. X. Preparation of substituted 2-aminoacetamides as sodium channel blockers. *PCT Int. Appl. WO 9926614 A1*, 3 Jun 1999, 46 pp.

103. Beatch, G. N.; Longley, C. J.; Walker, M. J. A.; Wall, R. A. Aminocycloalkyl cinnamide compounds for arrhythmia and as analgesics and anesthetics. *PCT Int. Appl. WO 2000051981 A1,* 8 Sep 2000, 79 pp.

104. Chapman, V.; Wildman, M. A.; Dickenson, A. H. Distinct electrophysiological effects of two spinally administered membrane stabilizing drugs, bupivacaine and lamotrigine. *Pain* **1997**, 71(3), 285-295.

105. Klamt, J. G. Effects of intrathecally administered lamotrigine, a glutamate release inhibitor, on short- and long-term models of hyperalgesia in rats. *Anesthesiology* **1998**, 88(2), 487-494.

106. Trezise, D. J.; John, V. H.; Xie, X. M. Voltage- and Use-Dependent Inhibition of Na+ Channels in Rat Sensory Neurons by 4030W92, a New Antihyperalgesic Agent. *Br. J. Pharmacol.* **1998**, *124*, 953-963.

107. Clayton, N. H.; Collins, S. D.; Sargent, R.; Brown, T.; Nobbs, M.; Bountra, C.; Trezise, D. J. The Effect of the Novel Sodium Channel Blocker 4030W92 in Models of Acute and Chronic Inflammatory Pain in the Rat. *Br. J. Pharmacol.* **1998**, *123*, 79P.

108. Collins, S. D.; Clayton, N. M.; Nobbs, M.; Bountra, C. The Effect of 4030W92, a Novel Sodium Channel Blocker, on the Treatment of Neuropathic Pain in the Rat. *Br. J. Pharmacol.* **1998**, *123*, 16P.

109. Gutser, U. T.; Friese, J.; Heubach, J. F.; Matthiesen, T.; Selve, N.; Wilffert, B.; Gleitz, J. Mode of antinociceptive and toxic action of alkaloids of Aconitum spec. *Naunyn-Schmiedeberg's Arch. Pharmacol.* **1998**, 357(1), 39-48.

110. Ameri, A. The effects of Aconitum alkaloids on the central nervous system. *Prog. Neurobiol.* **1998**, 56(2), 211-235.

111. Keith, R. QX-314 inhibits ectopic nerve activity associated with neuropathic pain. *Brain Res.* **1997**, 771(2), 228-237.

112. Berger, J.; Flippin, L. A.; Hunter, J. C.; Loughhead, D. G.; Weikert, R. J. Preparation of N-[2-(2,6-dimethylphenoxy-1-methylethyl)]ethylamine as sodium channel blocker. *PCT Int. Appl. WO 9727169 A1*, 31 Jul 1997, 37 pp.

113. Perucca, E. The new generation of antiepileptic drugs: Advantages and disadvantages. *Br. J. Clin. Pharmacol*. **1996**, 42, 531-543.

114. Wang, G. K.; Strichartz, G. R. Therapeutic Na+ channel blockers beneficial for pain syndromes. *Drug Dev. Res.* **2001**, 54(3), 154-158.

115. Tasso, S. M.; Bruno-Blanch, Luis E.; Estiu, G. L. Pharmacophore model for antiepileptic drugs acting on sodium channels. *J. Mol. Modeling* **2001**, 7(7), 231-239. http://link.springer.de/link/service/journals/00894/papers/1007007/10070231.pdf

116. Pevarello, P.; Bonsignori, A.; Caccia, C.; Amici, R.; McArthur, R. A.; Fariello, R. G.; Salvati, P.; Varasi, M. Sodium channel activity and sigma binding of 2-aminopropanamide anticonvulsants. *Bioorg. Med. Chem. Lett.* **1999**, 9, 2521-2524.

117. Shimojo, M.; Takasugi, K.; Yamamoto, I.; Funato, H., Mochizuki, H.; Kohsaka, S. Neuroprotective action of a novel compound-50463- in primary cultured neurons. *Brain Res.* **1999**, 815, 131-139.

118. Zimanyi, I.; Weiss, S. R. B.; Lajtha, A.; Post, R. M.; Reith, M. E. A. Evidence for a common site of action of lidocaine and carbamazepine in voltage-dependent sodium channels. *Eur. J. Pharmacol.* **1989**, 167, 419-422.

119. Gleitz, J.; Friese, J.; Beile, A.; Ameri, A.; Peters, T. Anticonvulsive action of (±)-kavain estimated from its properties on stimulated synaptosomes and Na^+ channel receptor sites. *Eur. J. Pharmacol.* **1996**, 315, 89-97.

120. Catterall, W. A.; Gainer, M. Interaction of Brevetoxin with a new receptor site on the sodium channel. *Toxicon* **1985**, 23 (3), 497-504.

121. Worley, P. F.; Baraban, J. M. Site of anticonvulsant action on sodium channel: autoradiographic and electrophysiological studies in rat brain. *Proc. Natl. Acad. Sci. USA.* **1987**, 84, 3051-3055.

122. Modest, E. J.; Farber, S.; Foley, G. E. Structure-biological activity relationships in a series of biologically active dihydrotriazines. *Proc. Am. Ass. Cancer Res.* **1954,** 1, 33.

123. Modest E. J. Chemical and biological studies on 1,2-dihydro-s-triazines. II three-component synthesis. *J. Org. Chem.* **1956,** 21, 1-13.

124. Kim, K. H.; Dietrich, S. W.; Hansch, C. Inhibition of dihydrofolate reductase. 3. 4,6-diamino-1,2-dihydro-2,2-dimethyl-1-(2-subtituted-phenyl)-*s*-triazine inhibition of bovine liver and mouse tumor enzymes. *J. Med. Chem.* **1980**, 23, 1248.

125. Dietrich, S. W.; Smith, R. N.; Fukunaga, J. Y.; Olney, M.; Hansch, C. Dihydrofolate reductase inhibition by 2,4-dihydrotriazines: a structure-activity study. *Arch. Biochem. Biophy.* **1979**, 194 (2), 600-611.

126. Bami, H. L. Studies in dihdydrotriazines. *Current Sci.* **1954**, 23, 124.

127. Matthews, D. A.; Bolin, J. T.; Burridge J. M.; Filman D. J; Volz K. W.; Kraut J. Dihydrofolate reductase – the stereochemistry of inhibitor selectivity. *J. Biol. Chem.* **1985** 260 (1), 392-399.

128. Kim, K. H.; Dietrich, S. W.; Hansch, C. Inhibition of dihydrofolate reductase. 3. 4,6-diamino-1,2-dihydro-2,2-dimethyl-1-(2-substituted-phenyl)-*s*-triazine inhibition of bovine liver and mouse tumor enzymes *J. Med. Chem.* **1980**, 23, 1248-1251.

129. Dietrich, S. W.; Smith, R. N.; Fukunaga, J. Y.; Olney, M.; Hansch, C. Dihydrofolate reductase inhibition by 2,4-diaminotriazines: a structure-activity study. *Arch. Biochem. Biophy.* **1979**, 194 (2), 600.

130. Bami, H. L. Studies in dihydrotriazines. *Current Sci.* **1954**, 23, 124.

131. Dayagi, S.; Degani, Y. In *The Chemistry of the Carbon-nitrogen Double Bond*; Patai, S., Ed; Wiley-Interscience: New York, **1970**; pp 61.

132. In *Dictionary of Organic Compounds*, 5th edition; Buckingham, J., Ed; Chapman and Hall: London, **1982**.

133. Liu, K. J. *Org. Chem.* **1980**, 45 (19), 3916-3918.

134. Sharghi, H; Sarvari, M. H. Selective synthesis of *E* and *Z* isomers of oximes. *Synlett.* **2001**, 1, 99-101.

135. Witek, S.; Bielawski, J.; Bielawski, A. New pesticides and intermediates. Part VII. Some azaalkenyl derivatives of N-phenylurea and N-phenylcarbamic acid. *Polish J. Chem.* **1981**, 55 (12), 2589-2600.

136. Gawinecki, R.; Kolehmainen, E.; Kauppinen, R. ^{1}H and ^{13}C NMR studies of *para*-substituted benzyloximes for evaluation of the electron donor properties of substituted amino groups. *J. Chem Soc. Perkin Trans. 2* **1998**, 1, 25-30.

137. Trofinov, B. A.; Korostova, S. E.; Balabanova, L. N.; Mikhaleva, A. I. Pyrroles from ketoximes and acetylene. VI. Study of conditions for the reaction of aceto- and propiophenone oximes with acetylene. *Zhurnal Organicheskoi Khimii* **1978**, 14 (8), 1733-1736.

138. Heyliger, S. O.; Goodman, C. B.; Ngong, J. M.; Soliman, K. F. A. The analgesic effects of tryptophan and its metabolites in the rat. *Pharmaco. Res.* **1998**, 38 (4), 243-250.